7-1-2011

Parallel simulation of reinforced concrete sructures using peridynamics

Navid Sakhavand

Navid Sakhavand
Candidate

Civil Engineering
Department

This thesis is approved, and it is acceptable in quality and form for publication:

Approved by the Thesis Committee:

, Chairperson

PARALLEL SIMULATION OF REINFORCED CONCRETE STRUCTURES USING PERIDYNAMICS

by

Navid Sakhavand

B.S. Civil Engineering, Sharif University of Technology, 2008

THESIS

Submitted in Partial Fulfillment of the
Requirements for the Degree of

Master of Science

Civil Engineering

The University of New Mexico
Albuquerque, New Mexico

May, 2011

DEDICATION

To my Beloved Mom who loves me, like nobody

To my Dear Dad who supports me, like nobody

To my sisters, Nooshin and Nahal

ACKNOWLEDGEMENTS

I owe my utmost gratitude to Prof. Walter Gerstle, my advisor, for his patience, support, guidance and understanding during the time of my research.

I am heartily thankful to my co-advisor, Prof. Susan Atlas, whose encouragement, supervision and support enabled me to develop an understanding of the subject.

It is a pleasure to thank Dr. Stewart Silling whose kind concern and consideration regarding my research and my academic achievements is acknowledged.

I would also like to express gratitude to Prof. Timothy Ross and Prof. Percy Ng, members of my committee, for their comments and suggestions.

Also, I thank the Center for Advanced Research Computing for the use of facilities and help in harnessing the supercomputers.

Lastly, I offer my regards and blessings to my family, my friends, and all of those who supported me in any respect during the completion of my thesis.

PARALLEL SIMULATION OF REINFORCED CONCRETE STRUCTURES USING PERIDYNAMICS

by

Navid Sakhavand

B.S. Civil Engineering, Sharif University of Technology, 2008

ABSTRACT OF THESIS

Submitted in Partial Fulfillment of the
Requirements for the Degree of

Master of Science

Civil Engineering

The University of New Mexico
Albuquerque, New Mexico

May, 2011

PARALLEL SIMULATION OF REINFORCED CONCRETE STRUCTURES USING PERIDYNAMICS

by

Navid Sakhavand

B.S., Civil Engineering, Sharif University of Technology, 2008

M.S., Civil Engineering, University of New Mexico, 2011

ABSTRACT

The failure of concrete structures involves many complex mechanisms. Traditional theoretical models are limited to specific problems and are not applicable to many real-life problems. Consequently, design specifications mostly rely on empirical equations derived from laboratory tests at the component level. It is desirable to develop new analysis methods, capable of harnessing material-level test parameters.

To overcome limitations and shortcomings of models based on continuum mechanics and fracture mechanics, Stewart Silling introduced the concept of peridynamics in 1998. Similar to molecular dynamics, peridynamic modeling of a physical structure involves simulating interacting particles subjected to an empirical

"force field". The evolution of interacting particles determines the deformation of the structure at a given time due to the applied boundary condition.

As a particle-based model, peridynamics requires the repeated evaluation of many particle interactions which is computationally demanding. However, with today's inexpensive computing hardware, parallel algorithms can be utilized to run such problems on multi-node supercomputers with fast interconnects. However, existing codes tend to be domain-specific with too many built-in physical assumptions.

In this work, a novel method for parallelization of any particle-based simulation is presented which is quite general and suitable for simulating diverse physical structures. A scalable parallel code for molecular dynamics and peridynamics simulation, PDQ, is described which implements a novel *wall method* parallelization algorithm, developed as part of this thesis. PDQ partitions the geometric domain of a problem across multi-nodes while the physics is left open to the user to decide whether to simulate a solvated protein or alloy grain boundary at the atomic scale or to simulate cracking phenomena in concrete via peridynamics. A further extension of PDQ brings more flexibility by allowing the user to define any desired number of degrees of freedom for each particle in a peridynamics simulation.

At the end of this thesis, plain, reinforced and prestressed concrete benchmark problems are simulated using PDQ and the results are compared to available design code equations or analytical solutions.

This research is a step toward next level of computational modeling of reinforced concrete structures and the revolutionizing of how concrete is analyzed and also how concrete structures are designed.

TABLE OF CONTENTS

LIST OF FIGURES

1. INTRODUCTION

1.1. Motivation

Concrete, a quasi-brittle material, has been commonly used in civil engineering structures such as bridges, buildings and dams. Concrete cracks under loading, causing discontinuities in the displacement field. In fact, concrete contains many micro-cracks even before loading. Figure 1.1 and Figure 1.2 illustrate failure behavior in some reinforced concrete structures.

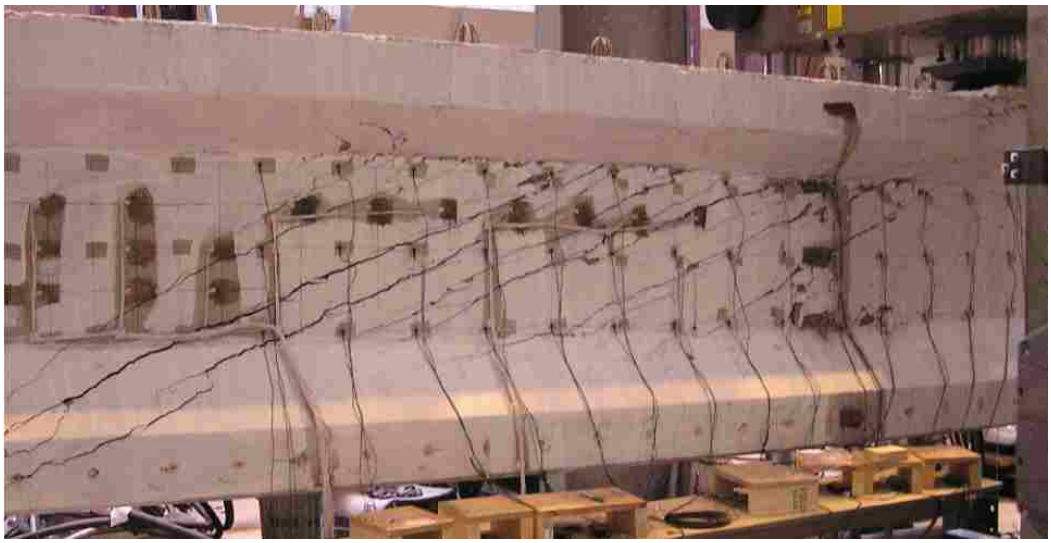

Figure 1.1 – Shear failure of a prestressed concrete beam, from [Runzell et al. 2008]

Figure 1.2 - Damaged column at Olive View Hospital, from [Steinbrugge 1992]

Computational modeling of civil engineering structures is an active area of research. Displacement discontinuities (cracks) make modeling of concrete structures challenging. Continuum mechanics [Mase *et al.* 2009] and finite elements methods [Huebner *et al.* 2008] address many problems in solid mechanics. However, the implicit assumption of continuity of the displacement field prevents these methods from bing capable of predicting cracking in materials. Researchers have applied fracture mechanics [Anderson 2010] in an attempt to overcome these issues. The smeared crack approach, the discrete crack approach, and the discrete element approach are among the models based upon fracture mechanics. In smeared-crack models, the cracks are represented through changes of the material constitutive equations instead of changes in the geometry as with discrete models. Sensitivity of results to the mesh is the major deficiency with

smeared crack models [Nguyen and Chun 2005]. In discrete crack models, long equations with many empirical factors based upon nonlinear fracture mechanics theory are utilized to predict the direction of crack propagation. The problem geometry and the finite element mesh are incrementally altered as cracks propagate [Cusatis *et al.* 2006]. Both discrete crack and discrete element approaches require redefinition of the geometry in the predicted location of nucleation of discontinuity [Silling 1998]. Such approaches confines formation of spontaneous discontinuities (cracks).

In light of the limitations of these traditional approaches, it is desirable to develop new analysis methods which can model cracking behavior of quasi-brittle materials. Such methods should address real-life problems in the field of structural engineering such as reinforced and prestressed concrete structures.

With today's access to powerful supercomputers, concepts similar to molecular dynamics can be utilized to model cracking phenomenon in concrete. Molecular dynamics is a computer simulation method wherein particles are modeled at the atomistic scale and Newton's equations are applied to each atom at each time step of the simulation. Interactions between atoms require calculation of the forces acting between them. These forces are based on empirical spring models, electrostatics, and the underlying quantum mechanics of the electrons in the atoms [Allen and Tildesley 1987].

Applying molecular dynamics to quasi-brittle materials would involve specifying an appropriate force field for such material, representing how the consisting atoms interact. Determination of such force field is beyond the level of interest of a structural engineer. In addition, as a rough estimation, a 6m x 0.6m x 0.3m concrete beam contains approximately 10^{28} atoms (based on atomic spacing of silica). Today's most powerful

supercomputers are able to run molecular dynamics simulations up to several billions (10^9) of particles only [Kadau *et al.* 2006].

1.2. Background

As discussed in the previous section, many researchers have tried to advance the traditional models of continuum mechanics, finite elements and fracture mechanics and reduce their limitations in applying them to quasi-brittle materials. In addition, molecular dynamics is impractical for simulating large-scale structural engineering problems. A more unified, conceptually simple, and general approach which is applicable to quasi-brittle materials is "peridynamics", presented next.

1.2.1. Peridynamics

To overcome the limitations and shortcomings of models based on continuum mechanics and fracture mechanics, Stewart Silling, at Sandia National Laboratories, introduced the concept of peridynamics [Silling 1998]. The term "peridynamic" comes from the Greek words "peri", meaning "near", and "dynamic", meaning "force" [Silling 1998].

Peridynamics, although similar to, is not the same as molecular dynamics. In peridynamics, the material domain is thought of as an infinite number of infinitesimal interacting particles. Particles closer than a particular distance, called the *material horizon*, interact with each other. The interacting forces between particles are calculated through empirical particle interaction relations. Particles move in accordance with Newton's second law.

1.2.2. Molecular dynamics

In molecular dynamics, the forces acting between atoms are assumed to be functions strictly of current particle positions. Peridynamics, on the other hand, uses a *reference configuration* of particles as well as their current positions to calculate interacting forces. In addition, in peridynamics, inter-particle forces may depend upon the history of particle motions.

In molecular dynamics, Newton's laws of motion are integrated to evolve the motion of the particles (atoms) in the system. The general algorithm is that first, particles interact and total forces acting on each particle are computed. Next, by integrating numerically in time, new particle positions are computed. The process is repeated until a desired time period has reached, typically to several nanoseconds. The time series record of the motion of a given atom is called a *trajectory*. Thermodynamic statistics may be extracted from the set of trajectories recording the motion of all the atoms.

Even with the fastest computers, it takes a very long time to run molecular dynamics simulations on a single machine, if it is even possible due to limited per-node memory. Consequently, running simulations on parallel processors is common for molecular dynamics problems. For this purpose, specific algorithms are devised and implemented as parallel codes. In principle, these algorithms are applicable to any multi-particle system including peridynamics as long as particles and the force field are suitably defined. The next section presents an overview of the concept of parallel computing.

1.2.3. Scalable parallel computing

Similar to molecular dynamic systems, peridynamic systems require a large number of interacting particles. Assuming one-inch spacing between particles in a cuboidal grid, more than 300,000 particles are needed to model a typical 3'x2'x30' concrete beam. The large number of particles required in realistic simulations makes peridynamics computationally expensive, although feasible. A considerable amount of research has been conducted to address these high computational requirements. Optimizing methods of calculation, use of specialized hardware and advanced computational approaches are among researchers' efforts. Barney lists the following physical and practical reasons why simply building ever faster serial computers is insufficient to address large-scale problems [Barney 2010]:

- The speed of a serial computer is directly dependent upon the limited speed of data transmission through its hardware.
- The number of transistors that can be placed on a chip is limited by atomic size.
- Using a larger number of commodity processors is less expensive than making a single processor faster with the same (or better) performance.

Parallel algorithms allow researchers to run multi-body simulations on multi-node machines. Parallel algorithms divide a simulation into parts and assign each part to a single processor. Every processor is responsible for a designated part of the problem.

1.3. Objectives of thesis

Early in this research, several peridynamic codes were developed by the author, using FORTRAN 90 and Matlab, to simulate some simple specific problems. Matlab codes were developed to analyze the output data and illustrate the deformed shapes. For example Figure 1.3 depicts a two-dimensional cantilever beam, consisting of 31500 particles, under a uniform vertical load applied at the top of the beam.

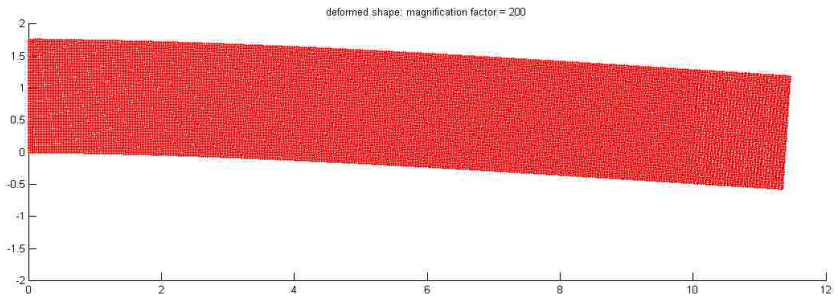

Figure 1.3 – 2D cantilever beam subjected to uniform downward loading

For 0.07 seconds of simulation time, it took two hours to run this problem on an Intel® Dual-Core™ CPU T3400 @ 2.16 MHz laptop computers with 4 GB of RAM. The beam is plain concrete with a simple linear force field. Running real problems with hundreds of thousands or millions of particles and sophisticated peridynamic pairwise force models is unrealistic on such a machine. Parallel machines and parallel algorithms are mandatory to solve real, large-scale problems.

In the course of explaining the possibility of determining a *de novo* general peridynamics simulation code, the author's advisor, Prof. W. Gerstle, encountered a similar effort underway in the UNM Department of Physics and Astronomy (research group of Prof. S. R. Atlas). A previously developed object-oriented parallel molecular dynamics (MD) code, PDQ [Atlas *et al.* 1996, Reynders *et al*. 1996, Atlas 1999], was undergoing a complete redevelopment effort in order to take advantage of the object-oriented and modular benefits of C++ and FORTRAN 90, without the concomitant syntactical and performance issues that can be encountered in these languages. The new version of PDQ would also be designed to accommodate a novel charge-transfer (reactive dynamics) force field developed at the University of New Mexico [Valone and Atlas 2006, Atlas and Valone 2011].

In light of the high-level similarities between peridynamics and molecular dynamics simulations ("particles" interacting via a "force field"), and the need for a fast, parallel code capable of flexible, large-scale computations, it was decided that a collaboration between the two groups would be of mutual benefit. This effort was initiated in the fall of 2009, and included the author, Prof. W. Gerstle, Prof. S. R. Atlas, and a graduate student in Physics and Astronomy, Vijay Janardhanam.

This joint effort culminated in the development of a novel parallel algorithm for particle-based simulations, implemented in a completely re-written version of PDQ. PDQ[1] (parallel dynamics Quantum) is an integrated code which is able to simulate molecular dynamics as well as peridynamics problems. This thesis presents the new parallelization algorithm and its implantation in PDQ. The code is designed to balance generality,

[1] Also, in idiomatic English, "PDQ" means "fast".

flexibility and speed in solving problems and to address complex state-of-the-art research problems difficult to answer before in both peridynamics and in molecular dynamics.

1.4. Scope of thesis

In this thesis, a novel method for parallelization of particle-based molecular dynamics and peridynamics models is introduced. This new method, termed the "wall method", utilizes a spatial decomposition approach together with Plimpton's message passing method [Plimpton 1993]. Implementation of this scheme within PDQ is explained.

This thesis is divided into five chapters: Introduction, Literature Review, Implementation of Wall Method in PDQ, Example Problems, and Conclusions.

Chapter Two is a literature review, divided into three sections. The first section introduces the concept of peridynamics and peridynamic models and covers some recent work on peridynamics. In the second section, algorithms and techniques that are used in developing PDQ are reviewed. The last section reviews existing parallel simulation codes for peridynamics and molecular dynamics.

Chapter Three explains the computational implementation of the novel wall method parallelization algorithm. The resulting scalable parallel code, PDQ, is able to solve molecular dynamics as well as peridynamics problems with millions of particles.

Chapter Four, "Example Problems", contains several peridynamics simulations using PDQ. Several reinforced and prestressed concrete elements are simulated and the results are discussed.

The final chapter reviews the contribution of this thesis to computational science and parallel computing and to the ability to solve important, practical peridynamic problems in civil engineering. Possible improvements in the code in the aspects of speed-up, adding more features and generalizing the code to solve more comprehensive problems, are proposed in the final chapter.

A PDQ user manual for peridynamics is provided as an appendix at the end of this thesis, which explains how to run peridynamic problems using PDQ. Preparation of input files, running the code and post processing the output data are explained.

2. LITERATURE REVIEW

This chapter contains three main sections. In the first section, the theory of peridynamics is explained and compared to continuum mechanics and molecular dynamics. Various peridynamic models are reviewed. The second section is a review of computational algorithms and techniques for parallelization of Newtonian-particle simulations. The third section introduces and evaluates existing codes for molecular dynamic and peridynamics simulations. The final section summarizes the literature review and provides the justification for our current research.

2.1. Peridynamics

Since partial derivatives are used to determine the relative displacement, continuum mechanics fails to correctly predict nucleation and propagation of discontinuities in solid mechanics problems. Although regularization techniques based on continuum mechanics and fracture mechanics received achievements to varying degrees, they do not allow spontaneous discontinuities to occur (Section 1.1).

In 1998, Silling proposed peridynamics [Silling 1998], which is based upon integral rather than differential equations. Because differentiation of the displacement field is not required, peridynamics is well-behaved even if there is a discontinuity in the displacement field. Therefore, unlike in the fracture mechanics [Anderson 2005], there is no need to explicitly model cracks, as they emerge naturally.

To computationally solve peridynamic problems, the model may be discretized as a finite number of interacting particles, although the discretization is not part of the

peridynamic model *per se*. Because the interaction of particles is at a finite distance, peridynamics is a nonlocal model. The interaction distance in peridynamics is called the *material horizon*, which may be considered as a material property.

Figure 2.1 illustrates the peridynamic model, showing relative displacement, relative position vectors and the force vector between a pair of particles.

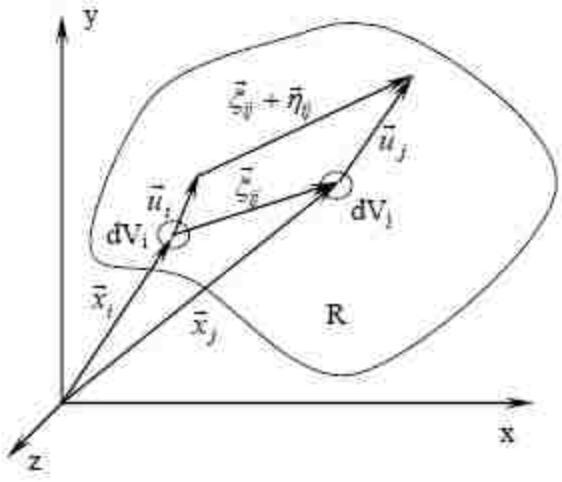

Figure 2.1 – Terminology for peridynamic model

The peridynamic formulation proposed by Silling is defined by the following equation:

$$\vec{L}(\vec{x},t) = \int_R \vec{f}\left(\vec{u}(x',t) - \vec{u}(\vec{x},t), \overrightarrow{x'} - \vec{x}\right) dV_j \qquad \forall x \in R, \qquad 2.1$$

where $\vec{L}$ is the force per unit volume acting on particle volume, dV_i, at location $\vec{x}$, due to interaction with volume dV_j located at $\overrightarrow{x'}$, through a force function $\vec{f}$. $\vec{u}$ is the displacement field and $\vec{x}$ is the reference configuration. The force function f is called the

pairwise force function. Silling uses the following notation for the relative displacement and the relative reference position vectors, respectively:

$$\vec{\eta} = \overrightarrow{u'} - \vec{u}, \quad \vec{\xi} = \overrightarrow{x'} - \vec{x} \tag{2.2}$$

Based on Newton's second law, the peridynamic equation of motion is given by

$$\rho\ddot{\vec{u}} = \overrightarrow{L_u} + \vec{b}, \tag{2.3}$$

where b is the external force density, in units of force per volume.

Silling has shown that classical elasticity problems can be modeled using peridynamics. In addition, the original peridynamic formulation results in material isotropy, in a sufficient distance (material horizon) away from the boundary of the geometric domain [Silling 1998].

Some attempts have been made to improve and generalize peridynamics, as well as to integrate it with other frameworks such as finite elements. Some of these efforts are reviewed in the next sections.

2.1.1. Micropolar peridynamic modeling

In 2005, Gerstle, Sau and Silling extended peridynamics by adding moments and rotation equations to the original peridynamic formulation [Gerstle *et al.* 2005]. The resulting model was called the *micropolar peridynamic model*. In this model pairwise moments, as well as pairwise forces, act between particles (Figure 2.2).

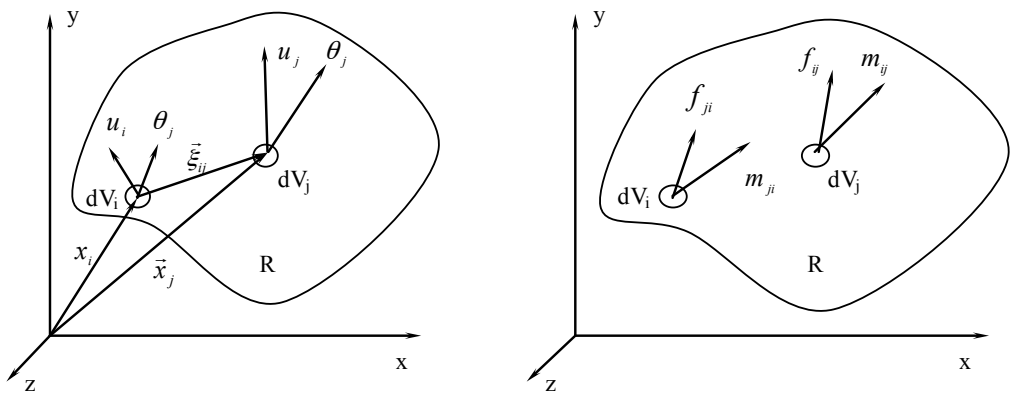

(a) Kinematic Terminology (b) Kinetic Terminology

Figure 2.2 - Terminology for micropolar peridynamic model (from [Gerstle, Sau and Silling 2005])

The micropolar peridynamic model applies Newton's second law of motion for moments and rotations to the peridynamic model:

$$\overrightarrow{dm_\iota}\,\overrightarrow{\ddot{u}_\iota} = \sum d\vec{F}, \qquad 2.4$$

$$\overrightarrow{dI_\iota}\,\overrightarrow{\ddot{\theta}_\iota} = \sum d\vec{M}, \qquad 2.5$$

where $\sum d\vec{F}$ is the force vector and $\sum d\vec{M}$ is the moment vector acting on the free body of an infinitesimal particle. $\overrightarrow{dm_i}$ is the differential mass and $\overrightarrow{dI_i}$ is the differential mass moment of inertia of particle *i*. In the quasi-static case the linear and rotational accelerations are zero.

The micropolar peridynamic model formulation in the quasi-static case yields:

$$\int_R \vec{f}_{ij}\left(\vec{\eta},\vec{\xi},\vec{\theta}\right) dV_j + \vec{b}_i = \vec{0}, \qquad 2.6$$

$$\int_R \vec{m}_{ij}\left(\vec{\eta},\vec{\xi},\vec{\theta}\right) dV_j + \vec{m}_i = \vec{0}, \qquad 2.7$$

where $\vec{\eta}, \vec{\xi}$ and $\vec{\theta}$ are relative displacement, relative position and relative rotation, respectively between particles i and j with volumes dV_i and dV_j. In analogy to $\vec{f}_{ij}$, the pairwise force function, $\vec{m}_{ij}$ is the pairwise moment function between two particles. The pairwise moment function has three components with the units of moment per volume squared. Note that although by Newton's third law, the mutual forces $\vec{f}_{ji}$ and $\vec{f}_{ij}$ are equal, $\vec{m}_{ij}$ is not necessarily equal to $\vec{m}_{ji}$.

Micropolar peridynamic model generalizes peridynamics to cover materials with Poisson's ratios different from 1/4 [Gerstle *et al.* 2005]. The current version of PDQ does not allow for micropolar peridynamics. However, a peridynamic-specific version, which accepts multiple user-defined degrees of freedom, is available. This version of the code can model micropolar peridynamic problems (Section 2.1.1), and is in the process of being integrated with the official PDQ release.

2.1.2. Peridynamic states

Difficulties occur in applying the original (*bond-based*) peridynamic model, proposed by Silling in 1998, to phenomena such as plasticity [Silling 2008]. The original approach oversimplifies the interaction between the particles in the sense that the mutual force between two particles is assumed to be independent of the positions of other nearby particles. For example, bond-based peridynamics is unable to model plasticity [Silling 2008].

In an effort to overcome these difficulties, Silling *et al.* introduced the concept of *peridynamic states* [Silling *et al.* 2007]. In the constitutive model, the deformations and

the forces have *states*. The deformation state is the deformation field within the material horizon of a particle. The *force state* is the collection of all pairwise forces acting on a particle. The constitutive model is the relationship between deformation states and force states. The *state-based* model is a generalization of the *bond-based* model.

Introducing the state-based theory, Silling *et al.* replaced the original peridynamic equation of motion by

$$\rho(x)\ddot{\vec{u}}(x,t) = \int_{H_x}\{\vec{T}(x,t)(x'-x) - \vec{T}(x',t)(x-x')\}dV_{x'} + b(x,t), \qquad 2.8$$

where H_x is spherical region centered at x with the radius of the material horizon. T is the *force vector state* field.

State-based peridynamic modeling is computationally more demanding than the original bond-based peridynamic model. However, the state-based theory seems to be very promising for modeling certain phenomena like plasticity [Silling *et al.* 2007]. PDQ is currently being modified to allow the implementation of the state-based theory.

In 2007, Gerstle *et al.* developed several peridynamic codes using Matlab. They simulated an over-reinforced concrete beam with a rebar at the top. The state-based micropolar peridynamic model used in their simulation is shown in Figure 2.3 [Gerstle *et al.* 2007a, 2007b].

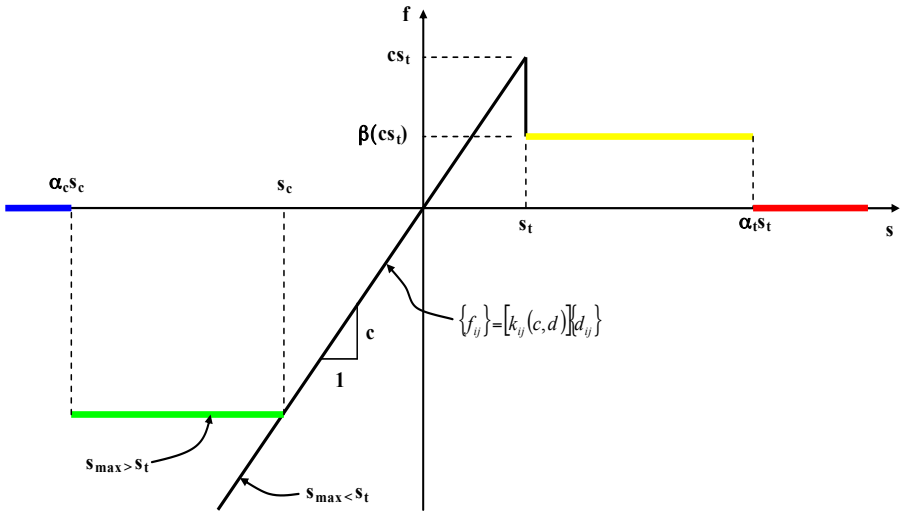

Figure 2.3 - Micropolar constitutive model for concrete (from [Gerstle et al. 2007b])

In this micropolar model, the pairwise force function between a pair of particles depends on the axial stretch, s, of the peridynamic link between those particles as well as on the maximum stretch, s_{max}, of any other peridynamic link connected to either of the particles [Gerstle *et al.* 2007b].

Flexural cracks were observed at the start of failure, followed by shear cracks as shown in Figure 2.4. Nucleation of additional shear cracks and compression failure at the lower left corner of the beam progressed as the simulation continued. The beam was modeled in 2D with 7500 particles subjected to a downward force at the top right corner. Figure 2.4 shows the state of pairwise forces at the end of the simulation: per Figure 2.3, yellow is in tension plateau, red is after complete tension failure, green is in compression plateau and blue is after complete compression failure.

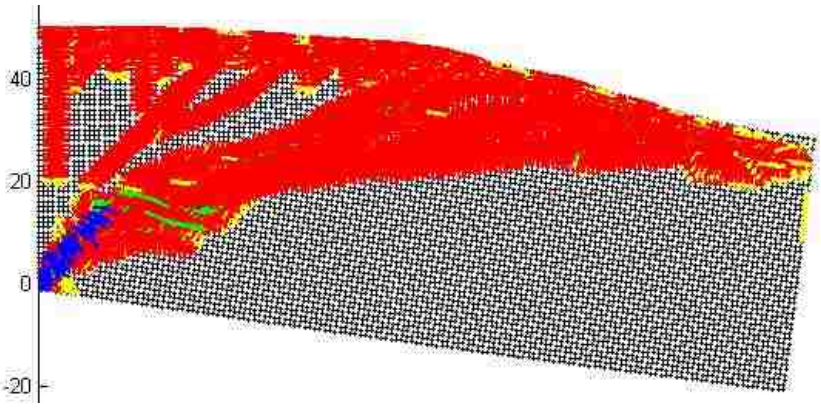

Figure 2.4 - Shear beam at ultimate stage (from [Gerstle, Sau and Aguilera 2007])

As Gerstle *et al.* stated in their paper, it took four hours to solve this problem on a Toshiba Satellite Intel® Core™ 2 CPU T550 @ 1.66 MHz laptop computer with 1.99 GB of RAM.

2.1.3. Implementation of peridynamics within finite element framework

The peridynamic method was implemented in a finite element framework by Gerstle *et al.* in 2007 [Gerstle, Sau and Silling 2007]. The model is initially meshed with finite elements. If, during the simulation, an element approaches the strain-softening regime of the strain-stress curve, the element is replaced with a grid of peridynamic particles as shown in Figure 2.5. This adds more degrees of freedom to the problem at softening locations. Using only peridynamic particles to model the problem adds to the accuracy of the solution. However, this method increases the number of degrees of freedom and consequently the simulation time substantially. The propagation of a crack in a cantilever concrete beam using peridynamic finite element is shown in Figure 2.5.

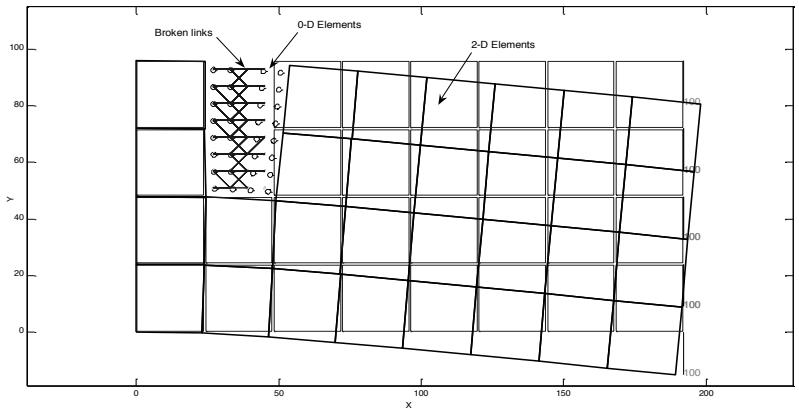

Figure 2.5 – Example of finite element implementation of peridynamic method (from [Gerstle, Sau and Silling 2007])

The size of the finite elements must be large compared to the material horizon. Using finite elements with smaller size than the material horizon produces more degrees of freedom than necessary. Also when the finite element size is approximately the same as the material horizon, it is more reasonable to use individual peridynamic particles.

2.1.4. Multi-physical peridynamics

Multi-physical phenomena are of interest to many engineers. The diverse nature of mechanisms in multi-physical processes adds to the complexity of the problems. Gerstle *et al.* have applied peridynamics to a multi-physical model [Gerstle *et al.* 2008].

In 2008, Gerstle *et al.* published a paper on applying peridynamics to simulate mechanical, thermal, electrical, and atomic diffusion processes which often account for the failure of integrated circuits (electromigration). It was noted that peridynamics

simulation of electromigration simplifies the modeling and can be used to describe the physical behavior of interconnects [Gerstle *et al.* 2008]. Unlike previous simulation techniques, peridynamics provides a unified multi-physical modeling paradigm that allows discontinuities in the material to evolve.

In the peridynamic model for electromigration, the constitutive relations of solid mechanics, heat conduction, electric conduction and atomic diffusion, which normally involve differentiations at a point being replaced by integrations over a finite neighborhood of the point. The conservation equations governing these phenomena are applied at each point.

The multi-physics constitutive model includes fluxes of force, heat energy, electrical charge, and atoms. "Peridynamic kernels" [Gerstle *et al.* 2008] are used to represent the physical constitutive behavior of these processes. Table 2.1 shows the constitutive peridynamic models for electromigration.

	Solid Mechanics	Heat Conduction	Electric Conduction	Atomic Diffusion
Primary Field	Displacement, u_k	Temperature, T	Electrical Potential, Φ	Atomic Concentration, C
Peridynamic Kernel	PD Force, $f_{F,k}$	PD Heat Flux, f_q	PD Current Flux, f_j	PD Atomic Flux, f_J
Constitutive Relation	$f_{F,k} = f_{F,k}(\underline{\xi}_k, \eta_k, \ldots)$	$f_q = f_q(\underline{\xi}_k, \tau, \ldots)$	$f_j = f_j(\underline{\xi}_k, \phi, \ldots)$	$f_J = f_J(\underline{\xi}_k, \chi, \ldots)$
Conservation Equation	$\int_{H_F} f_{F,k}\, dV + b_k = \rho \ddot{u}_k$	$\int_{H_q} f_q dV + \overline{Q} = c_T \rho \dot{T}$	$\int_{H_j} f_j dV + \overline{J} = c_E \dot{\Phi}$	$\int_{H_J} f_J dV + \overline{\mathrm{K}} = c_D \dot{C}$

Definition of symbols (see Table I for previously defined symbols):

$f_{F,k}$ (vector) peridynamic force per unit volume squared
f_q peridynamic heat flow per unit volume squared
f_j peridynamic current flow per unit volume squared
f_J peridynamic concentration flow per unit volume squared
$x_{\alpha,k}$ (vector) position of point α in reference configuration
$\underline{\xi}_{\alpha\beta,k}$ (vector) relative position in reference configuration, $x_{\beta,k} - x_{\alpha,k}$
$u_{\alpha,k}$ (vector) displacement of point α in reference configuration
$\eta_{\alpha\beta,k}$ (vector) displacement difference between points α and β, $u_{\beta,k} - u_{\alpha,k}$
$\tau_{\alpha\beta}$ temperature difference between points α and β, $T_\beta - T_\alpha$
$\phi_{\alpha\beta}$ electric potential difference between points α and β, $\Phi_j - \Phi_i$
$\chi_{\alpha\beta}$ concentration difference between points α and β, $C_\beta - C_\alpha$
H_F, H_q, H_j, H_J peridynamic neighborhoods for various fluxes

Table 2.1 - Peridynamic fluxes, constitutive relations, and conservation equations for modeling electromigration (from [Gerstle et al. 2008])

Such a peridynamic model provides a theoretical framework to simultaneously model many phenomena observed in microchips, including electromigration, thermomechanical crack formation, and fatigue crack formation. In their work, Gerstle *et al.* presented a one-dimensional example problem, solved with the proposed peridynamic model.

The peridynamic model demonstrated satisfactory results and suggested that the peridynamic model has significant promise for the simulation of three-dimensional

problems exhibiting interfacial and cracking behavior [Gerstle *et al.* 2007]. PDQ provides an appropriate framework for solving such computationally-demanding problems.

2.2. Computational algorithms for parallel simulations

As discussed in Section 1.2.3, both peridynamics and molecular dynamics involve particle interactions. Simulating real-life problems requires tracking of millions of particles over a sufficient time period. Parallel computing is necessary for such large simulations. *Atom decomposition*, *force decomposition* and *spatial decomposition* are the principal parallelization methods that have been developed for molecular dynamics simulations. These methods are described next.

In the *atom decomposition* method, an approximately equal number of particles are assigned to each processor, regardless of the particles' positions. To calculate new positions, at each time step, all processors must exchange all particle information. This communication scheme is called *all-to-all communication*. Efficient algorithms implementing this method are described in [Bruck *et al.* 1994].

The *force decomposition* method was introduced by Hendrickson and Plimpton in 1992 [Hendrickson and Plimpton 1992]. In this method, a subset of pairwise forces is assigned to each processor. The forces between two particles might be calculated on a processor to which neither of the interacting particles belongs.

In *spatial decomposition* (also called the *geometric algorithm* [Fincham 1987]), each processor is responsible for a geometric subdomain of the problem. The particles residing on a subdomain are assigned to the associated processor. Some particles interact with neighboring particles on adjacent processors. Therefore, the adjacent processors

must exchange data. Interacting forces between a pair of particles on the same processor are calculated by that processor. If two particles are on different processors, one of the processors assumes responsibility for the force calculation. There is no need to calculate the mutual force, because according to Newton's third law, the interacting forces between a pair of particles have the same magnitude and are in the opposite direction.

The atom and force decomposition methods have the potential to divide computations evenly among the processors. This is called *load balancing*. In these methods, subdivision of computation does not depend upon particle position. The communication bandwidth required in the force decomposition method is global (all-to-all). In contrast, in the spatial decomposition method, the communication scheme is local. That is, the particles are reassigned to new processors if they move to a subdomain which is assigned to another processor, resulting in less time spent on inter-processor communications. In contrast to the atom and force decomposition methods, the communication time in the spatial decomposition method decreases as the range of interaction decreases [Plimpton 1995].

New algorithms, integrating force and spatial decomposition methods, have been recently introduced, showing high scalability and efficient load balancing. More details on these algorithms are provided in this section.

Choosing an algorithm for a molecular dynamics simulation is problem-dependent. Brown and Miagret note that the choice depends on factors such as the average number of particles per processor and the speed of the individual processors. When the number of particles per processor is high, the spatial decomposition algorithm is the most efficient one [Brown and Miagret 1999].

This chapter contains an explanation of several techniques in implementation of parallelization algorithms for molecular dynamics simulations which are provided in the literature. Plimpton's message-passing method is also introduced.

2.2.1. The neighbor list method

In 1967, Verlet suggested a technique for speeding up molecular dynamics simulations [Verlet 1967]. The idea is based on maintaining a list of neighbors for each particle, which facilitates searching for the particles with which each particle interacts. The lists are updated periodically. This method does not affect the force computation time but reduces the time spent in finding interacting particles.

In the original Verlet method, each particle has two surrounding spherical layers. The smaller sphere has a radius corresponding to the material horizon (range of interaction in molecular dynamics) and the larger sphere surrounds it. The thickness of the outer layer, called the "skin", is chosen so that it is guaranteed that nearby particles outside of the skin cannot move within the material horizon of the particle during the neighbor list update interval. The neighbor lists in such algorithms are usually reconstructed every 10-20 time steps [Allen and Tildesley 1987]. Fincham and Ralston proposed a modification for automatic update of the neighbor lists without predefining an interval [Fincham and Ralston 1981]. The total displacement of each particle since the last neighbor list update is monitored. When the displacement exceeds the thickness of the skin, the list is updated.

The neighbor list method is not currently implemented in PDQ. However, its combination with the "multi-cell" method could speed up the code, as explained in the next section.

2.2.2. The multi-cell method

The *multi-cell method* is at the heart of the new algorithm implemented in PDQ. Beazley and Lomdahl used the multi-cell method for their molecular dynamics simulation algorithm [Beazley and Lomdahl 1992]. In this method, similar to other spatial decomposition algorithms, the geometry of the problem is subdivided into cuboids, each of which is assigned to a processor. However, in addition, each cuboid is further subdivided into smaller cuboids, called *cells* [Beazley and Lomdahl 1992]. Using cells in the spatial decomposition makes it possible to locate a particle's neighboring particles more quickly, thus minimizing the time spent finding interacting particles. A cell stores information such as particle positions, velocities, masses, forces and particle types, in data blocks with sequential access capability, which further facilitates inter-processor communication.

Interaction between particles is either *inter-* (between) or *intra-* (within) cellular. First, all the particles within a cell interact and mutual forces are calculated. Next, particles interact with particles in adjacent cells, following the interaction path shown in Figure 2.6 [Melcuk *et al.* 1991]. By choosing the cell dimensions to be somewhat greater than the material horizon, interaction of particles within the material horizon is guaranteed. Taking advantage of Newton's third law, the number of necessary interaction paths is reduced from all adjacent cells to those shown in Figure 2.6.

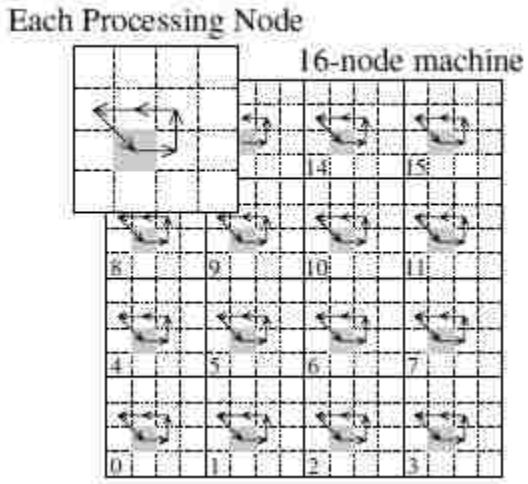

Figure 2.6 - Interaction path in multi-cell method in 2D, The gray colored cell interacts with adjacent cells following the path shown [Beazley and Lomdahl 1992], In this example, each node of the parallel machine has a single processor only

Cells lying adjacent to the boundary of processors may need to interact with cells on adjacent processors, necessitating communication between processors. In the Beazley and Lomdahl algorithm, whenever a cell needs to interact with a cell on an adjacent processor, the information required for that cell is sent and received immediately. This method of communication makes the total number of exchanged messages, in each time step, problem-dependent, because the number of the cells depends on the geometry of the problem as well as the total number of processors and the range of interaction [Beazley and Lomdahl 1992].

The multi-cell method could be combined with the Verlet neighbor list method for faster determination of interacting particles. In this method, particles interact only with

the particles in their neighbor lists. The cells help to construct the neighbor lists faster without looping over all the particles. The algorithm checks particles located only in the home cell and adjacent cells to maintain the neighbor list.

2.2.3. The midpoint method

In 2006, Dr. D. E. Shaw's research group introduced the midpoint method which is a combination of the spatial and the force decomposition algorithms (Section 2.2) [Bowers *et al.* 2006]. The midpoint method algorithm is a member of the class of "neutral territory" methods. Unlike traditional spatial decomposition methods, in neutral territory methods, the mutual force calculation between two particles might take place on a processor upon which neither particle resides [Bowers *et al.* 2006].

In the simple case of calculating pairwise forces between two particles, the processor, associated with the region containing the midpoint of the line connecting the two particles assumes responsibility for calculating the pairwise force (Figure 2.7). Nonetheless, like other spatial decomposition methods, each processor is responsible for maintaining and updating properties of particles it contains. As shown in Figure 2.7, the pairwise force between particles might be calculated on a processor upon which neither of the particles resides. For example the force between particle 2 and 5 is calculated in processor e.

Force calculation involving more than two particles takes place on the processor which contains the center of the smallest sphere containing all the particles [Bowers *et al.* 2006].

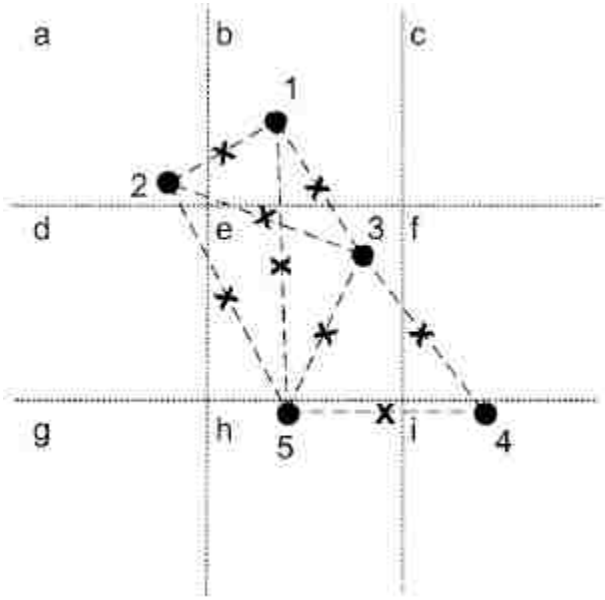

Figure 2.7 - Particles distributed in 3x3 processors [Bowers et al. 2006]

Bowers *et al.* have noted several advantages for this method over traditional spatial decomposition methods as well as other neutral territory methods [Bowers *et al.* 2006]. This midpoint method decreases required communication bandwidth by distributing the communication load over the network that links the processors. The amount of data in each direction of the network links (sending or receiving) are balanced more effectively using this method. Finally, they argue that it is the best choice for simulations involving both *bonded* (covalent) forces as well as *non-bonded* forces, involving three or more particles. Therefore, it is preferable to other spatial decomposition methods for biomolecular force fields, where covalent bond structures of molecules (bonded forces) as well as electrostatic and pairwise van der Waals interactions (non-bonded forces) contribute to the total force on a particle.

A problem that inevitably occurs when using spatial decomposition for a system that includes enforced molecular connectivity (intermolecular bonds between atoms) is that atoms of a particular molecule may be distributed over several processors [Brown and Miagret 1999].

2.2.4. Plimpton's method of processor communication

Parallelization of particle-based simulations requires communication between processors. Information necessary to calculate forces between particles on different processors is exchanged. This information is exchanged as a data package called a *message*. Communication between processors is called *message passing*.

In the spatial decomposition algorithm, message passing occurs between cuboids. Each cuboid requires access to information on adjacent cuboids. The simplest way is for each cuboid to ask directly for the necessary information from its adjacent cuboids as the need arises. In this case, each cuboid needs to communicate with twenty-six adjacent cuboids. Thus, in each time step, twenty-six received messages are required by each processor.

In 1993, Plimpton introduced a novel message-passing scheme for the spatial decomposition algorithm which reduces the required number of messages to six [Plimpton 1993]. Figure 2.8 illustrates Plimpton's method of message passing. The first step involves each processor pairing up with its East and West processors [Plimpton 1993]. For example, processor 2, as shown in Figure 2.8a, packs the necessary information in an appropriate data structure and sends it to the West processor (processor 1). Simultaneously, it receives a pack of data from East (processor 3). The received

information is stored on processor 2. Then the process is repeated in the West to East direction, *i.e.*, processor 2 sends a message to processor 3 and receives a message from processor 1. The second step involves pairing up in the North/South direction. The difference is that the messages exchanged in this step contain the information from the source processor itself, as well as the information received from its East and West processors in the previous step (processors 1 and 3). Finally, processors communicate in the Up/Down direction, sending and receiving the information of the plane, as shown in Figure 2.8c. In each step of Figure 2.8, the message sent by processor 2 is dark-colored. In a similar procedure, processor 2 and all other processors receive information from their respective twenty-six adjacent processors using the six message exchanges [Plimpton 1993].

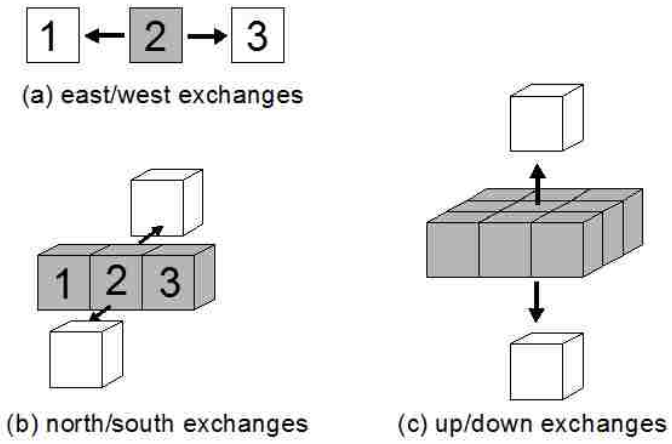

Figure 2.8 - Plimpton's method of message passing [Plimpton 1993]

Reducing the number of messages reduces *communication latency*. Communication latency is a fixed time interval required for passing a message which is

overhead (start-up time for preparing to send the message) and is independent of the size of the message.

PDQ benefits from Plimpton's method of message passing combined with the concept of "walls", as described in Section 3.5.

2.2.5. Zonal methods

Recently several MD research groups have modified their codes to utilize a *zonal methods* parallelization approach (Section 2.3). Zonal methods have been described in detail in recent papers, reviewed in [Bowers *et al.* 2006]. This class of parallelization algorithms integrates traditional spatial decomposition methods with a force decomposition method. Zonal methods rely on specific regions of space called *zones*. At each time step, each processor imports (receives) specific zones (regions) from the processors which are responsible for an adjacent physical subdomain of the global domain. Following the forces calculation, these regions are exported to those adjacent processors, *i.e.* the calculated mutual forces are sent back to adjacent processors. In fact, zones comprise the messages that are exchanged between processors. The goal of zonal methods is to reduce communication time, to avoid redundant force calculations, and to optimize scaling with respect to the number of processors for biophysical systems with hundreds of thousands of atoms and range-limited force fields [Bowers *et al.* 2007].

2.3. Existing parallel codes for MD and PD

Several parallel codes have been developed for molecular dynamics and peridynamics simulations: SpaSM, LAMMPS, GROMACS, Desmond, NAMD, and

EMU. Each of these parallel codes has been developed to solve a specific class of problems. Among these codes, EMU is the only specifically developed to solve peridynamics problems. LAMMPS was primarily developed for molecular dynamics simulations. However, in 2008, Parks *et al.* modified the code to implement peridynamics [Parks *et al.* 2008]. This section reviews some of existing scalable parallel molecular dynamics and peridynamics codes.

2.3.1. SPaSM

In the early 1990s, SPaSM (Scalable Parallel Short-range Molecular dynamics) was developed at Los Alamos National Laboratory [Beazley and Lomdahl 1994]. It was first implemented for the Thinking Machines CM-5 using the multi-cell spatial decomposition method, explained in Section 2.2.1. SPaSM was primarily developed for large-scale materials science and physics simulations of many particles. In 2006, SpaSM was ported to the BlueGene/L supercomputer which consists of 65,536 nodes, each with two IBM PowerPC 440 processors (at 700 MHz clock speeds) and 512 MB of memory [Kadau *et al.* 2006]. Solving benchmark problems with billions of particles, SpaSM showed excellent scaling properties, both in terms of problem size and parallel efficiency. The BlueGene/L architecture was used to simulate a molecular dynamics problem with 320 billion particles. However, each time step of the run required 20 seconds of real time; thus it remains unrealistic to model problems of this size on a real-time basis.

2.3.2. LAMMPS

In the mid-1990s, a cooperative research group from Sandia National Laboratories, Los Alamos National Laboratory and three companies (Cray, Bristol Myers Squibb, and Dupont) began to develop a large-scale parallel classical MD code [LAMMPS 2011]. The coding effort was led by Dr. Steve Plimpton at Sandia National Laboratories. LAMMPS was first coded in FORTRAN 77 and later converted to FORTRAN 90. The current version of LAMMPS is written in C++ and contains many new features and capabilities. The developers rewrote LAMMPS in C++ to make it object-oriented and modular. Nonetheless, writing the code in C++ instead of FORTRAN makes the code intuitively less extensible and makes the physics harder to read.

The spatial decomposition method is used for parallelization of the code. According to its website, LAMMPS supports simulations of a wide range of particle types and models such as atoms, coarse-grained particles (e.g. bead-spring polymers), united-atom polymers or organic molecules, all-atom polymers, organic molecules, proteins, DNA, metals, granular materials, coarse-grained mesoscale models, extended spherical and ellipsoidal particles, point dipolar particles, rigid collections of particles and hybrid combinations of these. In addition, LAMMPS provides various options for molecular dynamics force fields, ensembles, constraints, boundary conditions and different integrator methods. LAMMPS has been extended to address peridynamics simulations [Parks *et al.* 2008]; however, the peridynamics support is at a very early stage. LAMMPS is an open source code.

2.3.3. GROMACS

The GROMACS (GROningen MAchine for Chemical Simulations) package is developed at the University of Groningen in the Netherlands. It is primarily designed for molecular dynamics simulations of biomolecules such as proteins, lipids, and nucleic acids [Lindahl *et al.* 2001]. GROMACS was a re-write and re-development in the C language of another code developed by the same group in FORTRAN 77. GROMACS was intended to be faster than any existing code for simulating biomolecular systems, including NAMD and Desmond [Lindahl *et al.* 2001]. However, GROMACS is biased to gain maximal performance on smaller numbers of processors rather than a supercomputer. This is in contrast to interests of the developers of PDQ, which are to be able to simulate with good efficiency systems ranging from 100,000 biomolecule problems to millions of atoms or volume elements, and will be scalable to thousands of processors if required by the problem.

The GROMACS code utilizes the spatial decomposition algorithm with MPI. Efforts are ongoing to keep GROMACS updated with state-of-the-art computational algorithms. In 2007, a paper was published on upgrading GROMACS using the zonal method [Hess *et al.* 2008].

2.3.4. Desmond

Desmond is a molecular dynamics package originally designed for improved parallel scalability on commodity clusters [Bowers *et al.* 2006]. Commodity clusters are off-the-shelf parallel machines which have not been customized for any particular application. The code was primarily developed for simulation of a single very long

molecular trajectory for a biomolecular system with tens or hundreds of thousands of atoms [Bowers *et al.* 2006]. It is therefore not expected to be able to scale to billions of particles like SpaSM, which utilizes an underlying cell structure, also used in PDQ. Desmond implements an integrated force decomposition and spatial decomposition algorithm, which is based on the careful construction of tailored import regions for buffering inter-processor communication.

2.3.5. NAMD

Similar to Desmond and GROMACS, NAMD is a parallel molecular dynamics code designed for biophysical simulations. It is written in C++ and specialized to the biophysical domain, which does not support simulations with millions or billions of independent particles as required for atomistic material or peridynamics simulations.

2.3.6. EMU

EMU was developed by Dr. Stewart Silling at Sandia National Laboratories [http://www.sandia.gov/emu/emu.htm]. It was the first code which was designed specifically to implement the peridynamic theory of solid mechanics. The code was primarily written to solve pure dynamics problems involving impact, failure due to fracture etc. EMU was designed as a research code rather than for broad production use, although a user manual is provided [Silling, personal communication, 2011]. It is unable to accept externally-applied forces and peridynamic force models are limited. In EMU, problem parameters are defined by editing an input file and a graphical interface is included to help visualize the results.

The author used EMU prior to collaborating on the development of PDQ. Gerstle, Sakhavand and Chapman simulated a lap splice problem using EMU [Gerstle *et al.* 2010]. The same problem was simulated again using PDQ, and the results are discussed and compared in Chapter Five.

EMU shows promising results for certain simulated problems. However, the code supports a limited set of geometries, and the pairwise force and stretch relationship is limited to few built-in force fields. These limitations motivated the development of a general, parallel peridynamics capability through the collaboration on PDQ.

2.4. Summary

Several existing molecular dynamics and peridynamics codes have been reviewed in this chapter. Most have limitations ranging from a fixed selection of built-in force fields to limitations on defining different materials. LAMMPS is probably the only code which allows the user to use his/her own physical equations. Flexibility in addressing multi-physical phenomena and the ability to develop user-defined physical equations were of utmost importance in motivating the PDQ project. All reviewed codes other than LAMMPS are designed to address certain set of problems such as simulation of materials, biomolecules, etc. These codes lack the flexibility in supporting both *atomistic molecular dynamics* simulations, as well as *peridynamics* simulations of structural materials.

On the peridynamic side, a key motivation of the presented work was the desire to solve problems such as the prestressed concrete beam and the need for significant flexibility in defining and solving increasingly complex civil engineering problems. On

the MD side, the goal was to develop and implement advanced reactive charge transfer force fields in a flexible development environment for application to both biophysical and material systems.

PDQ is straightforward to understand, is general and extensible, and also provides enough flexibility for the user to easily define his/her own physical problems without having to be concerned about the parallelization aspects. In PDQ, the parallel compute engine is clearly separated from the engineering and physics equations as well as the input and outputs to give the user the flexibility to define his/her own pre- and post-processing modules. A new user does not have to have any knowledge of the specifics of MPI (message passing interface) or parallel computing in order to adapt and modify PDQ to suit his/her problem-specific needs.

The new parallelization algorithm, which is the heart of PDQ, is described in this thesis. The *wall method* algorithm benefits from some of the features explained in this chapter such as the multi-cell method of SpaSM and Plimpton's method of message-passing. The wall method algorithm and its implementation in PDQ are explained in the next chapter.

3. IMPLEMENTATION OF WALL METHOD IN PDQ

Similar to most parallel particle-based codes, PDQ uses a spatial decomposition method. The inter-processor communication scheme in PDQ uses Plimpton's message-passing approach which was introduced in Section 2.2.4. To reduce the number of required messages and their latency overhead, the concept of walls is described in Section 3.5. The philosophy is to decompose the geometry of the problem between the processors while hiding the parallelization from the user. This approach and the resulting high-level design of PDQ was based on the *vernet* electronic structure, a code previously developed at UNM [Atlas *et al.* 1998-2011].

In the peridynamic mode of PDQ, currently two files containing computer coding for the force field and the integration method are exposed to the user. The user can revise these files on his/her discretion and according to the specifics of the problem. Some examples of these files can be found in the peridynamics user manual for PDQ (Appendix A).

User access to these files provides considerable flexibility for the code, enabling it to be customized to virtually solve any particle dynamics problem in PD and MD. For instance, incorporation of multiple peridynamic materials can be accomplished through appropriate coding in the force and integration files. The prestressed concrete beam is an interesting example which contains concrete, reinforcing bars and prestressed bars.

This chapter explains the wall message passing method as well as its implementation in PDQ.

3.1. Mapping between `procCubes` and processors (processor layout)

In PDQ, the global geometric domain is assumed to be a cuboid which is subdivided into cuboids called `procCubes` (Figure 3.1).

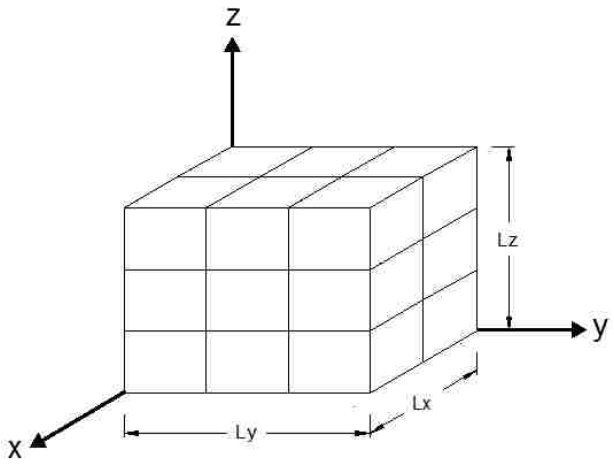

Figure 3.1 - Global physical domain subdivided into 2 x 3x3 = 18 `procCubes`

A `procCube` need not have sides of equal dimensions. Dividing the dimensions of the global domain (L_x, L_y and L_z in Figure 3.1) in the x, y, z directions by the number of processors in each direction (N_x, N_y and N_z), respectively, uniquely defines the `procCube` dimensions in each direction. Processor dimensions are computed in the subroutine `ComputeDerivedParams`.

The wall method incorporates the multi-cell method introduced in Section 2.2.2, and utilizes Plimpton's message passing method (Section 2.2.4) for its communication scheme. The concept of walls, discussed in Section 3.5, is used to minimize the number of passed messages.

PDQ utilizes the open source Message Passing Interface (MPI) [Pacheco 1998] to implement inter-processor communication. For this purpose, MPI assigns an integer

number to each processor whose value varies from zero to the total number of processors minus one ($N_x*N_y*N_z-1$). Each processor is recognized by this MPI-assigned processor ID at runtime, which provides a handle for addressing the each processor.

PDQ divides the geometry of the problem into `procCubes` and assigns each `procCube` to a specific processor. There is a one-to-one relationship between processors and `procCubes`. A `procCube` thus embodies a geometric as well as computational subdomain of the problem.

To link the processors with their `procCubes`, the `procCubes` must be identified in the physical domain. A three-dimensional topological coordinate system is used to identify each `procCube`. In this system, the ξ, η and ζ axes are respectively associated with the x, y and z axes in the Cartesian coordinate system. The coordinates of `procCubes` in the ξ, η and ζ directions vary from zero to the number of processors in that direction, minus one (N_x-1, N_y-1, N_z-1).

An example of a global physical domain with eighteen `procCubes` is shown in Figure 3.2. Each `procCube` in the three-dimensional coordinate system is identified by three IDs. In this particular example, the first ID is the ξ coordinate which varies from zero to one, the second ID, the η coordinate, varies from zero to two and the third ID, representing the ζ coordinate, also varies from zero to two.

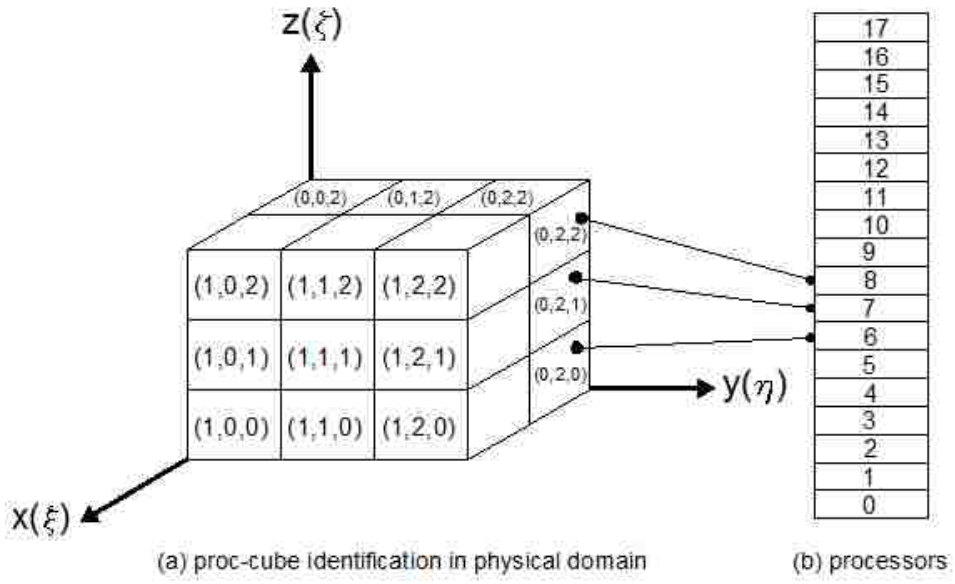

Figure 3.2 - Processors and associated `procCubes`*. Processors 6, 7, and 8 are connected to their associated* `procCubes` *as examples*

To associate processors and `procCubes`, a function was written which provides a mapping between the two coordinate systems.

In the PDQ subroutine `ProcLayout`, two mapping functions between the coordinate systems are constructed. The first function prepares a mapping from the MPI-defined one-dimensional coordinate system to the three-dimensional topological coordinate system. Following Equation 3.1, the MPI-assigned ID of a processor is accessed, given the three `procCube` IDs (i, j, k).

$$PMap3Dto1D(i,j,k) = i * Nz * Ny + j * Nz + k, \qquad 3.1$$

where i, j, k are the three integer IDs in the 3D coordinate system, and N_y and N_z are the total number of processors in the y and z directions, respectively. The MPI processor ID values are stored in the matrix `PMap3Dto1D`.

The second mapping in the subroutine `ProcLayout` helps find the `procCube` IDs (i, j, k) if the processor ID is provided. This is the inverse of the first mapping. The three coordinate values (i, j, k) of each `procCube` are kept in the lookup table `PMap1Dto3D`.

3.1.1. Identification of adjacent processors

Each `procCube` must communicate with its adjacent `procCubes`. Subroutine `ProcLayout` determines the adjacent `procCubes` of each `procCube`. Each `procCube` in the global physical domain at most has 26 adjacent `procCubes` (6 sharing faces, 12 sharing edges and 8 sharing vertices). However, because Plimpton's message passing method (Section 2.2.4) is used in PDQ, only 6 `procCubes`, which share faces, must be recognized by the home `procCube`. In PDQ, positive and negative ξ, η and ζ directions are associated with South, North, East, West, Up and Down directions, respectively, as shown in Figure 3.3.

If the home `procCube` is identified in the ξ, η, ζ coordinate system as (i, j, k), the required neighboring faces will be as follows:

North `procCube`	=	$(i-1, j, k)$	corresponding to $-\xi$ direction
South `procCube`	=	$(i+1, j, k)$	corresponding to $+\xi$ direction
East `procCube`	=	$(i, j+1, k)$	corresponding to $+\eta$ direction
West `procCube`	=	$(i, j-1, k)$	corresponding to $-\eta$ direction
Up `procCube`	=	$(i, j, k+1)$	corresponding to $+\zeta$ direction
Down `procCube`	=	$(i, j, k-1)$	corresponding to $-\zeta$ direction

These adjacent `procCubes` are computed and saved for each `procCube` at the start of a run. During a simulation, each `procCube` has access to the processor IDs of its six adjacent `procCubes` using the `PMap3Dto1D` array. Figure 3.3 shows the processors and their IDs for the example previously illustrated in Figure 3.2. As an example, processor 17 saves six of its adjacent processors as follows:

North processor	=	8
South processor	=	no processor exists
East processor	=	no processor exists
West processor	=	14
Up processor	=	no processor exists
Down processor	=	16

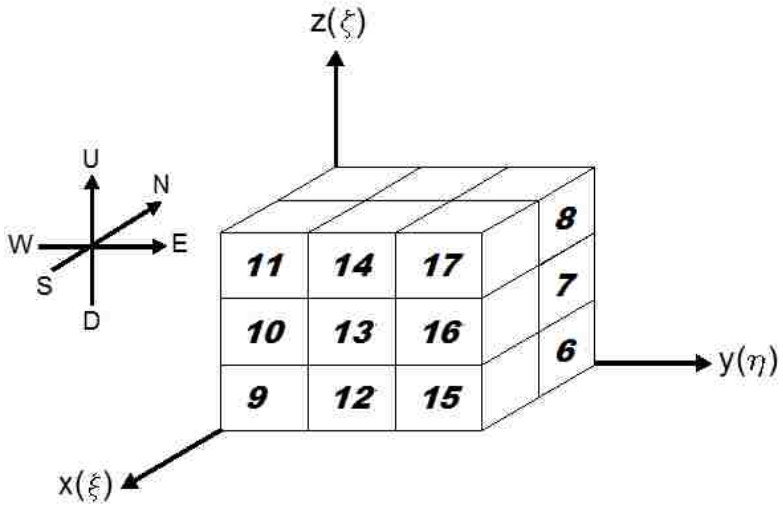

Figure 3.3 - Interchangeable coordinate systems

3.1.2. Periodic boundary conditions (PBC)

In most peridynamic problems, particularly those in which civil engineers are interested, there are boundaries for the geometry of the problem. In accordance with the domain decomposition of such problems, processors on the domain boundary will not have adjacent processors, as shown in Figure 3.3. In PDQ, when a processor lacks an

adjacent processor, the ID of the adjacent processor is assigned the value -1. Some problems (mostly in molecular dynamics) are better simulated with periodic boundary conditions (PBC) [Allen *et al.* 1987]. With PBC, it is assumed that the global domain is replicated through the space in all the directions. Therefore, when a `procCube` lies on the boundary of the global domain, it is surrounded by adjacent `procCubes` in all directions.

Replication of the example domain of Figure 3.3 in the *y-z* plane is depicted in Figure 3.4. The hatched `procCubes` act as virtual neighbors of the `procCubes` on the boundary of the real global domain. As an example in Figure 3.4, processor 17 will have all its 6 neighbors as follows:

North processor	=	8
South processor	=	8
East processor	=	11
West processor	=	14
Up processor	=	15
Down processor	=	16

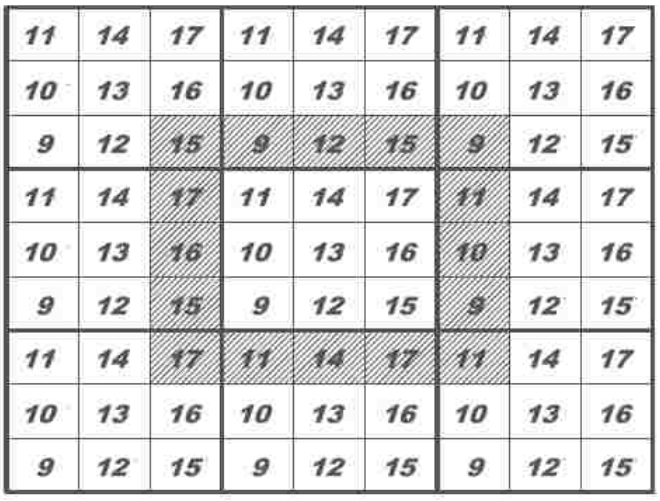

Figure 3.4 - Periodic boundary condition in 2D

After execution of subroutine `ProcLayout` in PDQ, each processor knows its own IDs in both the 3D and the 1D coordinate systems and also knows its West, East, South, North, Up and Down processors in either the PBC or non-PBC scheme.

3.2. Identification and mapping of cells (cell layout)

In a further level of decomposition in PDQ, each `procCube` is subdivided into cuboids called *cells*. This is analogous to what is done in SpaSM. The function of the cell is to facilitate keeping track of neighboring particles. As mentioned in Section 2.2.2, the cell dimension must be slightly larger than the material horizon to guarantee that particles interact only with particles in their containing or adjacent cells.

The cell dimension in each direction is also governed by the `procCube` dimension in the same direction. The product of the cell dimension and the number of the cells in a given direction must be exactly equal to the `procCube` dimension in that direction.

In the subroutine `CellLayout`, each `procCube` is partitioned into cells. Similar as with the `procCubes`, the cells are identified by two sets of IDs: an integer number for the 1D coordinate system and three integers for the 3D coordinate system.

Mapping mechanisms, similar to those in the subroutine `ProcLayout` are provided in the subroutine `CellLayout`. The only difference is that in the 1D coordinate system for cell layout, the cell IDs start from one and continue to the total number of cells in the home `procCube`. Such numbering prevents a cell with zero ID, facilitating array indexing in the code. Note that zero cell IDs are avoided only in the 1D cell coordinate system.

Figure 3.5 illustrates an example `procCube`. In this figure, the cells are shown with their ξ, η and ζ coordinates and their corresponding single IDs in a larger font. The numbering pattern is exactly the same as in `procCube` layout except for the above-mentioned difference. In this example, each `procCube` has five, four and three cells in x, y and z directions, respectively.

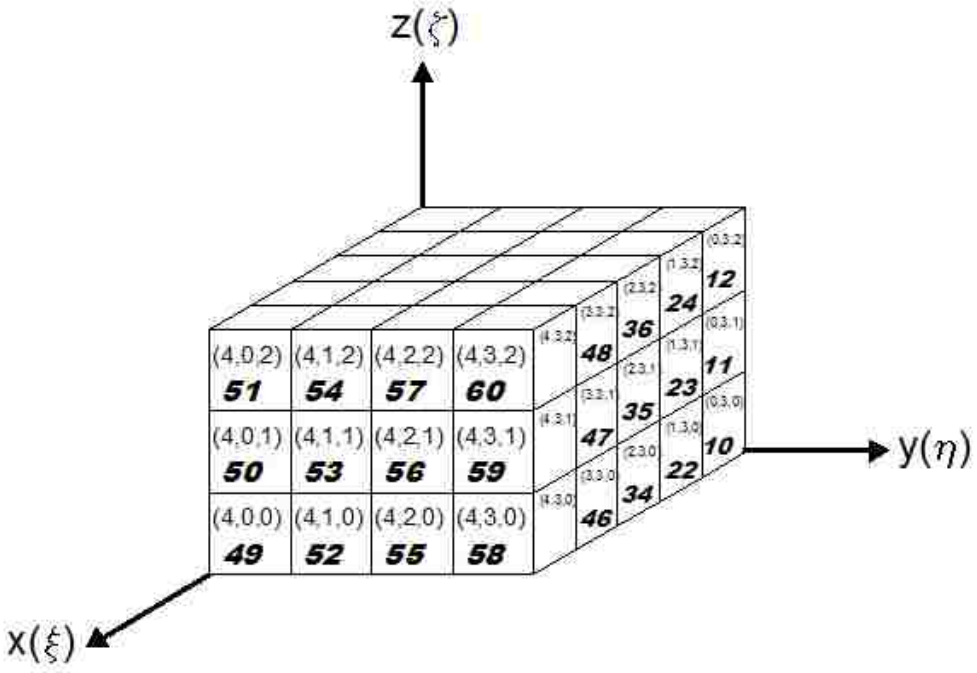

Figure 3.5 – A `procCube` and its cells. Cells are indexed from 1 to 60 in the 1D coordinate system

3.3. Particle allocation to processors

All the particles lie on the global domain which is subdivided into `procCubes`. Particles are allocated to the `procCubes` in the subroutine `SetupProblem`. Before

calculating acting forces, each `procCube` has a copy of the attributes of all the particles in the global domain. Each `procCube` independently identifies the particles it contains based on particle positions.

According to a particle's x, y and z positions in the global domain, three IDs are determined for each particle. These IDs are similar to `procCube` IDs in the 3D Cartesian coordinate system (ξ, η, ζ) of `procCubes`, although in this step, they are defined for the particles not `procCubes`. Similar to `procCube` IDs in the 3D coordinate system, their values vary from zero to the total number of processors in that direction minus one (N_x-1, N_y-1, N_z-1). Using `PMap3Dto1D` lookup array, defined in the section on processor layout (Section 3.2), the appropriate ID in the 1D coordinate system is defined for each particle.

The processor compares the computed particle ID in the 1D coordinate system with its own processor ID. If these IDs match, the particle belongs to that `procCube` and particle information, including position, velocity, mass, material type, reference position, etc. is copied from the global arrays into the corresponding local `procCube` arrays.

When reading particle information from the input files, each particle is assigned a unique global ID which remains unchanged during the simulation. The global particle IDs start from one and increase sequentially to the total number of particles. The purpose of the global IDs is to keep track of particles in the global domain. The global particle IDs are accessible within all the subroutines and should not be confused with the computed particle IDs calculated when allocating particles to `procCubes`.

Particles residing of a `procCube` are also assigned a local ID which remains unchanged while the particle stays on that `procCube`. These local IDs facilitate access to particle atttributes in the local arrays and help to keep track of particles in the local

domain of a procCube. If a particle leaves a procCube and enters a new procCube, a new local ID is assigned to it by the new home procCube.

After each processor executes the SetupProblem subroutine, the procCubes know their contained particles and have their particle attributes in local arrays.

3.4. Particle allocation to cells (Linked List and Head arrays)

As discussed in the previous section, particles are identified in their home procCube by their assigned local ID. Each procCube stores the particle local IDs in two arrays: the Linked List array and the Head array. These arrays allow each particle to recognize its cell. The Linked List and Head arrays are used to access necessary particles and their attributes during particle interactions.

The Head array acts as the door to other particles inside each cell. The size of this one-dimensional array is equal to the total number of the cells within a procCube. The first element of the Head array is the local ID of an arbitrary particle on the first cell. The second element contains the local ID of a particle in the second cell and similarly each element of the Head array addresses to one arbitrary particle in the associated cell.

The particle local IDs from the Head array are used in the Linked List array to access other particles in a particular cell. Each element of the Head array points to an element in the Linked List array, which on one hand, is the particle local ID of the next particle and on the other hand, points to the next element in the Linked List array.

Figure 3.6 shows the first and second cells in a sample `procCube` with their particles and their local IDs. The corresponding `Linked List` and `Head` arrays of that `procCube` are also shown in the figure.

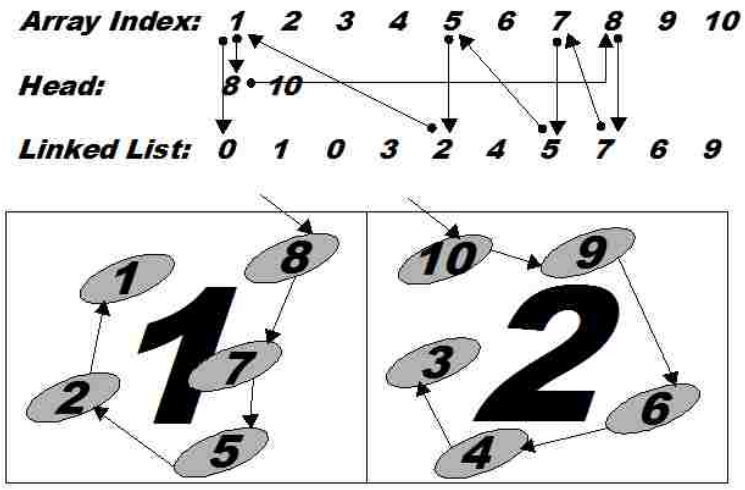

Figure 3.6 - Cells 1 and 2, `Linked List` and `Head` Arrays (Adapted from [Allen and Tildesley 1987])

The code starts from the 1st element of the `Head` array. The value of 8 in the first element, points to the particle 8 (local ID). Also it directs the code to find the next particle of cell 1, in the 8th element of the `Linked List` array which is 7. Again, 7 is the local ID of the next particle and points to 7th element of the `Linked List` which is 5. The procedure will go on until the 2nd element of the `Linked List` points to the 1st element which is zero. Zero value indicates that all the particles in that cell are processed. The code will move on to the 2nd element of the `Head`. The procedure continues until all the cells of a `procCube` are processed.

3.5. Interaction paths

Each particle potentially interacts with particles within all the cells adjacent to its home cell. Each cell in each `procCube` knows where to look for its neighboring cells. In other words, each cell knows which cells it interacts with. Each adjacent cell that a particular cell needs to interact with is on the "interaction path" of that specific cell. Subroutine `DefineInteractPath` defines the interaction path for each cell.

The same as with `procCubes`, each cell has at most 26 adjacent cells. However, due to Newton's third law, the interacting force between a pair of particles can be calculated one time because the mutual force has the same magnitude but is in the opposite direction; therefore, only one-half of the neighboring cells need be included in the interaction path. Figure 3.7 shows the 13 neighboring cells on the interaction path of the dark colored cell. The figure illustrates two planes of the example `procCube` of Figure 3.5 separately. The illustrated pattern is analogous to the 2D interaction path introduced in Section 2.2.2, now in three-dimensions. This interaction path following the displayed orientation of the axes and numbering is arbitrarily defined and used in PDQ.

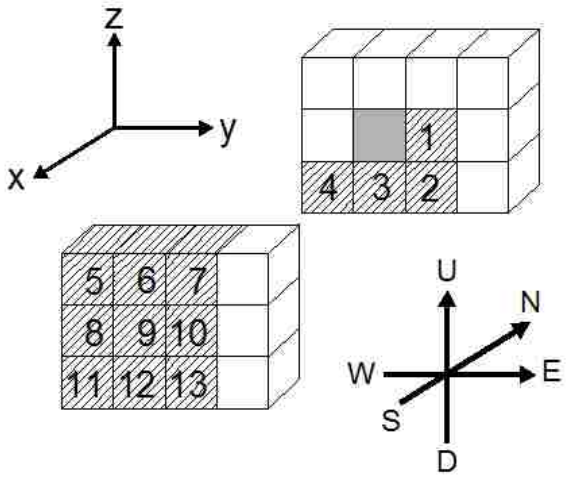

Figure 3.7 - Cells and their interaction paths

It is appropriate here to mention that the interaction paths of the cells located on the boundary of the global domain have less than 13 cells. With PBC, all the cells, no matter where they are located, have exactly 13 cells in their interaction paths.

Three steps are taken in `DefineInteractPath` to determine the interaction paths. In the first step, six IDs are defined for each neighboring cell on the interaction path of each cell. The first three IDs are the ξ, η and ζ coordinates of the adjacent cell with which the home cell interacts. These coordinates are computed with the facilities developed in cell layout (Section 3.2) and they help locating the adjacent cells on their home `procCube`. To identify on which `procCube` each adjacent cell resides, the ξ, η, and ζ coordinates of each adjacent cell's home `procCube` are also saved which constitutes the second stored set of IDs.

Cells located on the boundary of a `procCube` may have an interaction path with cells on adjacent `procCubes`. A cell located on an adjacent `procCube` will be on its boundary plane. A plane of cells, one cell deep, located on the boundary of a `procCube`, is called a *wall*. According to their locations within the home `procCube`, these walls are named the North, South, East, West, Up and Down walls. The boundary cells find their adjacent cells on foreign processors through these walls. Walls are components of the messages exchanged between adjacent `procCubes`. How the walls help to create the messages is explained in detail in Section 3.6.

A wall has its own local geometric domain. Therefore, cells of a wall have coordinates local to the domain of their home wall as well as that of the home `procCube`. The ξ, η and ζ coordinates of the adjacent cells, defined in the first step, are local to their containing `procCube` coordinate system. In the second step of defining interaction paths,

if an adjacent cell is on an adjacent `procCube`, its ξ, η and ζ coordinates are found in the local domain of its home wall. Next, using the mapping mechanism introduced in cell layout, ξ, η and ζ cell coordinates either local to the wall domain or to the `procCube` domain, are mapped to cell IDs in the one-dimensional coordinate system. An illustration of a sample `procCube` and its walls in different directions is shown in Figure 3.8.

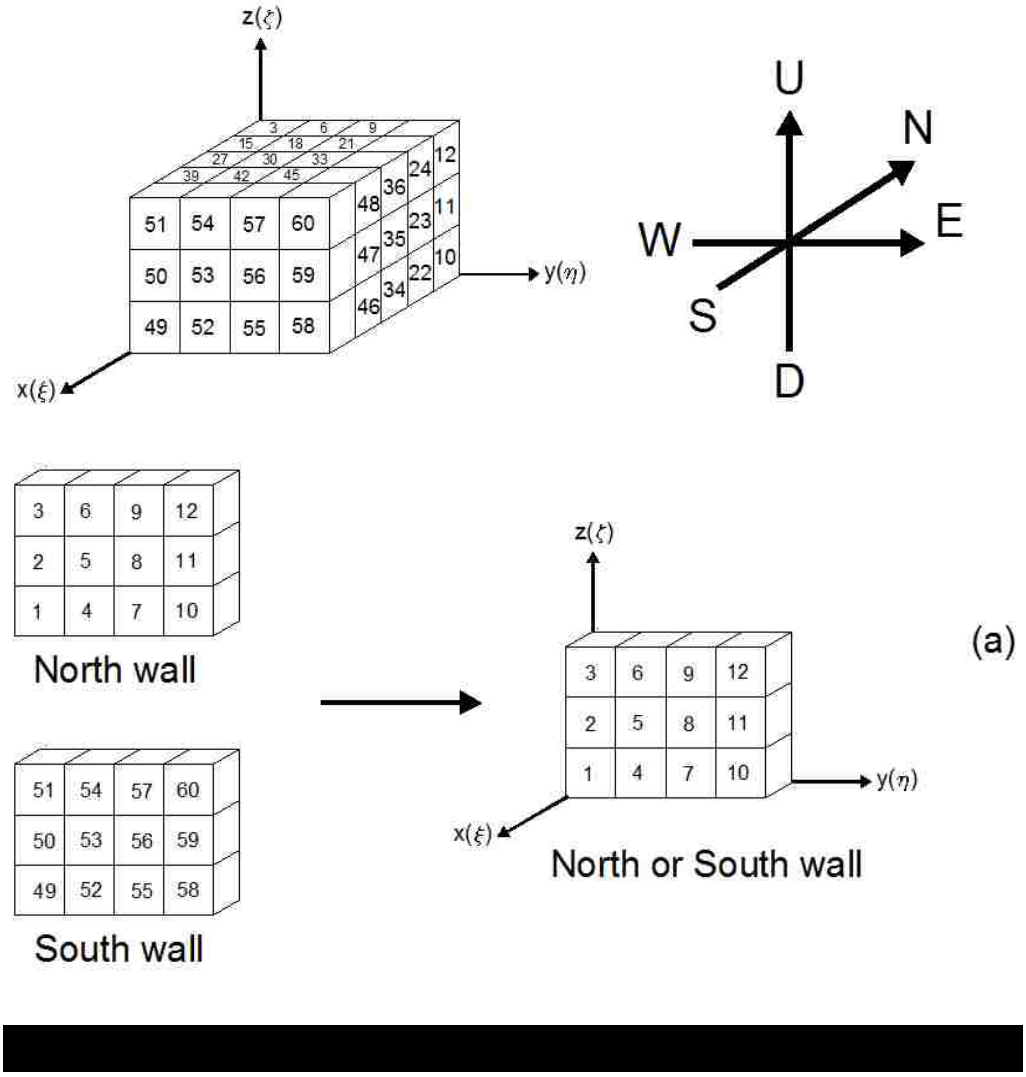

Figure 3.8 – An example `procCube` and its walls, (a) cells IDs of the North and the South walls local to the `procCube` domain mapped to the wall domain

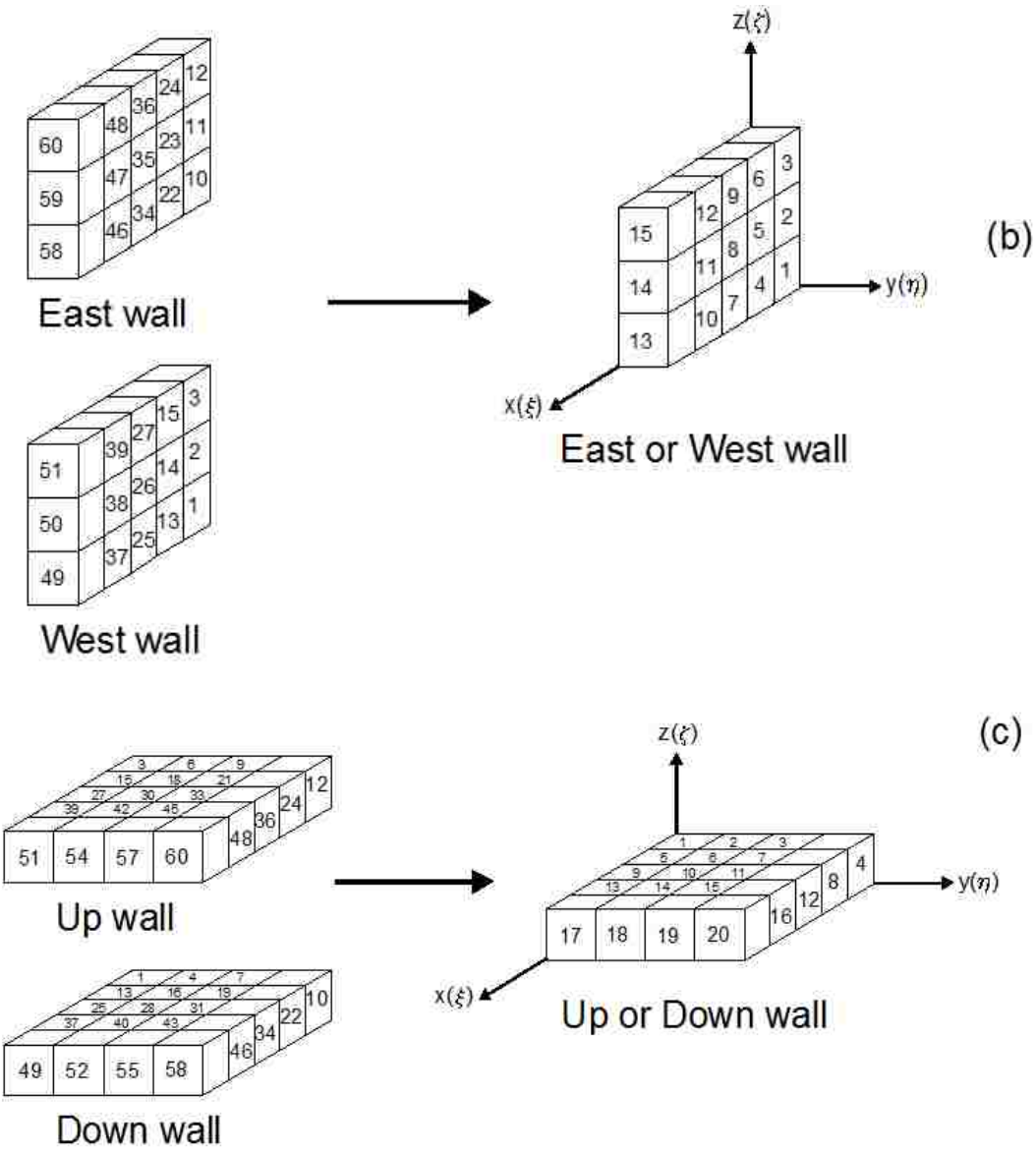

Figure 3.8 (continued) – An example `procCube` *and its walls, (b) cells IDs of the East and the West walls local to the* `procCube` *domain mapped to the wall domain (c) cells IDs of the Up and the Down walls local to the* `procCube` *domain mapped to the wall domain*

As was earlier mentioned and will be elaborated in the next section, during processor communication, the walls constitute the components of the messages exchanged between adjacent processors. When a wall is received from an adjacent processor, its information is stored appropriately for later access. Therefore, a predefined set of IDs is devised in the code for each received wall, according to its relative position to the home `procCube`.

These IDs are used to store and address the indices of exchanged buffer matrices (messages). Each ID refers to a specific location relative to the home `procCube`. For instance, the adjacent `procCube` located to the southwest of the home `procCube` will be recognized with ID number 5. Therefore, the wall received from the southwest adjacent `procCube` is stored and addressed, using ID number 5. PDQ benefits from careful assignment of these IDs to the received walls in specific order, which obviates packing and unpacking of exchanged data.

In the final step of defining the interaction path for each cell, the interaction path is divided into two sets. The cells which reside on the home `procCube` are distinguished from those on foreign `procCubes`. The two matrices generated for this purpose are `PathinHomeProc` and `PathinAdjProc`. This separation of the interaction paths is necessary for particle interaction (Section 3.7). In addition, if fewer than 13 cells in the interaction path are required for a particular cell (as with a boundary cell in non-PBC), non-existing paths are excluded from the interaction path array. After the interaction paths are defined, each cell has the local cell IDs of its adjacent cells (local to the `procCube` if on the home `procCube` and local to the home wall if on an adjacent

procCube). If the interaction path points to a cell on an adjacent procCube, the appropriate ID of that procCube is known to the home cell.

3.6. Particle communication

If a processor needs information located on an adjacent processor, message passing is required. The necessary data is delivered from the source processor to the asking processor. Message passing is enabled by the physical network links that are provided in the architecture of the multi-node machine connecting all the processors to each other.

To calculate the forces acting on particles, each particle must interact with its neighboring particles. However, some of these neighboring particles are located not on the home procCube, but on adjacent procCubes. Therefore, the necessary information must be received by the home processor. The subroutine ParticleComm is responsible for sending and receiving the necessary data using MPI commands.

A procCube is potentially surrounded by up to 26 procCubes, which implies that 26 messages are needed for each processor in each time step. With Plimpton's method of message passing (Section 2.2.4), all the data is sent by only six messages. Taking full advantage of Newton's third law further reduces the 6 messages to 5. According to the interaction paths shown in Figure 3.7, a cell never asks for information from its North (-*x* direction) plane. Therefore, if a cell is on the edge of a procCube, there is no need for the information of the adjacent cells on its North plane, which is the "south" wall of the "north" procCube. Consequently, there is no need to exchange the "south" walls between the processors and the necessary messages are reduced to 5.

The concept of the walls is used in PDQ combined with Plimpton's method of message passing. The messages are, in fact, composed of the walls. Walls are received in buffers which are constructed in such a way that their particles' home cells and home `procCubes` are known. The structure of buffer matrices has been explained in interaction paths. As explained in Section 2.2.4, the idea of Plimpton's method is that in some steps of message passing, some parts of received buffers are sent themselves as messages. Thus, each `procCube` potentially works as the source to send a message, as the destination to receive a message and also as a *transmitter*, *i.e.,* it relays some of the received messages to other `procCubes`.

In PDQ, all of the `procCubes` receive all the information they need in five steps (messages). Figure 3.9 shows how necessary messages are received by the purple object which is assumed to represent the home `procCube`. The orange objects are neighboring `procCubes`. It is very important to note that the figure only illustrates how the messages are received by the purple `procCube`. However, the purple `procCube` also sends its information to its adjacent `procCubes` as well, and the identical procedure is performed simultaneously by all of the `procCubes`, in parallel.

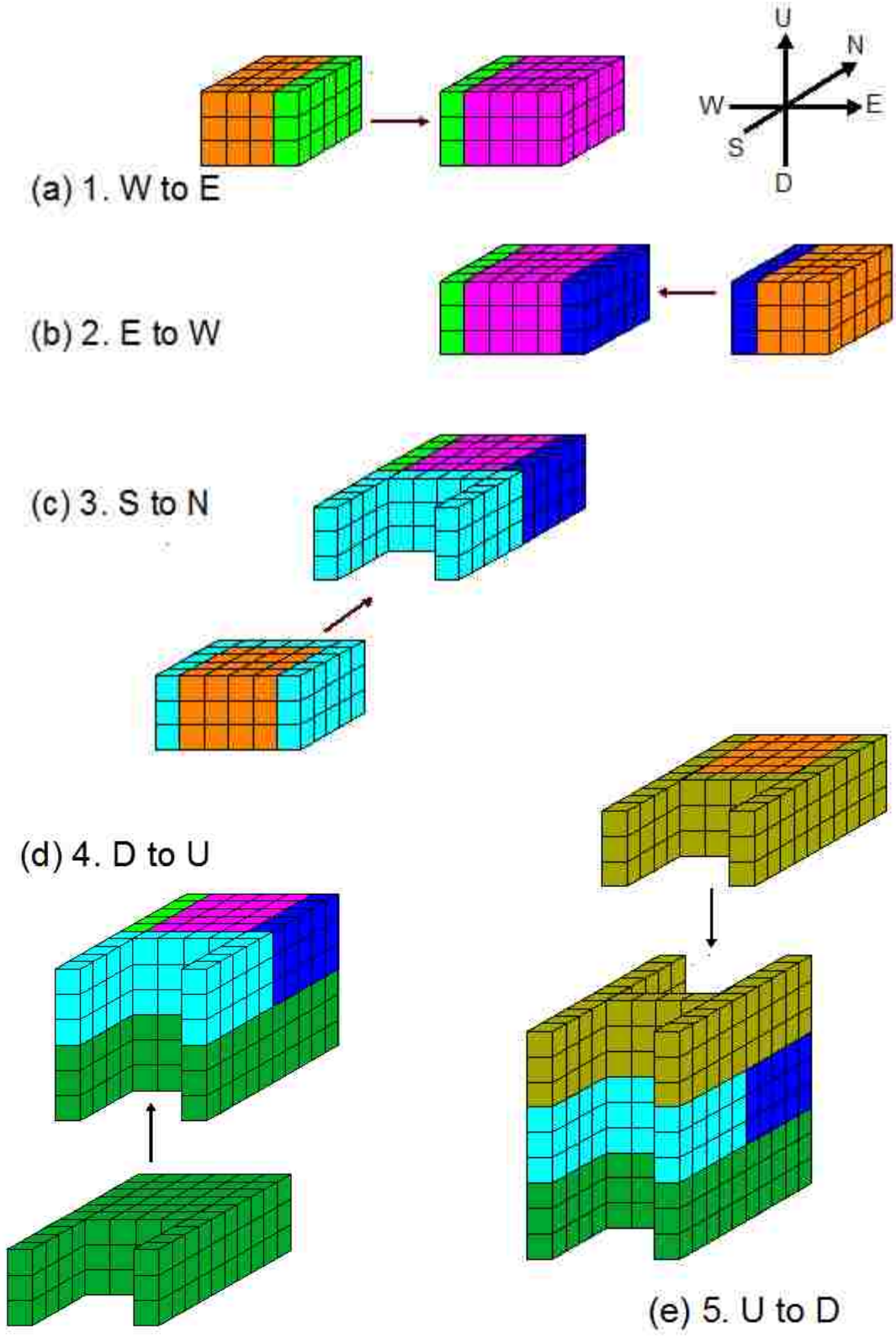

Figure 3.9 - Message passing five steps

In the first step, simultaneously, all procCubes send their East walls to their East procCube and receive a wall from their West procCube. After the first step, all the procCubes have the received the wall of their East procCube which is saved in the appropriate place in the receiving procCubes. This is illustrated graphically in Figure 3.9a where the green wall, sent by the East processor, is attached to the home procCube.

The second step involves exchange of information in the East-to-West direction. Each procCube sends its West wall to the West procCube and receives a wall from the East. After the second step, the procCubes have received walls from West and East procCubes. In Figure 3.9b the blue wall represents the received buffer from the East by the home procCube.

In the third step of message passing, all procCubes send the North walls to their North procCubes and receive walls from the South. In this step, the size of the message is roughly three times the size of the messages exchanged in the E-W and W-E message-passing steps, because the message includes three walls: the North wall of the South procCube as well as the walls previously received from the East and West procCubes of the South procCube. Thus the home processor receives the North wall of its South processor and the East and West walls of the processors located on southwest and southeast of the home processor in one package. Figure 3.9c shows the received message from South procCube in light blue.

In the third step of message passing, as well as fourth and fifth steps, procCubes not only send and receive data they need, but also send previously received walls to adjacent procCubes.

From the walls received from southeast and southwest `procCubes`, the home `procCube` requires only a column of the cells which are shown in yellow in Figure 3.10. The rest of the cells of the walls, received from southeast and southwest `procCubes`, are not required, although they are exchanged.

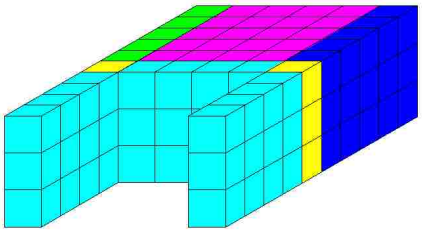

Figure 3.10 – Third step of receiving adjacent walls, necessary columns from southeast and southwest `procCubes` shown in yellow

The fourth message, shown in Figure 3.9d, contains six walls: the walls previously received by the Down `procCube` from its East and West in the first step, three walls received by the Down `procCube` from South as explained in step three, and the up wall of the Down `procCube`. All of this information is sent in one pack of data (one message) by the Down `procCube`. Simultaneously, the home `procCube` sends such information to its own Up `procCube`.

The last step is similar to the fourth one. Six walls, including five walls previously received from nearby `procCubes`, along with the Down wall of the Up `procCube` are sent down and received by the home `procCube`. At the end of the final step all the `procCubes` have received the necessary data (Figure 3.9e).

As noted earlier, due to Newton's third law, there is no need for data exchange in the direction of North to South which reduces the number of messages to five. As

explained before, benefiting from Newton's third law obviates exchange of information from North to south.

Every `procCube` needs only the information in the boundary cells of adjacent `procCubes` which creates one cell-deep shell around the home `procCube`. However, as illustrated in Figure 3.9e, some unneeded cells are transferred to the home `procCube`. In fact, there is a surfeit of exchanged data. More research is required to determine if, in this particular method, the advantage of a reduced number of messages outweighs the disadvantage of passing more information than is absolutely required.

3.7. Particle interaction

This section explains how particle interacting forces are calculated. Subroutine `Interact` does this in three steps. In the first step, all the particles, that reside on a specific cell and are within the material horizon of each other, interact. In the second step, the interactions between a particle and the neighboring particles which lie outside the home cell but within the home `procCube` are computed. Such particles are accessible by `PathinHomeProc`, constructed in defining interaction paths. In both steps, the interacting particles are within the home `procCube` and all required information to calculate the interaction forces is accessible via local arrays. In the final step of interaction, cells having interaction paths on adjacent `procCubes` interact with those adjacent cells. These interaction paths have been previously stored in array `PathinAdjProc`. The predefined IDs introduced in the second step of defining interaction paths are used to find the appropriate data through buffer arrays. At the end of

this step, all inter-particle forces on all particles have been calculated for the specific time step.

Benefiting from Newton's third law, only half of the interaction forces need be calculated. Each interaction force has a mutual force with the same magnitude and direction but with opposite sign. These mutual forces must be added to the total force acting on the other particle. For the interactions inside the home `procCube`, the reaction forces are added to local force arrays immediately after the calculation of the interaction forces. For interactions with particles on foreign `procCubes`, the mutual forces are stored in specific buffer arrays called `ForceAdjBuf`. These arrays are sent to adjacent `procCubes`, where the corresponding particles reside. On home `procCubes`, received mutual forces are added to local force arrays to sum the total forces acting on each particle.

3.8. Message components (beams, columns, and cornices)

The most efficient code sends and receives the least number of messages which contain only the necessary data. Reducing the number of exchanged messages decreases the computation latency (Section 2.2.4). Latency is largely a function of the speed of light, and in most fiber optic cables it results in about 4.9 microseconds of latency for every kilometer. One of the wall message-passing method's strengths is that it reduces the number of necessary exchanged messages to 5 as opposed to 6 in Plimpton's original method. However, there is a surfeit of data exchanged in this method which might counterbalance its speed. It is unclear how these two factors balance each other. Clarifying this issue requires further research.

The size of the messages can be reduced by sending only the necessary data. To prevent over-sending information, new objects with a similar functionality as with the walls should be defined. In consistent with previous naming convention, these objects can be names *beams*, *columns*, and *cornices*. Figure 3.11 illustrates these objects, where the walls are colored cyan, columns are yellow, beams are orange and cornices are shown green.

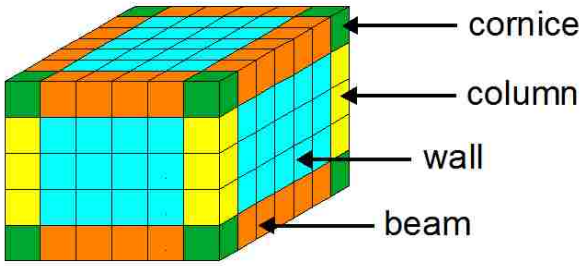

Figure 3.11 – Walls, beams, columns and cornices are components of the messages

Using these objects in creating the messages adds another step to forming the messages. The messages must be packed appropriately before sending and be unpacked in the destination `procCube`. There are predefined MPI commands for packing and unpacking data. However, packing and unpacking of data, while reducing communication time, require more computation time. More research is required to determine if doing so will speed up the code.

3.9. Force communication

As was discussed in previous section, the mutual forces calculated on foreign `procCubes` are sent to associated `procCubes`. Subroutine `ForceComm` is responsible for sending and receiving force buffer arrays which contain the mutual reaction forces.

The same message-passing idea used in particle communication is implemented in force communication with some alterations. The process involves sending and receiving five messages in the reverse process as for the particle communication procedure (Section 3.6). The only difference is that in each step of message passing, the receiver processor adds up the forces acting on particles received from different sender processors.

3.10. Integration

After calculating the total force acting on all particles, the positions and velocities of all the particles are updated in the integration subroutine. Using Newton's second law, its acceleration of every particle is calculated based on its mass and the applied force. The updated velocity is computed given the acceleration and velocity at the previous time step. The particle position is updated using the new velocity and previous position.

There are several integration methods in the literature. The molecular dynamics mode in PDQ offers two options: the "Velocity Verlet" integration method and the "Leapfrog" method. Other methods include finite difference methods such as the "predictor-corrector" algorithm, the "Gear predictor-corrector" algorithm and the "Runge-Kutta-Gill" method [Allen and Tildesley 1987]. The integration source code file in peridynamics mode of PDQ is exposed to the user to enable alternative integration scheme to be replaced.

3.11. Particle shuffling

A necessary feature for the code is particle shuffling. This involves transferring particles to new `procCubes` and cells. When particle displacements are not negligible compared to the radius of interaction, particles may leave their home `procCubes` and cells and move into adjacent `procCubes` and cells. It is necessary to transfer particles from their home `procCube` (to which the particles originally belong) to new `procCubes`. This involves deleting alterable particle attributes from the local arrays of the home processor, and inserting this information to the new processor local arrays. Relocation of particles to an adjacent `procCube` is possible for particles lying on the walls of the `procCubes`. Currently, the developed parallel algorithm is being revised to address particle shuffling in PDQ. Particle shuffling is very important particularly for molecular dynamics simulations, wherein large displacements, compared to the cutoff distance of the particles, occur.

3.12. Generalization of degrees of freedom

Modifying PDQ to handle user-defined degrees of freedom is a necessary feature of PDQ which gives PDQ unique generality and flexibility. Several steps need to be done to supply this capability to PDQ. The most important step, which has been implemented in the current version of PDQ, involves modifying the communication subroutines, `ParticleComm` and `ForceComm`. These subroutines basically contain MPI send and receive commands. The indices of arrays and array sizes, which are to be exchanged, are pre-calculated based upon the number of degrees of freedom of the

problem. In peridynamics simulation, number of degrees of freedom is an input parameter in the main input file. Its value is set to three as a default value for molecular dynamics simulations. A new extension of PDQ has been developed which fully addresses generalized degrees of freedom for peridynamics simulations. Solving similar problems with available versions showed a slowdown in calculation time. The latest version seems to be more than three times slower than the original version. This reduction in speed is expected as the modified version utilizes multi-dimensional arrays for particle and force field attributes instead of one-dimensional arrays used in the original version of PDQ. Processors spend more time on calculating the address of a certain element of a multi-dimensional array in the memory. Memory address finding process takes place much quicker for one-dimensional arrays. Further research is required to minimize the effect of using multi-dimensional arrays on the speed of the code.

3.13. Summary

The wall method message passing algorithm was explained in this chapter. In addition, details of the parallel scheme used in PDQ and the implementation of the wall method message passing were described.

The source code in peridynamic mode of PDQ is divided into two sections. The main source code contains the parallelization scheme where it takes place behind the user's eye. Some of the source code is open to the user to define desired force field and integrating method. Editing these files does not require any knowledge of the parallelization method. To help the user to edit these source code files, create necessary input files and analyze the outputs, a user manual is provided.

Several example problems are simulated using PDQ which are presented in the next chapter. The user is able replicate the simulated problems using the user manual (Appendix A).

4. EXAMPLE PROBLEMS

This chapter presents the results from six example problems in civil engineering simulated using PDQ. The example problems include a plain and a reinforced (RC) concrete cantilever beam, a plain and a reinforced simply supported concrete beam, a lap splice pullout problem and a prestressed (PS) bulb T beam. The first four problems are canonical, relatively simple problems in structural analysis for which the strength can be simply calculated from solid mechanics equations. The lap splice pullout problem was previously simulated by Gerstle, Sakhavand and Chapman [Gerstle *et al.* 2010] using EMU. The shear failure mechanism of a prestressed bulb T beam is a problem of interest to many civil engineers. Figure 1.1, in the Introduction section of this thesis, illustrates shear cracking of a prestressed concrete beam under loading in a laboratory test.

The presentation of these results serves two purposes: validating the code, and demonstrating the range of problems that can be tackled using peridynamics.

For all these problems, the initial minimum and maximum natural frequency of vibration of the problem is determined using a commercial finite element simulation package, SAP2000 11.0.8 (Computers and Structures, Inc., Berkeley, California). The total duration of the simulation is determined based on the minimum natural frequency. The maximum frequency is used to determine the time step of the problem in the preprocessing step (Appendix A).

Both concrete and steel are treated as nonlinear elastic, but this should not matter if no unloading of links occurs. The constitutive model used in the simulations for concrete is shown in Figure 4.1.

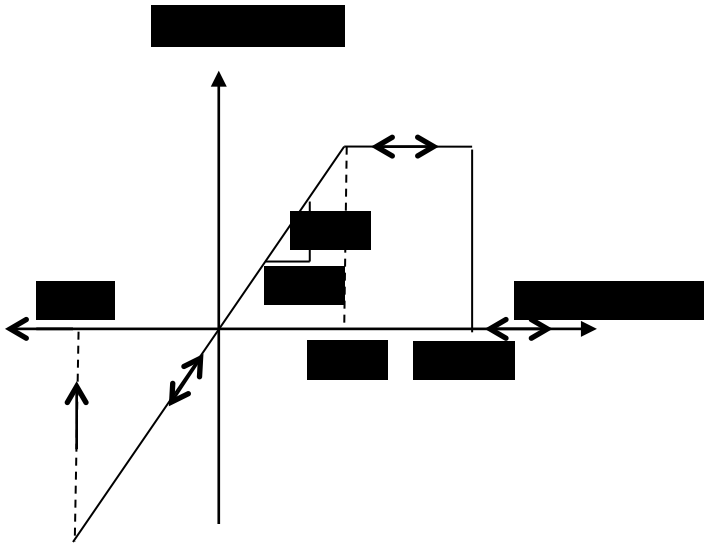

Figure 4.1 – Peridynamic constitutive model for concrete

The following material properties are used for steel and concrete unless otherwise specified for particular problem:

Steel:
Young's modulus E = 29000 ksi
Poisson's Ratio: ν = 0.3
Density: ρ = 490 lb/ft^3
Yield strain: s = 0.01 in/in

Concrete:
Young's modulus E = 3605 ksi
Poisson's Ratio: ν = 0.25
Density: ρ = 145 lb/ft^3
Critical stretch: $S_{tension}$ = 1.387x10^{-4} in/in, $S_{compression}$ = 1.1x10^{-3} in/in

E', the peridynamic constant, is calculated from [Gerstle *et al.* 2007]:

$$E' = \frac{6E}{\pi\delta^4(1-2\upsilon)}, \qquad 4.1$$

where δ is the material horizon. In all of the simulated example problems, the material horizon is set to be equal to $3''$.

Figure 4.2 shows the peridynamic pairwise force function for steel.

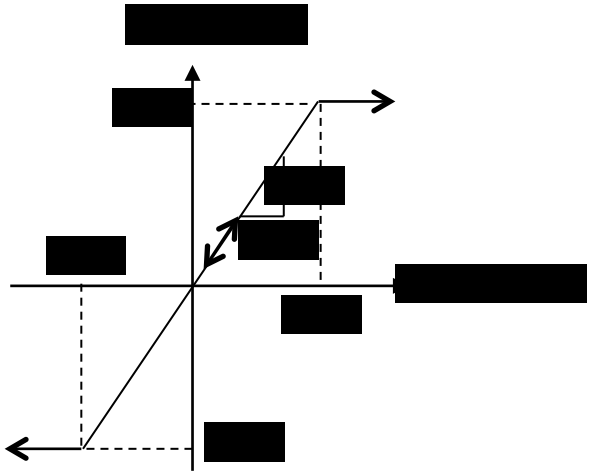

Figure 4.2 – Peridynamic constitutive model for steel

To simulate the bond-slip behavior between the steel bars and the concrete, the interaction between steel and concrete particles is simulated as concrete-concrete except that the calculated pairwise force and the critical stretches are both multiplied by a factor of three. This is the recommended factor in the EMU user manual.

Black regions in the figures illustrate particles having more than specified percentage of broken links. A link breaks when the previously existing interacting force between a pair of particles turns zero. Post-processing tools allow choosing the specified percentage of damaged links.

All the simulations were performed on the `nano` Linux parallel supercomputer at the University of New Mexico Center for Advanced Research Computing (CARC). `nano`'s specifications are as follows:

- Dell PowerEdge 1950 nodes

- 36 nodes each with dual 2.33 GHz dual core Intel Xeon processors
- 144 processors total
- 8 GB/node of local memory (RAM)
- 73 GB/node of local disk
- Myrinet2 Interconnect for fast inter-node communication
- 3 TB temporary scratch storage

In general, not all nodes are available for production computing. One node is reserved for debugging purposes and one node is reserved for maintenance.

4.1. Plain concrete cantilever beam

In the first example, a 3D concrete beam, subjected to a downward force (Figure 4.3), is simulated with PDQ. A similar 2D example was previously simulated by Sau [Sau 2008] with a different peridynamic model on a single processor. Sau states that solving such a problem requires a lot of memory and computer run time [Sau 2008], suggesting that this might be a good test problem for PDQ on a parallel supercomputer.

The simulated problem is a three-dimensional concrete beam of 200" length, with a rectangular cross section of 30" wide and 50" deep. Three planes of particles in the cross section of the beam are constrained in all the directions at the left end. The problem consists of a cubical grid of $200\times50\times30 = 300{,}000$ particles spaced at 1" with a material horizon of 3".

The model is subjected to a uniform force at the free end of the beam. The external force is applied to two planes of particles at the right end. The total applied force P is calculated as follows:

$$P = \frac{force}{particle} \times (total\ number\ of\ loaded\ particles = 2 \times 50 \times 30). \quad 4.2$$

The model is illustrated in Figure 4.3.

Figure 4.3 – Description of cantilever plain concrete beam

In a mechanics of material analysis, the maximum stress forms at the fixed end of the beam and is calculated as:

$$\sigma_{max} = \frac{M.c}{I} = \frac{P.L.c}{I}, \quad 4.3$$

where M is the resulting moment, I is the moment of inertia of the cross section, L is the total length of the beam, P is the total applied load and c is the half vertical length of the cross section.

The fracture strength of concrete is computed from:

$$f_r = 7.5\sqrt{f_c'}, \quad 4.4$$

where f_c' is the 28-day compressive strength of concrete.

With $L = 200"$, $f'_c = 4000$ psi, $c = 25"$, $I = \frac{50^3 x 30}{12} = 312500$ in^4, and by substituting f_r from Equation 4.4 in Equation 4.3, it is estimated that the beam should start cracking at $P = 30$ kips.

The force is linearly increased as a function of time shown in Figure 4.4.

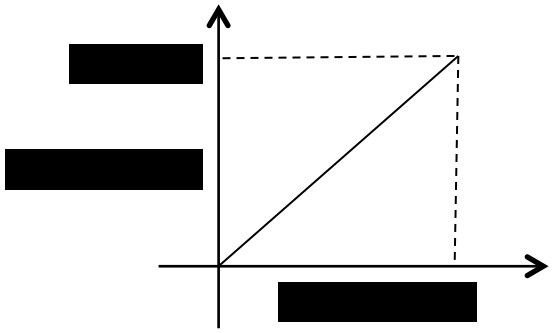

Figure 4.4 – Applied force vs. time

The simulation time step is 0.34×10^{-5} sec. A magnified 100x view of the beam deformation at different time steps is shown in Figure 4.5. The applied force at each particular time step is shown in each frame. Particles with 20% or more damage are shown in black. The beam suddenly starts cracking when the applied force approaches 30 kips.

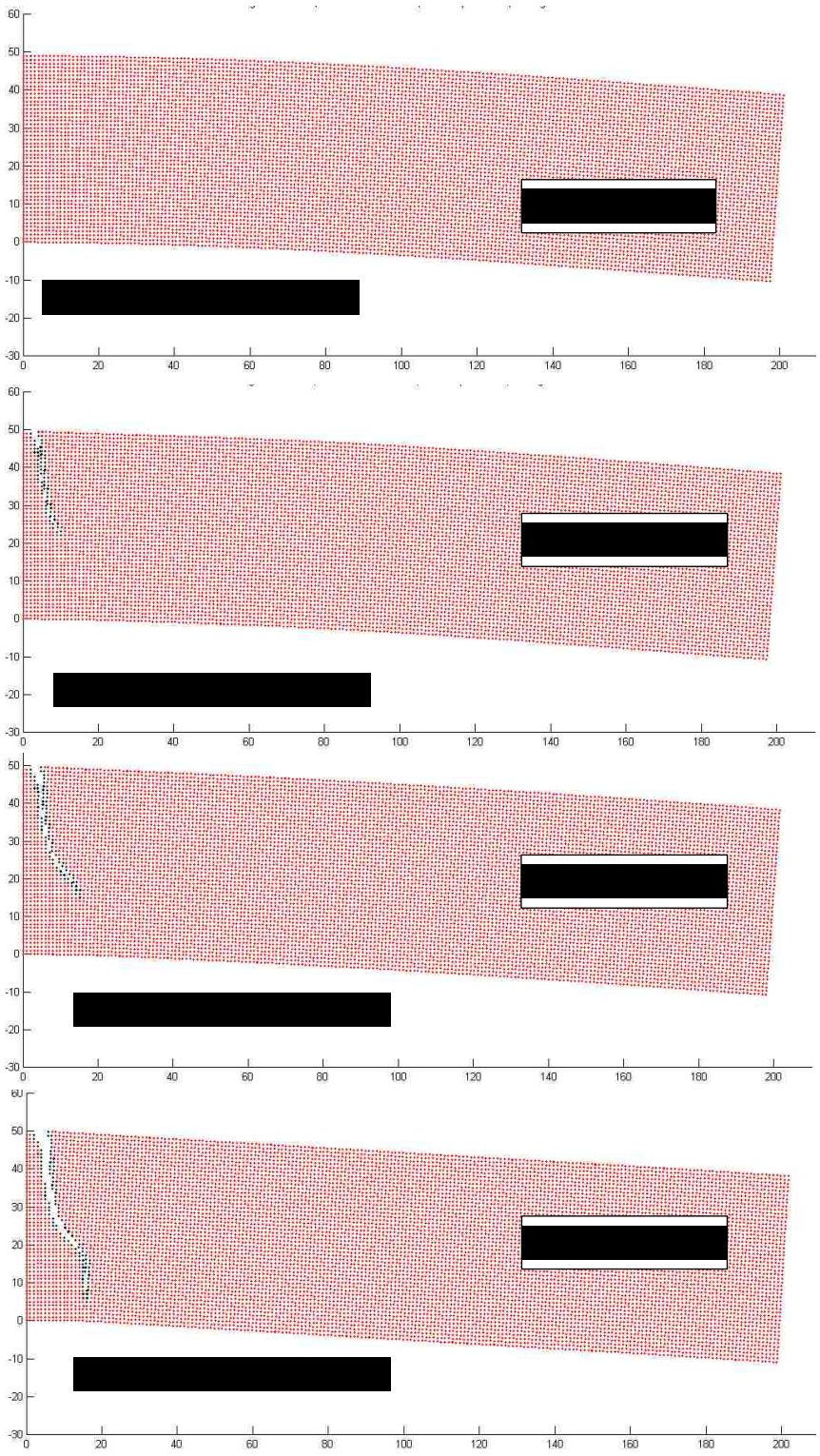

Figure 4.5 – Deformed shape of cantilever plain concrete beam using PDQ

Figure 4.6 shows absolute value of the displacement of a point located at the bottom right side of the beam, drawn according to the applied force. As the load is increased, the magnitude of the displacement is consequently increased. At the time the beam reaches its ultimate strength, the rate of change of displacement starts to increase and the displacement approaches an infinite value.

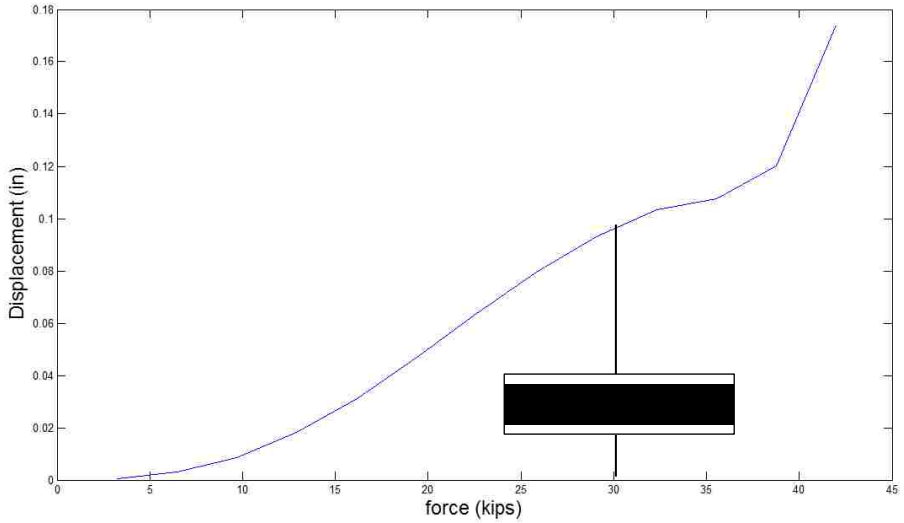

Figure 4.6 – Displacement vs. force plot

The value of the ultimate load estimated from Figure 4.6 is comparable to the calculated strength of the beam from the mechanics of materials equations.

4.2. Reinforced concrete cantilever beam

This is the same as problem number one except that the beam is now reinforced with three steel bars. The reinforcement ratio is 0.014. Figure 4.7 shows details of the model.

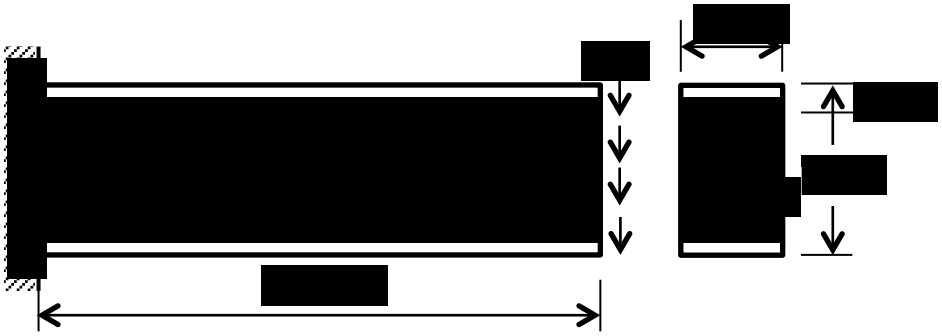

Figure 4.7 – Description of cantilever reinforced concrete beam

The model consists of 300,600 particles located in a box grid of one-inch spacing. The boundary conditions are similar to the previous example problem. Three planes of particles in the cross section of the beam are restrained from moving in all the directions on the left side. The load is applied to two planes of particles on the right side of the bam.

The American Institute of Concrete (ACI) design code specifies that the shear strength of a reinforced concrete beam can be calculated from:

$$V_c = 2\sqrt{f_c'}\, b_w d. \qquad 4.5$$

With $b = 30"$, $f_c' = 4000$ psi, and $d = 46.5"$, the maximum shear strength of the beam is predicted as $V_c = 175$ kips.

Similar to the first example, a force linearly increasing by time (Figure 4.4), is applied to two planes of particles at the right end of the beam.

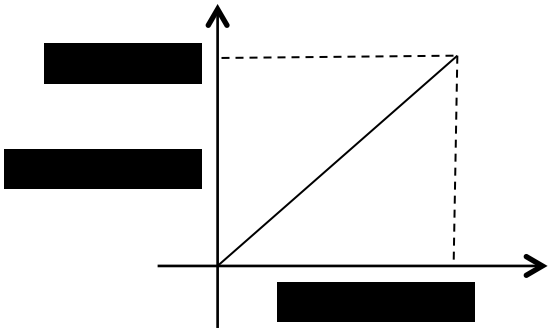

Figure 4.8 – Applied force vs. time

The simulation time step is 0.18×10^{-5} sec, which is smaller than the plain concrete example, because steel increases the strength of the beam, thus decreasing the minimum period ($\omega = \sqrt{\frac{k}{m}} = \frac{2\pi}{T}$).

Snapshots from 100x magnified deformation of the cantilever beam at different time steps are shown in Figure 4.9. Particles with more than 20% damage are shown in black. For clarity, only the outer periphery of concrete is shown in the figure. Figures on the left are 3D view of the same time step which is shown on the right in 2D.

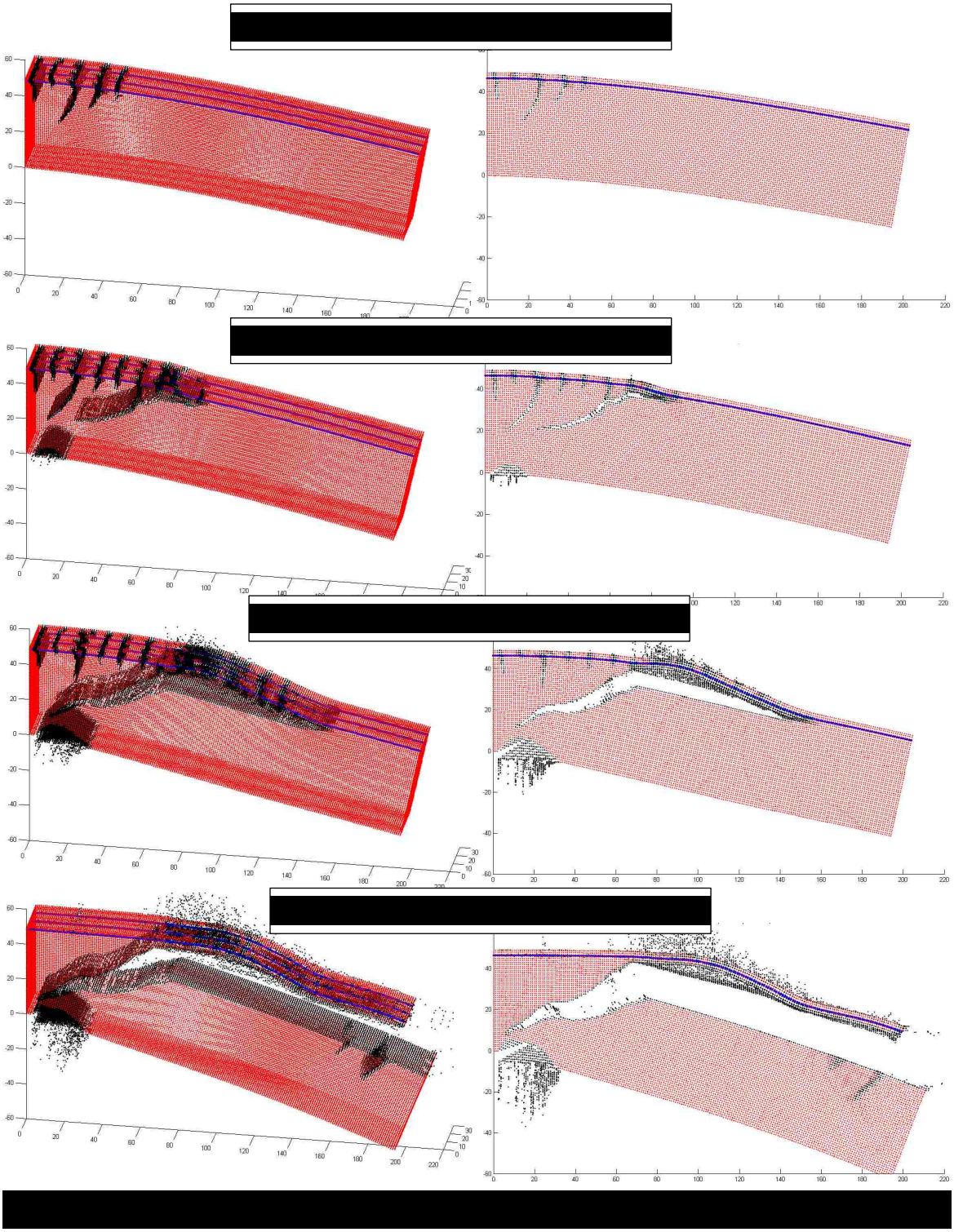

Figure 4.9 – Deformed shape of cantilever reinforced concrete beam

Propagation of flexural and shear cracks are observed in Figure 4.9. Crushing of concrete also is visible at the left bottom corner of the beam. The simulation took approximately 3 hours to run on `nano` using 32 processors.

The absolute value of the displacement of a particle located at the bottom right corner of the beam is shown in Figure 4.10, according to the increasing applied force.

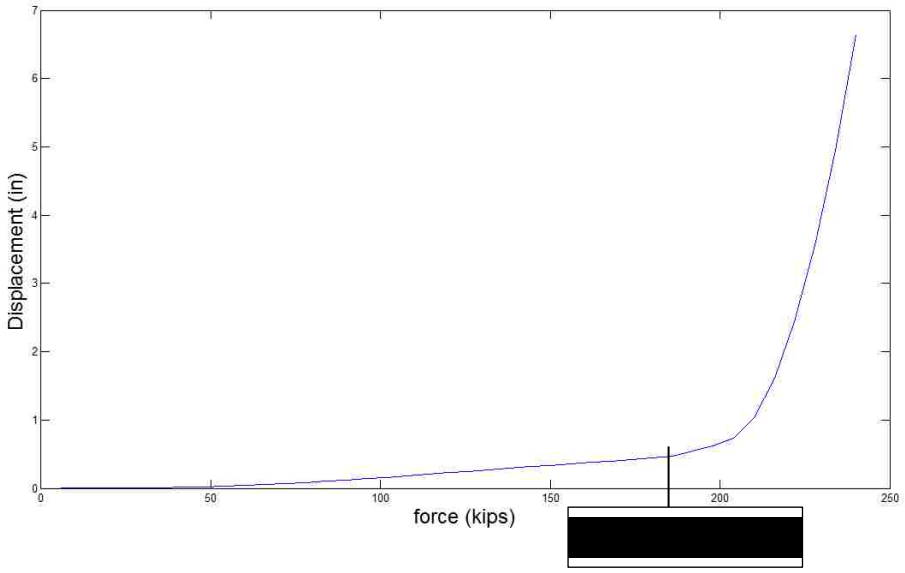

Figure 4.10 – Displacement vs. force plot

Such displacement vs. force plot can be used to determine strength of a beam. Sudden change in the rate of increase of the displacement takes place when the beam is not able to hold any larger loading (ultimate strength of the beam). The estimated value of the ultimate strength from the displacement vs. force plot (180 kips) is comparable to the ultimate shear strength computed using ACI equations (175 kips).

4.3. Simply supported plain concrete beam

The failure of a simply supported concrete beam is a famous problem in fracture mechanics. The beam is simulated using PDQ and is subjected to a uniform load applied at the top of the beam. The model description is shown in Figure 4.11.

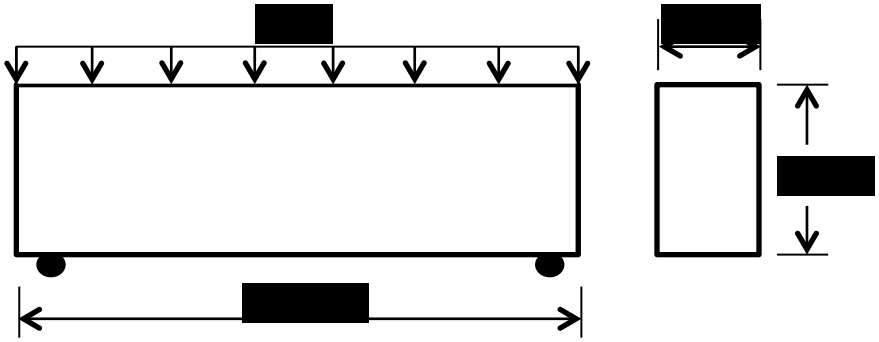

Figure 4.11 – Description of simply supported plain concrete beam

The beam consists of 375,000 particles with 1″ spacing between particles. The problem is simulated with the pairwise force function shown in Figure 4.1.

As the maximum stress happens at the bottom middle of the beam, it is expected that first cracks will nucleate in that area. The maximum normal stress is:

$$\sigma_{max} = \frac{M_{max}.\times c}{I}. \qquad 4.6$$

The fracture strength of concrete is computed from:

$$f_r = 7.5\sqrt{f_c'} \qquad 4.7$$

From classical beam theory, the maximum moment and shear for a simply supported beam are:

$$M_u = \frac{w\times l^2}{8}, \qquad V_u = \frac{w\times l}{2} \qquad 4.8$$

With $L = 250"$, $f'_c = 4000$ psi, $c = 25"$, $I = \frac{50^3 x 30}{12} = 312500$ in^4, and by substituting f_r from Equation 4.7 in Equation 4.8, the strength of the beam is calculated as $w = 760$ lb/in.

The beam is under a uniform force applied at two top layers of the particles. The force is increased linearly as the simulation advances.

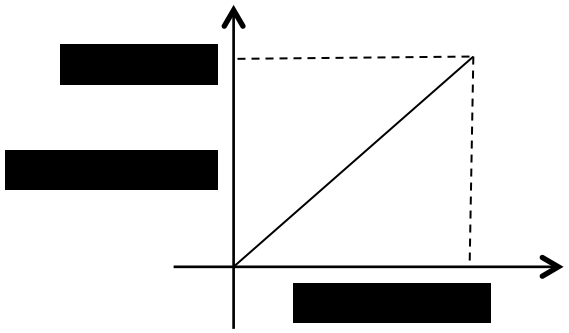

Figure 4.12 – Applied force vs. time

The deformed shape of the beam using PDQ is shown in Figure 4.13. Each frame shows a snapshot of the simulation at a certain time step and includes the applied force at that time step. Particles with 20% or more damage are shown in black. The deformation is magnified 100 times. As shown in Figure 4.13, a sudden failure occurs when the load reaches to 765 lb/in, which is comparable to the calculated strength of 760 lb/in.

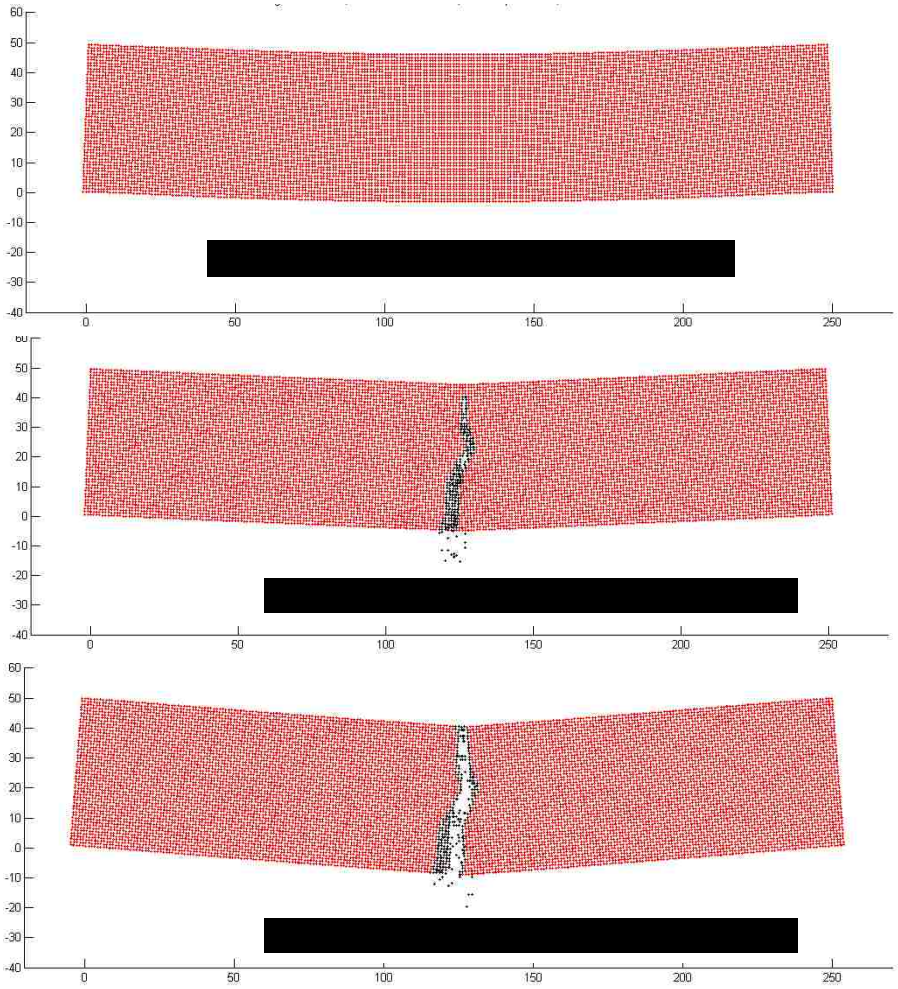

Figure 4.13 – Simulation results of simply supported plain concrete beam

4.4. Simply supported reinforced concrete beam

Studying shear failure mechanism in a reinforced concrete beam is an interesting area of research which has led to the development of shear provisions in the civil engineering design codes such as ACI and AASHTO. Figure 4.14 shows formation and propagation of shear cracks in a simply supported reinforced concrete beam.

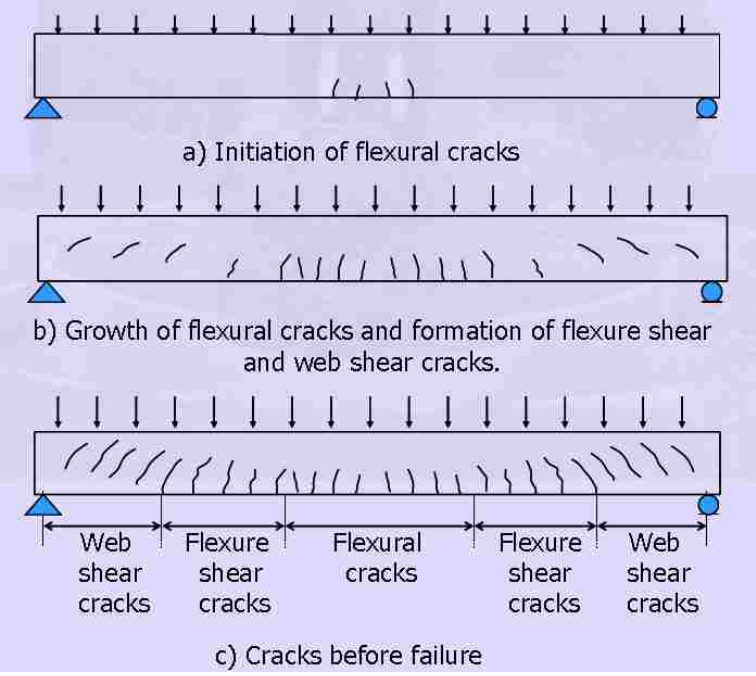

Figure 4.14 – Formation of cracks in a simply supported reinforced concrete beam

In this example, the previous example of unreinforced concrete beam is over-reinforced with three steel bars. The reinforcement ratio is $\rho = 0.01$. That means concrete starts crushing before steel yields. Properties of reinforcement bars and concrete are the same as in the cantilever beam example problem. Cross section of the beam is shown in Figure 4.15.

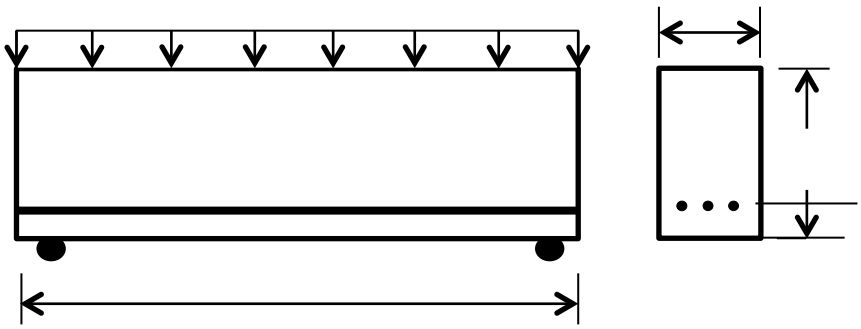

Figure 4.15 – Description of simply supported reinforced concrete beam

The ACI specifies that the shear strength of a concrete beam can be calculated from:

$$V_n = V_c = 2\sqrt{f_c'}\, b_w d, \qquad 4.9$$

where b_w is the width of the beam, d is the distance between steel bars and farthest in-compression fibers of concrete, and f_c' is the 28-day strength of concrete.

With $b_w = 30"$, $f_c' = 4000$ psi, and $d = 46.5"$, the maximum shear strength of the beam is calculated approximately as $V_c = 175$ kips. The beam is subjected to a uniform force at the top which is increasing proportional to the time.

If V_c equals the maximum nominal shear force V_u, the value of the uniform applied force, *w,* which produced V_c will be:

$$w = \frac{2V_c}{l} = \frac{2\times 175000}{250} = 1400\ \frac{lb}{in} \qquad 4.10$$

A uniform force, which is a linear function of time, is applied to the two top layers of particles. Nucleation and propagation of shear cracks are observed as shown in Figure 4.16.

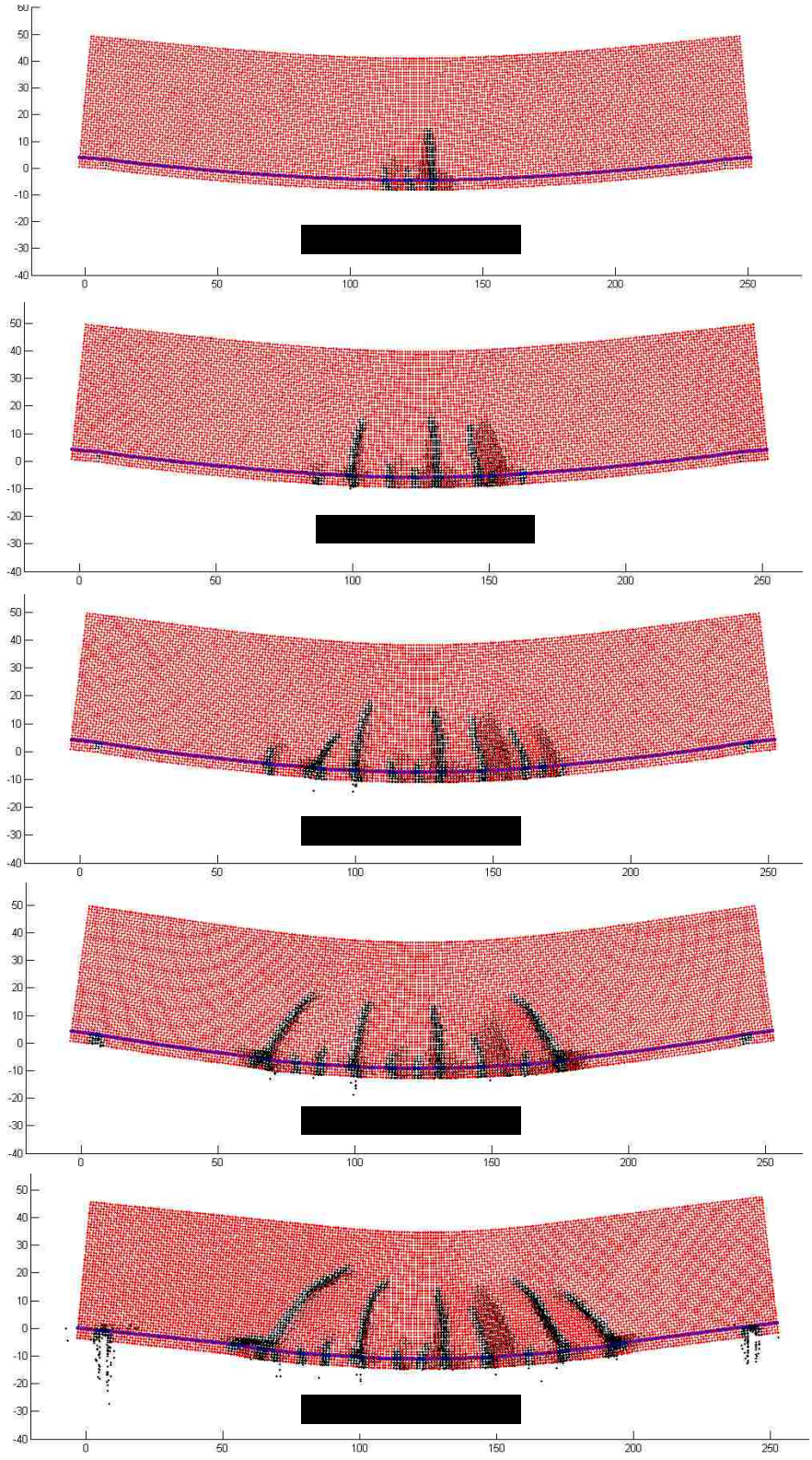

Figure 4.16 – Deformed shape of simply supported reinforced concrete beam using PDQ

The absolute value of the displacement of a particle located at the middle top of the beam is plotted against the time (Figure 4.17). The displacement becomes unstable at the time when force is approximately 1300 lb/in. This value can be compared to the calculated strength of 1400 lb/in.

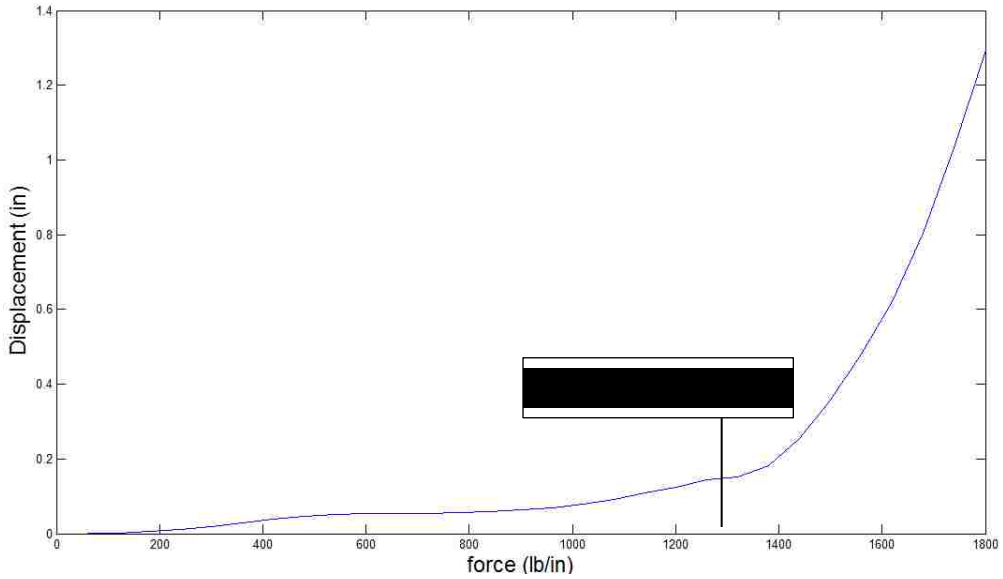

Figure 4.17 – Displacement vs. force plot

4.5. Lap splice pullout

Gerstle, Sakhavand and Chapman [Gerstle, Sakhavand and Chapman 2010] simulated the reinforced concrete lap splice problem in 2010 using EMU. The results were compared to a finite element model using ANSYS (ANSYS, Inc., Canonsburg, Pennsylvania) and experimental laboratory tests. The same problem is solved using PDQ and the results are compared. The problem consists of a cylinder of concrete with two bars embedded in the concrete as shown in Figure 4.18.

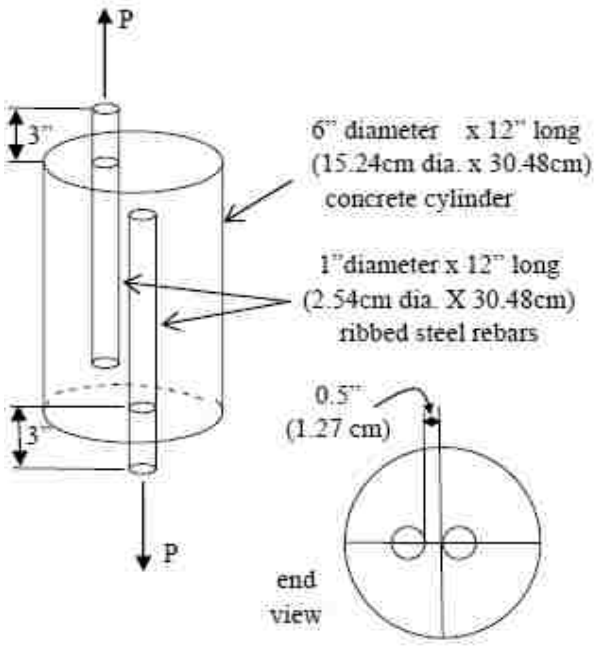

Figure 4.18 – Lap splice problem detail [Gerstle, Sakhavand and Chapman 2010]

The dimensions and material properties are kept the same as in the paper by [Gerstle *et al.* 2010].The bars are 12" long and 1" diameter and protrude from each end of a 12" long and 6" diameter concrete cylinder. The problem was modeled with the following material properties:

Steel:
Young's modulus E = 29000 KSI (200 GPa)
Poisson's Ratio: ν = 0.3
Yield Stress: Fy = 150 KSI (1.03 GPa)
Mass Density: ρ = 15.22 slug/ft^3 (7850 kg/m^3)
Sound Speed: c = 15130 ft/s (4612 m/s)

Concrete:
Young's modulus E = 3504 KSI (25 GPa)
Poisson's Ratio: ν = 0.22
Tensile Strength: Fy = 0.6 KSI (4.13 MPa)
Mass Density: ρ = 4.50 slug/ft^3 (2400 kg/m^3)
Sound Speed: c = 8310 ft/s (2533 m/s)
Fracture energy: GF = 1.0 lb-in/in^2 (175.1 N-m/m^2)

The lap splice problem is in dynamic, not static, equilibrium. The top part of the bar protruding from the top of the concrete is subjected to a uniform upward velocity of 7.87 in/s during the run. Similarly, the bottom part of the bar protruding from the bottom of the concrete is subjected to a uniform downward velocity of 7.87 in/s. The protruding parts of the bars are restricted from moving in the plane of cylinder base.

Figure 4.19 shows some figures from the simulation using EMU [Gerstle *et al.* 2010]. The black particles show damaged regions.

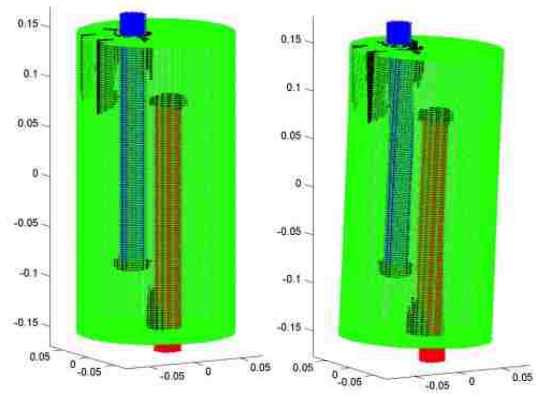

t = 0.00072 s
(a)

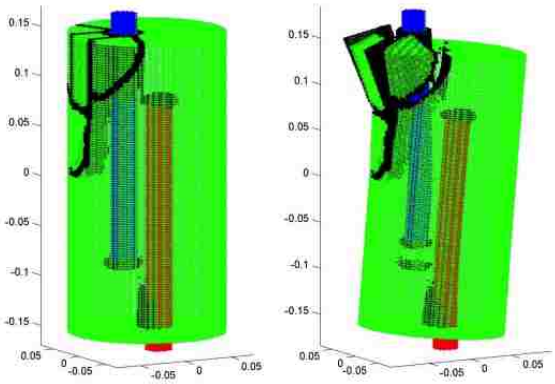

t = 0.0014 s
(b)

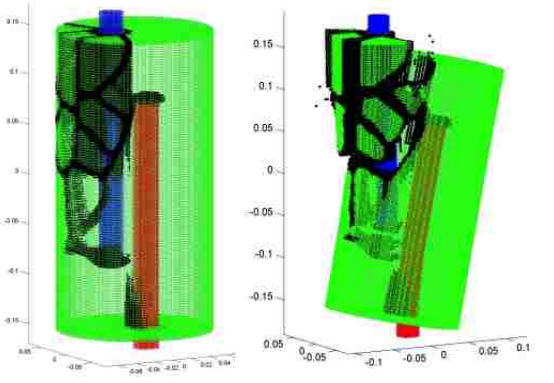

t = 0.0022 s
(c)

Figure 4.19 - Undeformed and deformed shapes at three simulation times from EMU [Silling 2003]. Deformation is magnified by a scale factor of 50. Particles with more than 30% of peridynamic links being broken are displayed as black [Gerstle, Sakhavand and Chapman 2010].

The lap splice pullout problem is also simulated using PDQ. The peridynamic constitutive model (pairwise force and stretch relationship) used for concrete is shown in Figure 4.1. The material properties are the same as used in EMU.

There are certain differences between the codes. EMU uses state-based peridynamic model (Section 2.1.2) whereas the results from PDQ are based on the original bond-based peridynamic theory. Figure 4.20 shows the results of the lap splice problem using PDQ subjected to a 7.87 in/sec velocity applied in opposite direction to the protruding sections of steel bars.

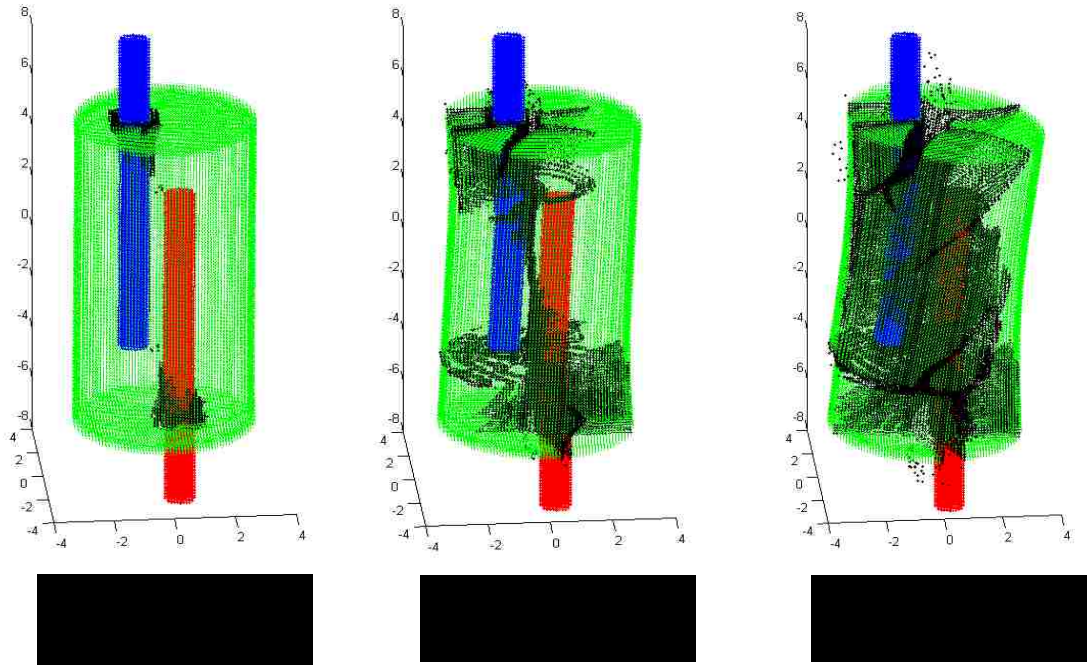

Figure 4.20 – Lap splice problem simulated with PDQ (7.8 in/sec pullout velocity), particles with more than 35% or more damage are shown in black

The time step used is 0.18×10^{-6} sec. Comparing figures from EMU simulations to those from PDQ simulations, shows that cracking pattern starts similarly and diverges as the simulation moves forward. Comparison of the figures according to their time step shows that propagation of cracks occurs much faster in PDQ than in EMU. Although the same parameters used in EMU have been used in PDQ for simulating this problem, the force fields might be different. The parameters used in the force filed in EMU are not clearly defined, thus using different parameters might account for the discrepancy in the results.

The same problem has been solved with a slower applied velocity (2.00 in/sec). The results are shown in Figure 4.21.

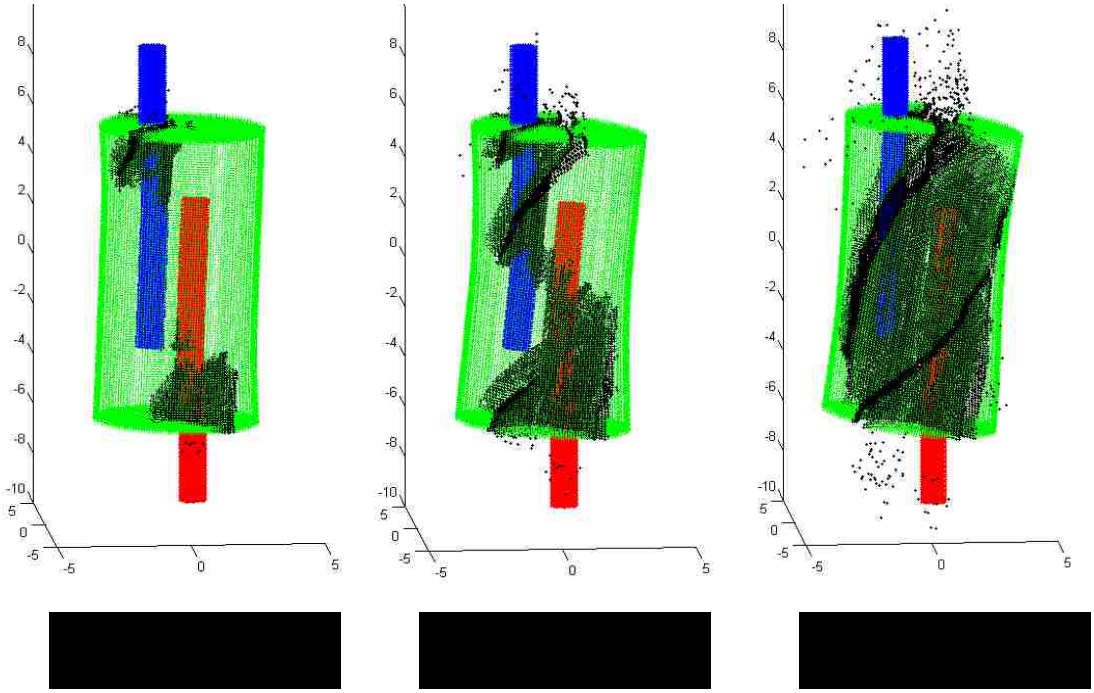

Figure 4.21 – Lap splice problem simulated with PDQ (2.0 in/sec pullout velocity), particles with more than 35% or more damage are shown in black

In another simulation run, a 0.5 in/sec constant velocity is applied to the protruding section of steel bars. Figure 4.22 illustrates the results.

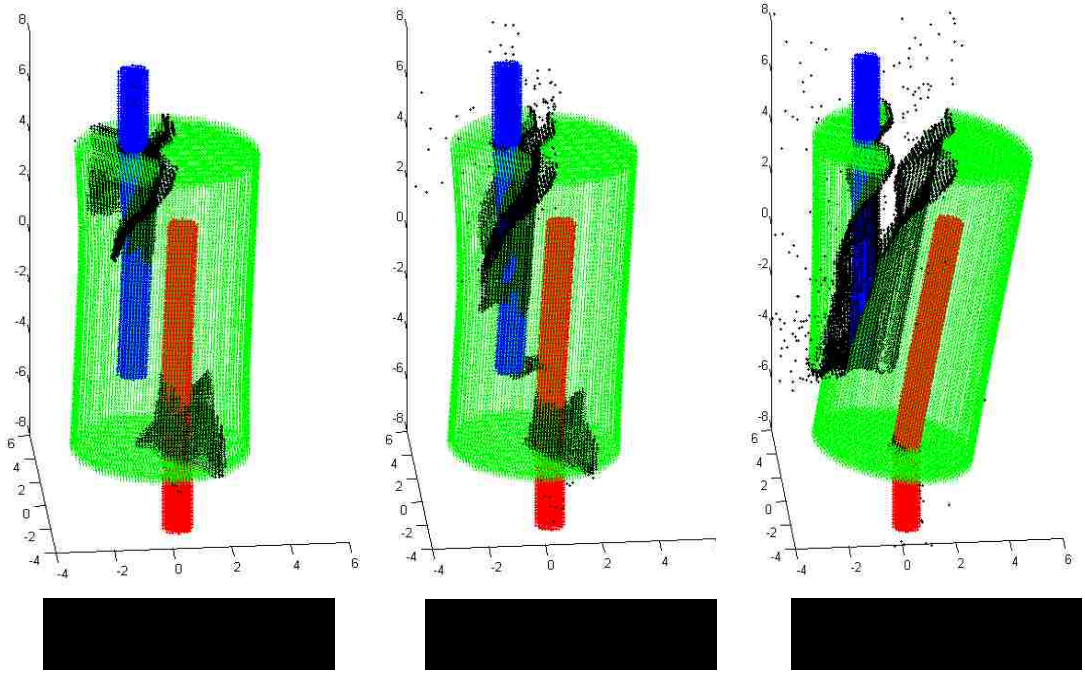

Figure 4.22 – Lap splice problem simulated with PDQ (0.5 in/sec pullout velocity), particles with more than 17% or more damage are shown in black

It is interesting to observe how the pattern cracking differs as the velocity is reduced.

4.6. Prestressed concrete beam

A prestressed concrete beam is simulated using PDQ. The cross section of the beam is a BT-72 (shown in Figure 4.23), which is mostly used as bridge girders.

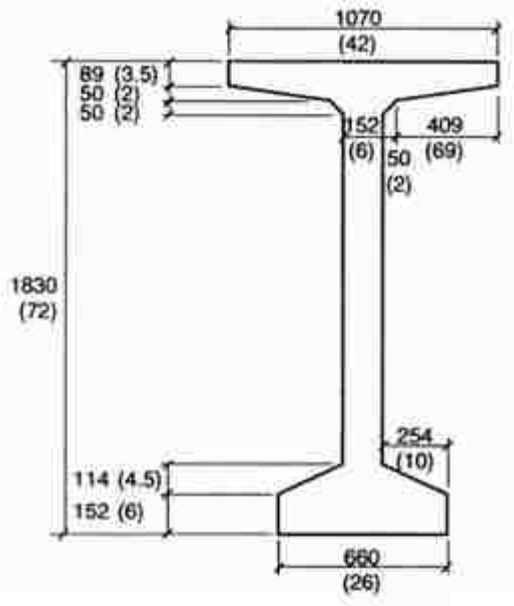

Figure 4.23 – Cross section of BT 72 beam, The dimensions are in millimeters (inches in parentheses)

The beam is 9.5 meters long and simply supported on two ends. The beam consists of 341,471 particles and is subjected to a downward load applied to a narrow strip at the top of the beam. The beam is reinforced with straight and prestressing strands as shown in Figure 4.24.

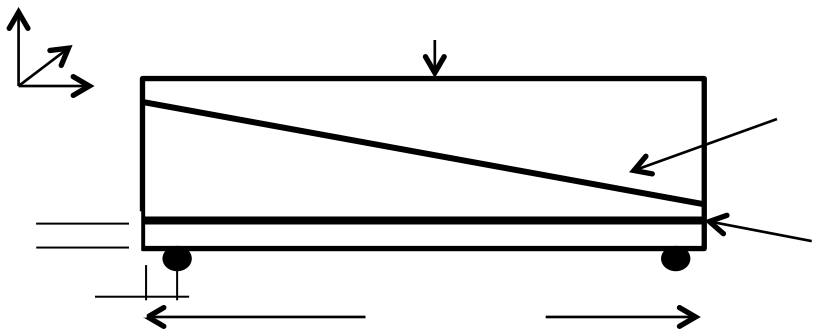

Figure 4.24 – Details of simply supported prestressed concrete beam

The pattern of reinforcing strands is shown in Figure 4.25. Eight reinforcing bars and three prestressing strands are inserted in the beam. Each reinforcing bar has an area of 400 mm^2 and each prestressing strand has an area of 450 mm^2.

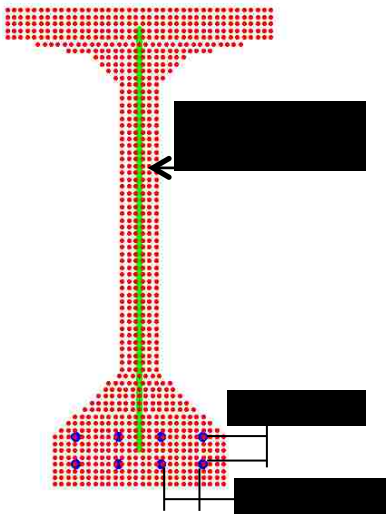

Figure 4.25 – Details of the strands in the prestressed bulb T beam

Two lines of particles in the *x*-direction and two lines in the *z*-direction are restrained from moving in *z*-direction. The top middle strip of the beam (two lines of particles in *x*-direction and two lines of particles in *z*-direction) are subjected to a downward force, P.

The deformed beam is shown in Figure 4.26 and Figure 4.27 at different time steps. The black particles show particles with more than 10% damage. The deformation is magnified 100 times. The time step used in this simulation is 0.18×10^{-5} sec.

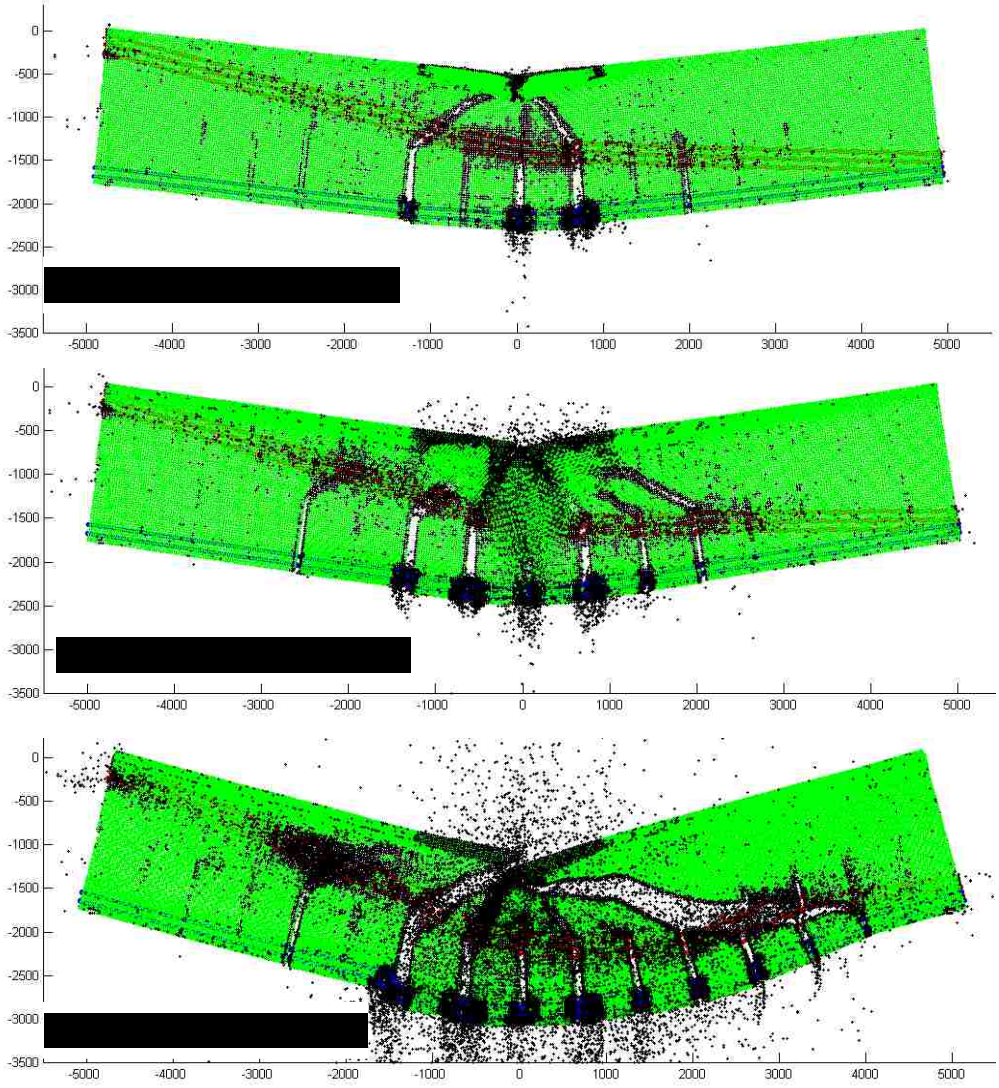

Figure 4.26 – 2D view of the BT72 beam simulation results

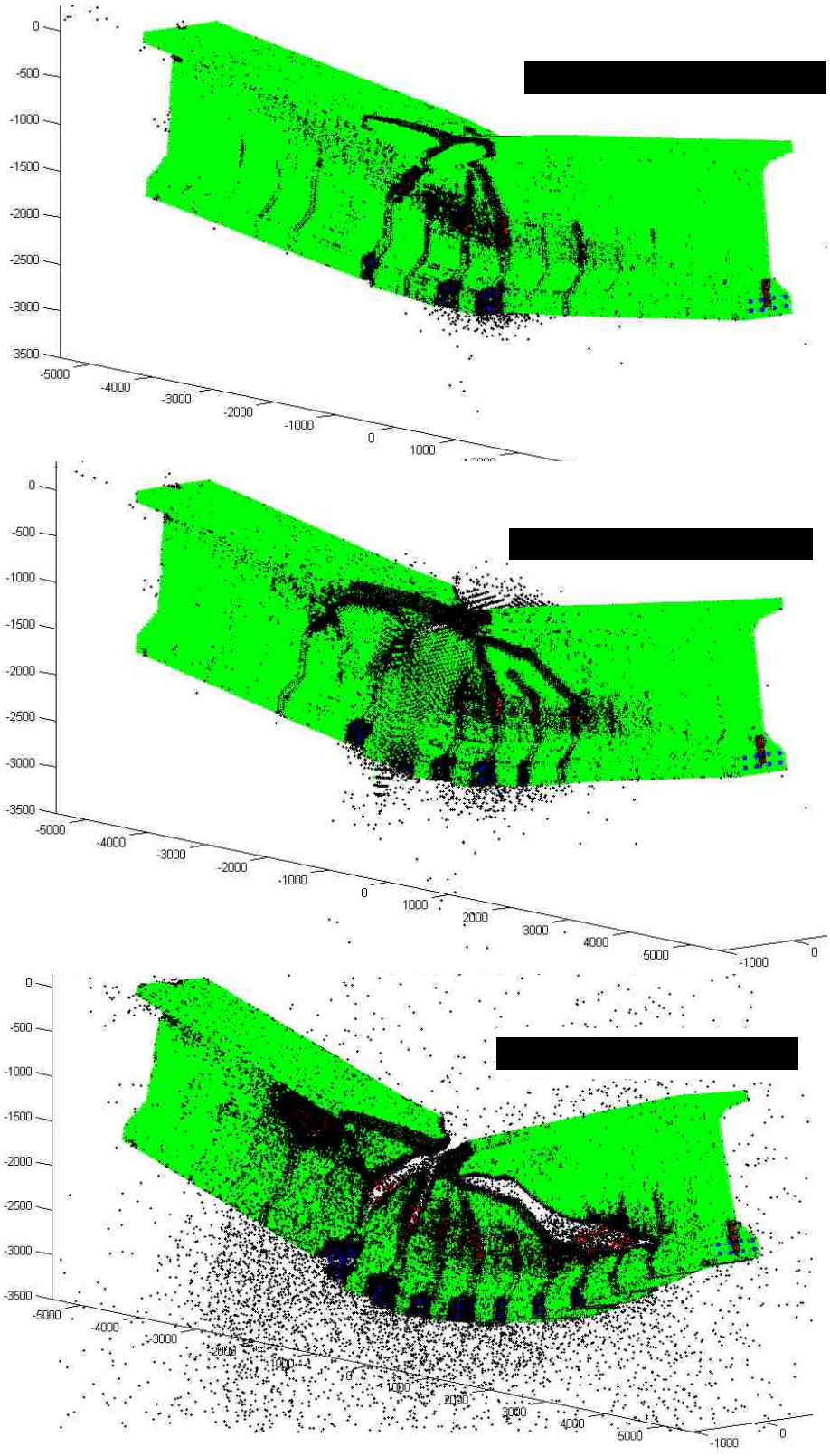

Figure 4.27 – 3D view of the BT72 beam simulation results

Cracking starts with the flexural cracks in the bottom flange. As the simulation advances, shear cracks nucleate and propagate in the web of the beam. In this example, the simulation results from PDQ are qualitatively presented. Quantitative comparison can be done by incorporation of ACI code provisions for designing prestressed girders used in bridges.

4.7. Scalability and timing performance

Scalability is how the performance of a system, network or process changes in accordance with the increased load. Consequently, a scalable system is a system whose performance improves proportionally with the hardware added.

As computational hardware prices drop, low-cost commodity systems are increasingly used for high-performance computing. The parallelization algorithms used for parallel particle-based simulations are desired to scale, *i.e.*, they must be suitably efficient and practical when applied to simulations of a large number of particles. In the context of high performance computing, *speedup* refers to how much a parallel algorithm is faster than a serial algorithm. Speedup is defined by Equation 5.11.

$$S = \frac{T_s}{T_p}, \qquad 4.11$$

where S is speedup, T_s is the calculation time using one processor and T_p is the calculation time using a parallel algorithm for a specific number of processors.

In an ideal scalable algorithm, calculation time is inversely proportional to the number of processors used, for the same problem with the same size. Figure 4.28 shows the calculation time per 1000 time steps against number of processors for the lap splice pull out problem with 362,677 particles.

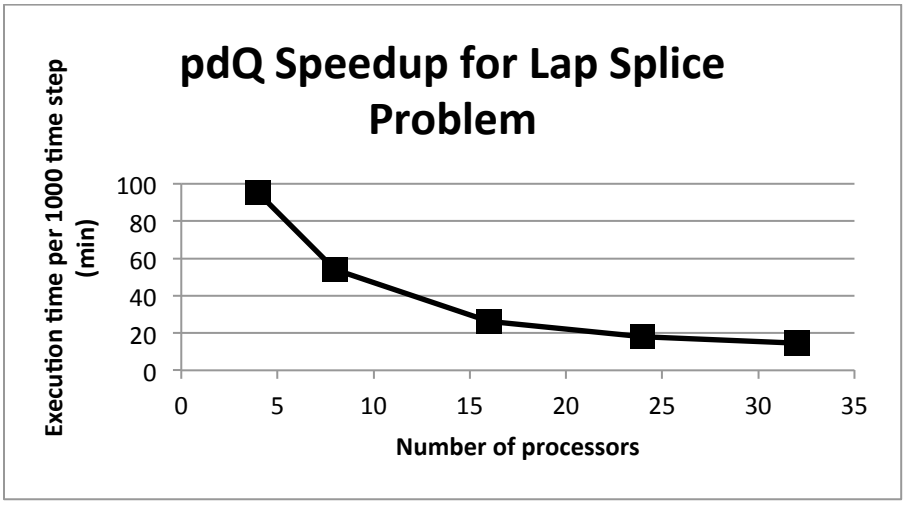

Figure 4.28 – Speedup for the lap splice pullout problem with 362677 particles

Gerstle *et al.* [Gerstle, Sakhavand and Chapman 2010] tried to estimate the total simulation time of a given problem in EMU using Equation 5.11:

$$T = K \times \frac{N \times C}{P}, \qquad 4.12$$

where K is processor-seconds per particle-time step, P is the number of processors, N is the total number of particles and C is the number of simulation time steps.

For the lap splice pullout problem, this factor is calculated to be approximately $1.8x10^{-4}$ for EMU, while in PDQ, K is $0.7x10^{-4}$ for this problem. In PDQ, for the other problems, K varies from approximately $0.4x10^{-4}$ to $0.7x10^{-4}$ processor-seconds per particle per time step. Substituting $K = 0.55x10^{-4}$ in Equation 6.1 with $N = 10^6$, $P = 1000$ and $C = 70{,}000$, T will be around one hour. The author plans to run PDQ on `encanto`, a supercomputer with 14,000 processors, which will allow simulating real-life problems in several hours using PDQ.

Preliminary timing performance analysis of PDQ shows that, in most of the simulations, approximately 8% of simulation time is spent on the inter-processor communication. 4.5% is approximately spent on particle communication and 3.5% is spent on force communication. Force calculation is dominant in an MD or PD simulation and takes 80%-90% of simulation time, depending on the problem specifics. Time integration takes less than 1% of the calculation time. The rest of the calculation time is spent on reading input files, initialization and outputting the results. These percentages mostly depend on the geometry of the problem (how the particles are located in the space) and also on how wisely the number of processors in each direction.

5. CONCLUSIONS

This chapter is divided into two sections. In the first section the parallel algorithm and the developed code, PDQ, are summarized. The advantages and limitations of PDQ are outlined. Also, the example problems and the simulation results are reviewed. The second section discusses suggested improvements to the code.

5.1. Summary and conclusions

Peridynamics simulation promises the ability to observe the creation of spontaneous discontinuities in materials which distinguishes it from other traditional methods in solid mechanics analysis. Its particle-based nature necessitates many interactions of particles which is computationally expensive. Parallel machines are needed to run such large simulations.

A scalable parallel particle-based spatial domain decomposition algorithm, the *wall method message passing algorithm*, was developed in the present work. Implementation of this parallelization scheme in a parallel code, PDQ, was described. PDQ is able to simulate both peridynamics and molecular dynamics simulations. Pre- and post-processing tools are provided separately for the code. Simplicity, generality and speed were the main design targets for PDQ. Exposing part of the source code to the user leaves the physical details to the user; meanwhile, the complexities of parallelization are hidden from the user.

As part of this thesis, several problems in structural engineering such plain, reinforced, and prestressed concrete beam were simulated using PDQ. Nucleation and propagation of cracks were observed from the simulation results.

Shear failure of a reinforced cantilever beam was illustrated in this work. The predicted strength derived from the simulated results showed close consistency with the analytical solutions. Figures from the simply supported beam match laboratory tests. The lap splice problem previously solved by Gerstle *et al.* using EMU [Gerstle *et al.* 2007] was also simulated. The simulation figures from PDQ match with those from EMU at the earlier stages of the simulation; but, diverge at later stages. The origin of this discrepancy is under investigation.

The ability of PDQ to accept user-defined force fields and its decentralization of the computation engine and input/output modules provides considerable flexibility and generality for the code to address different types of simulations at different length from the atomistic to the mesoscale.

In most of the simulations, reported here, the figures from simulations show some of the cracks nucleated earlier, close back up as the simulation evolves. This occurs because as the previously separated particles get closer than the material horizon, new links form. To avoid the undesired reformation of broken links, PDQ will need to be modified to maintain a history of the links.

5.2. Future work

The following suggestions are made to improve PDQ. Some of them have been developed in a preliminary extension of PDQ.

Oversimplifications in the original peridynamic model [Silling 1998], led Silling and his colleagues to introduce the state-based peridynamic model [Silling *et al.* 2007]. Extending PDQ to take up the concept of the states will make it ideal for peridynamics simulations. It also will allow determination of history-based models. A possible approach is using the idea of "neighbor lists" (Section 2.2.1) which also can help to speed up the code by reducing the time spent on finding interacting particles.

The generalization of degrees of freedom has been developed in an extended version of PDQ for peridynamics. Although this extended version is slower than the original version of PDQ, it enables the user to simulate problems using micropolar peridynamics model. In addition, the extension of PDQ to accept any number of degrees of freedom for each particle will provide the ability to run simulations involving charge-transfer force field in molecular dynamics simulations.

Simulation of cracking in solid materials does not require a large deformation; therefore possible relocation of particles to adjacent processors can be neglected for such problems. However, particle shuffling (Section 3.11) is a crucial part for molecular dynamics and must be implemented in PDQ.

PDQ provides a strong tool for solving structural engineering problems. More research is required to determine more realistic peridynamic models which reflect material behavior in the large scale. Implementation of these modified models in PDQ and access to supercomputers with thousands of processors, promises ability to simulate real-life structures such as a full bridge in a reasonable amount of time.

Today, cloud computing is an emerging concept in computational science which refers to the providing computational resources for the user via computer network

without bothering the user with the details of inner workings [The Economist 2009]. Utilizing a parallel code such as PDQ via the concept of cloud computing will enable a user to run peridynamic parallel simulations from his/her own laptop. This might be a venue to commercialize a structural analysis and design parallel code, which can be used as easy as other available commercial structural analysis and design simulation packages.

APPENDIX

Appendix A. pdQ User Manual for Peridynamics Simulations

A. PDQ User Manual for Peridynamic Simulations

This appendix provides the user manual to utilize PDQ for peridynamics simulations in the University of New Mexico supercomputer environment. This section of the thesis will be incorporated into a more general PDQ manual for both PD and MD at a later date. It is assumed that the user has basic programming expertise in FORTRAN 90, since several subroutines require user programming for customization. Some source code files are exposed to the user to give the user flexibility in defining sophisticated models.

A.1. Introduction

This manual is for PDQ peridynamics users. First install a terminal connection on your computer. `ssh` is a secure terminal connection which is accessible from `http://it.unm.edu/download/`. Cygwin/X (`http://x.cygwin.com`) and PuTTY (`http://www.chiark.greenend.org.uk/~sgtatham/putty/download.html`) are other free ssh/ftp clients which can also be used.

It is assumed that users have an account on a cluster a parallel supercomputer (e.g. `nano` or `pequena`) at the Center for Advanced Research Computing (CARC) at UNM, where PDQ is currently installed. If not, go to the CARC website (`http://www.hpc.unm.edu/`) and apply through the Project/Account link.

We assume the user is familiar with FORTRAN 90, Unix/Linux and with a Unix editor such as `vi` or `emacs`. The user can find a list of basic commands for Unix at `http://www.rain.org/~mkummel/unix.html` and for the `vi` editor at

http://www.lagmonster.org/docs/vi.html. Also the user can access a FORTRAN 90 tutorial at http://www.cs.mtu.edu/~shene/COURSES/cs201/NOTES/fortran.html or refer to [Metcalf *et al.* 2004].

A.2. Getting started

To log onto the supercomputer nano at the CARC, at the command prompt type:

```
ssh -X username@nano.hpc.unm.edu.
```

The -X suffix provides access to graphical connections. For instance, Matlab can be launched from nano if the -X suffix is used. Since Matlab should not be run at the head node of the super computer, an interactive session on nano should be obtained. Type qsub –I at the nano prompt. Once you have been assigned a node on nano, type Matlab.

PDQ uses a repository based upon the code-versioning software Subversion (http://en.wikipedia.org/wiki/Apache_Subversion). The PDQ repository can be viewed using a web browser at https://www.hpc.unm.edu/svn/cgi-bin/viewvc.cgi. To access the repository the user needs a username and password. To obtain access to the PDQ SVN repository contact Dr. Susan Atlas at the UNM Physics and Astronomy Department.

Next, create a directory named PDQ in your home directory. Then move to the PDQ directory and to check out the source code from the repository, type:

```
svn co https://www.hpc.unm.edu/svn/PDQ/src.
```

Now you have a directory /PDQ/src in your account.

A.3. Make a directory for each model

In the directory `/PDQ/PDsamplefiles` of the repository, there are several predefined models for peridynamic problems. To check out the `Cant` model, for instance, while in the PDQ directory, type:

```
svn co https://www.hpc.unm.edu/svn/PDQ/PDsamplefiles/Cant.
```

Each sample model includes the following directories:

modelsrc

postProcessor

preProcessor

run

Each model in the `PDsamplefiles` directory contains two source files that are model-specific: `PDuserForce.F` and `PDuserInteg.F`. The rest of the source files must be copied from `/PDQ/src` in the repository to the model directory.

Now copy all the files in the `/PDQ/src` directory to `/PDQ/`*`modelname`*`/modelsrc`. The model now contains all of the necessary PDQ source code and is ready to be compiled and linked.

A.3.1. Description of the user file `PDuserForce.F`

To provide the user with the ability to define problem-specific models, the `PDuserForce.F` source code file is segregated from main source code files. The user can edit this file and should review it to understand the pairwise force model. In this section, the user file `PDuserForce.F` is briefly explained. As an example, the following

pages show the `PDuserForce.F` file of the `Cant` model, which simulates a plain (unreinforced) concrete beam.

`PDuserForce.F` contains multiple subroutines. The first subroutine `ForceCalcPD`, shown in Figure A.1, is the main subroutine for the force calculation from which other subroutines inside this file are called. In this subroutine the pairwise force between two given particles is calculated. The reference positions, material types and degrees of freedom, which according to the problem could be current positions, velocities, etc., of the particles `i` and `j`, are inputs to the subroutine. The calculated forces at the degrees of freedom are the outputs. After determining whether the particles lie within the peridynamic horizon, the `ConcConc` subroutine is called, as all the particles are of the same material type. However, if the particles were of different material types, different subroutines could be called with the help of "if statements" as is illustrated with the example problem, called `RCCant` in the repository.

In the `ConcConc` subroutine, shown in Figure A.2, the material parameters are defined and the forces are calculated and returned to the `ForceCalcPD` subroutine.

```
!-----------------------------------------------------------------------
      subroutine ForceCalcPD(xPosi, yPosi, zPosi,
     .                       xPosRefi,yPosRefi,zPosRefi,MatTypei,dvoli,
     .                       xPosj, yPosj, zPosj,
     .                       xPosRefj,yPosRefj,zPosRefj,MatTypej,dvolj,
     .                       xFij, yFij, zFij,Bondij)

!     Calculates force between particles for PD.
!     NS. 07/02/10.
!-----------------------------------------------------------------------
     use scalars
     use serialArrays
     use globalParameters
     implicit none

     integer i, j, MatTypei, MatTypej
     real xDist, yDist, zDist, rCutOff2, Dist2
     real xPosi, yPosi, zPosi
     real xPosRefi, yPosRefi, zPosRefi
     real xPosj, yPosj, zPosj
     real xPosRefj, yPosRefj, zPosRefj
     real xFij, yFij, zFij
     real dvoli, dvolj,Bondij

     rCutOff2 = rCutOff*rCutOff
     xDist = xPosj - xPosi
     yDist = yPosj – yPosi
     zDist = zPosj - zPosi

     !     ... calculate distance between i and j
     Dist2 = xDist**2 + yDist**2 + zDist**2

       if (Dist2 .LT. rCutOff2) then

           call  ConcConc(xPosi, yPosi, zPosi,
    .                     xPosRefi, yPosRefi, zPosRefi, dvoli,
    .                     xPosj, yPosj, zPosj,
    .                     xPosRefj, yPosRefj, zPosRefj, dvolj, Dist2,
    .                     xFij, yFij, zFij,Bondij)
       else

         xFij = zero
         yFij = zero
         zFij = zero
         Bondij = zero

       endif

     return
     end
```

Figure A.1 – `ForceCalcPD` subroutine in `PDForceFile.F file`

```
!-----------------------------------------------------------------------
      subroutine ConcConc(xPosi, yPosi, zPosi,
     .                    xPosRefi, yPosRefi, zPosRefi, dvoli,
     .                    xPosj, yPosj, zPosj,
     .                    xPosRefj, yPosRefj, zPosRefj, dvolj, Dist2,
     .                    xFij, yFij, zFij, Bondij)
!
!    Calculates force if both particles are concrete type.
!
!    NS. 07/02/10.
!-----------------------------------------------------------------------
      use scalars
      use serialArrays
      use globalParameters
      implicit none

      integer i, j
      real RefDist, str
      real Dist, Cosx,Cosy,Cosz, const,Dist2
      real xPosi, yPosi, zPosi
      real xPosRefi, yPosRefi, zPosRefi
      real xPosj, yPosj, zPosj
      real xPosRefj, yPosRefj, zPosRefj
      real xFij, yFij, zFij
      real dvoli, dvolj, dvolij,Bondij

      real , parameter ::  E_Conc   = 3.604E6
      real , parameter ::  nu_Conc  = 0.22
      real , parameter ::  St       = 1.387E-4
      real , parameter ::  Sc       = -1.110E-3

      const = six*E_Conc/(pi*(rCutOff**4)*(one-two*nu_Conc))

      RefDist = sqrt( (xPosRefi-xPosRefj)**2 +
     .                (yPosRefi-yPosRefj)**2 +
     .                (zPosRefi-zPosRefj)**2 )
      Dist = sqrt(Dist2)
      str = ( Dist - RefDist ) / RefDist

      if ((str.lt.St).and.(str.gt.Sc)) then
        Cosx = (xPosRefj-xPosRefi)/RefDist
        Cosy = (yPosRefj-yPosRefi)/RefDist
        Cosz = (zPosRefj-zPosRefi)/RefDist
        dvolij = dvoli*dvolj*const*str
        xFij = Cosx*dvolij
        yFij = Cosy*dvolij
        zFij = Cosz*dvolij
        Bondij = 1.0
      else
        xFij = zero
        yFij = zero
        zFij = zero
        Bondij = zero
      endif

     return
     end
```

Figure A.2 – `ConcConc` subroutine in `PDForceFile.F` file

A.3.2. Description of the user file `PDuserInteg.F`

`PDuserInteg.F` is the user file for integration which contains source code for integration. The user can edit this file to implement the time integration method of choice. A sample integration file for the `Cant` model is in Figure A.3:

```
!-----------------------------------------------------------------------
      subroutine IntegratePD
!     This subroutine implements the integration schemes used PD
!
!     NS. 03/21/10.
!-----------------------------------------------------------------------
      use scalars
      use serialArrays
      implicit none

      integer i

      do i = 1, numAtomsL

       if (xBCcode(i) .EQ. 0) then
        xAccel(i) = xForce(i)/particleMass(i)
        xVel(i) = xVel(i) + deltastep*xAccel(i)
        xPos(i) = xPos(i) + deltastep*xVel(i)
       endif

       if (yBCcode(i) .EQ. 0) then
        yAccel(i) = yForce(i)/particleMass(i)
        yVel(i) = yVel(i) + deltastep*yAccel(i)
        yPos(i) = yPos(i) + deltastep*yVel(i)
       endif

       if (zBCcode(i) .EQ. 2) then
        zAccel(i) = (zForce(i)-14.0*istep/totSteps)/particleMass(i)
        zVel(i) = zVel(i) + deltastep*zAccel(i)
        zPos(i) = zPos(i) + deltastep*zVel(i)

       elseif (zBCcode(i) .EQ. 0) then

        zAccel(i) = zForce(i)/particleMass(i)
        zVel(i) = zVel(i) + deltastep*zAccel(i)
        zPos(i) = zPos(i) + deltastep*zVel(i)

       endif

      enddo

     return
     end
```

Figure A.3 – `PDIntegFile.F` for example problem `Cant`

A.4. Making an executable: `PDQ.x`

To create the executable file for PDQ, denoted `PDQ.x`, the code is compiled and linked using the `make` command.

In the `/PDQ/`*`modelname`*`/modelsrc` directory, open the `Makefile` using `vi`. In the `Makefile`, about three pages down, find the section shown in Figure A.4.

```
#-----------------------------------------------------------------
# programming model, OS, and simulation (PD vs. MD) mode #defines
#-----------------------------------------------------------------
```

Figure A.4 – Simulation mode section in the PDQ `Makefile`

Below this section title, there are two flags that are important: `DMPIL` and `DSERL`. `DMPIL` is the flag that controls the compiling and linking the parallel version of PDQ. `DSERL` compiles and links the serial version of PDQ. Of the lines below, only one dependency should be uncommented by removing the pound sign.

```
    #DMPII    = -Dmpi_IBM -Dmpi -DIBM
    #DMPIG    = -Dmpi_SGI -Dmpi -DSGI
    #DMPIL    = -Dmpi_LIN -DMPI -DLIN
    DMPIL          = -DMPI

    #DSERI    = -Dserial_IBM -Dserial -DIBM
    #DSERG    = -Dserial_SGI -Dserial -DSGI
    #DSERL    = -Dserial_LIN -Dserial -DLIN

    DPARALLEL = $(DMPIL) $(DSERL)
```

Figure A.5 – Parallel or serial dependency flag in the PDQ `Makefile`

We also need to specify at compile time whether the simulation mode is molecular dynamics (MD) or peridynamics (PD). This again is done by uncommenting the appropriate flag:

```
#SIMMODE  = -DMD
SIMMODE   = -DPD
DSIMMODE  = $(SIMMODE)
```

Figure A.6 – Simulation mode flag in PDQ `Makefile`

There are other flags in the `Makefile`; these flags should be set by the user in consultation with an applications specialist from the CARC user services group who can provide details of the environment of the parallel system being used for calculations (nano, pequena).

In the `/modelsrc` directory, type `make` to compile and link the program, thus creating an executable called `PDQ.x`.

After creating the executable file, copy `PDQ.x` from the `/modelsrc` directory to the *`modelname`*`/run` directory.

A.5. Preprocessing

The user can generate input files for PDQ or use those already provided in the run directory for the sample model. In the preprocessor directory for each model, there is a main preprocessing file. This file, which creates the input files for PDQ, should be named descriptively `PDpreprocess.F` or `BulbT.F` or `PullOut.F`, etc., depending on the model. For instance, in the `Cant` sample model, `PDpreprocess.F` produces a 3D cuboidal beam with specified external forces and boundary conditions that can be altered to create different input models.

For the `Cant` sample model, the user can edit `PDpreprocess.F` as desired and then make the executable `PDpreprocess.x` file in the `PDpreprocess` directory by typing `make`.

Run `PDpreprocess.x` by typing `PDpreprocess.x`. This application creates the six PDQ input files as output. The files are `RefConfig.dat`, `ParticleState.dat`, `Mass.dat`, `MatType.dat`, `BCs.dat` and also the main input file, `PDQPDInput.dat`, which includes global parameters such as the number of total time steps, the number of particles, etc.

Now copy the six files with `.dat` extensions (the input files) into the `modelname/run` directory.

A.5.1. Predefined geometries in the repository

A directory called `prePackage` is available in the repository which contains some files to make creating or excluding several predefined geometric shapes easier. These files contain functions which receive some geometrical properties as their input and return position arrays to create the desired geometrical shape. The returned data can be used in a main preprocessing file to create the desired models.

Currently the `prePackage` directory contains several files as follows:

`Insert.F` contains functions `InsertByPoints` and `InsertByangle` which is used to create lines of particles. It is useful for inserting reinforcing bars into concrete.

`Box.F` contains function `CreateBox` to create a box-shaped geometry which is useful to create a rectangular shaped concrete beam. Also it contains `DeleteBox` to exclude a box-shaped geometry out of an input geometry.

`Cylinder.F` contains functions `CreateCylinder` to create a cylindrical-shaped geometry and `DeleteCylinder` to exclude a box-shaped geometry out of an input geometry. These functions were used in the preprocessing `PullOut.F` file to create the lap splice problem.

Details on how to use specific functions can be found through the comments written inside their containing files. All these functions receive some information about geometric properties such as dimensions of a shape or desired spacing between particles. The returned data include created and modified particle position arrays and the total number of particles.

A.5.2. Description of input file `PDQPDInput.dat`

The main input file `PDQPDInput.dat` contains these sections:

A.5.2.1. Input file names

- `PDmatTypeFile`: includes material type of each particle.
- `PDparticleStateFile`: includes particles' current positions and velocities.
- `PDrefConfigFile`: includes reference positions of particles.
- `PDmassFile`: includes mass of each particle.
- `PDboundaryCondFile`: includes boundary conditions, constraints and loading.

A.5.2.2. Restart simulation related parameters

- `restart` is a number which the time step starts from. This is particularly useful when you stop the code while running, for example to check if it is

going as you wish, and would like to resume it again from the time step at which it was halted.

A.5.2.3. Main simulation related parameters

A.5.2.3.1. Particles

- `numAtoms` is the total number of particles.
- `atomDimFactor` is a fudge actor that ensures the sizes of local arrays are sufficient. The local arrays must be pre-allocated. This factor is used to guarantee that there will be enough space in the array for data storage. Although the size of the arrays are automatically computed in PDQ based on the geometry of the problem, in some cases, particularly those with irregular shapes, insufficient space can cause the code to crash with a core dump message. This indicates insufficient memory which can be solved by increasing the `atomDimFactor` parameter in the main input file. In no case should its value be less than 1.0. Increasing `atomDimFactor` results in larger local arrays which slows down the code as larger messages will be exchanged.
- `numDF` is the number of degrees of freedom per particle.

A.5.2.3.2. Simulation Box

- `xBoxDim` is the size of the global domain in the `x`-direction, which should be greater than the maximum `x`-position minus the minimum `x`-position of all the particles, and similarly for `yBoxDim` and `zBoxDim`. The code handles both positive and negative positions.

- `nxProc` is the number of the processor(s) in the `x`-direction. If the global domain has a longer dimension in a specific direction, it is suggested to use more processors in that direction and similarly for `nyProc` and `nzProc`. The product of these three integers is the total number of processors.
- `CellDimFactor` is a factor used to ensure that the cell dimension in each direction is slightly greater than the material horizon. `CellDimFactor` should be slightly greater than one.

A.5.2.3.3. Force-Field

- `rCutOff` is the length that defines the longest distance within which a particle interacts with other particles. It is also called the *material horizon* in peridynamics.

A.5.2.3.4. Integrator

- `deltaStep` is the time increment for numerical time integration. At each time step, updated accelerations, velocities and positions are calculated and integration happens. The time step is calculated automatically in the preprocessing files based on the bulk modulus, spacing between the particles and the density of the materials.
- `totSteps` is the total number of time steps requested in the simulation from the first time step.

A.5.2.3.5. Output parameters

- `dumpRestartSteps` is the number of time steps between which the restart files are written.

- `runID` is a user ID that appends to the filename of `PDQ`*`runID`*`.out`.

A.5.3. Generalized degrees of freedom

An extended version of PDQ for peridynamic simulations has been developed which accepts user-defined degrees of freedom for peridynamic simulations. This generalization gives PDQ a unique flexibility that distinguishes it from other PD codes. This version of the code allows the user to solve problems involving multi-physical phenomena. For instance, temperature can be included as a particle state variable. The modified version is also suitable for implementing the micropolar peridynamic model (Section 2.1.1). Another application of the modified version of PDQ is to enable the user to define specific parameters as degrees of freedom which, although not used in the force field, might be useful in another way. For instance, damage can be defined as a degree of freedom which can be used in post-processing.

In the modified version of PDQ for peridynamics, there are only three input files to PDQ: `ParticleAlterAttrsFile`, `ParticleFixedAttrsFile` and `PDQPDInput.dat`. The main input file `PDQPDInput.dat` remains the same as described in Section A.5.2 except the "input file name" section reduces to two files: `ParticleAlterAttrsFile` and `ParticleFixedAttrsFile`.

`ParticleAlterAttrsFile` includes all particle-alterable attributes that change as the simulation runs. These attributes include particle positions in *x*, *y* and *z* directions, particle velocities, temperature, damage percentage and all other attributes defined by the user that change during the simulation. On the other hand, the next file, `ParticleFixedAttrsFile` includes particle fixed (unchanged) attributes which do not

change during the simulation. Reference positions, mass, density, material type, etc. are among those attributes that remain constant during the simulation. In both these files the first column is the global particle ID. In `ParticleAlterAttrsFile`, the second, third and fourth columns contain the current particle `x`, `y` and `z` positions, respectively. The second, third and fourth columns in `ParticleFixedAttrsFile` contain the reference particle `x`, `y` and `z` positions, respectively. The order in which the other attributes appear in these files is arbitrarily defined by the user.

Given the information above, the user is completely responsible for deciding which file a particular attribute belongs to. Thus, the user should think carefully and fully understand the physics of the problem before running a simulation. The modified version of PDQ gives the user considerable flexibility, but simultaneously puts a burden of responsibility on the user. Although the order of attributes in the input files is specified by the user, it should be consistent with `PDuserForce.F` and `PDuserInteg.F` files. These files are exposed to the user to define the pairwise force relationship between a pair of particles and to define the desired integration method.

In the modified version of PDQ, six one-dimensional arrays are accessible by the user through the user source code files: `ParticleAlterAttrsi`, `ParticleAlterAttrsj`, `ParticleFixedAttrsi`, `ParticleFixedAttrsj`, `IntegFieldAttrsi` and `IntegFieldAttrsj`.

`ParticleAlterAttrsi` and `ParticleAlterAttrsj` contain alterable particle attributes of particles i and j respectively. The order which the attributes are saved in these arrays is the same as the order defined by the user when creating the

`ParticleAlterAttrsFile`. An example order of alterable attributes in `ParticleAlterAttrsFile` is shown in Figure A.7:

```
        0          1          2          3          4          5          6

  particleID  x-Position  y-Position  z-Position  x-velocity  y-velocity  z-velocity
```

Figure A.7 – Example of attributes order in `ParticleAlterAttrsFile`

If the order shown in Figure A.7 is defined by the user for "ParticleAlterAttrsFile" input file, the one-dimensional arrays "ParticleAlterAttrsi" and "ParticleAlterAttrsj" in the user source code files contain their elements in the order shown in Figure A.8.

```
ParticleAlterAttrsi(1) = x-position of i   ParticleAlterAttrsj(1) = x-position of j
ParticleAlterAttrsi(2) = y-position of i   ParticleAlterAttrsj(2) = y-position of j
ParticleAlterAttrsi(3) = z-position of i   ParticleAlterAttrsj(3) = z-position of j
ParticleAlterAttrsi(4) = x-velocity of i   ParticleAlterAttrsj(4) = x-velocity of j
ParticleAlterAttrsi(5) = y-velocity of i   ParticleAlterAttrsj(5) = y-velocity of j
```

Figure A.8 – Example of attributes order in `ParticleAlterAttrsi` and `ParticleAlterAttrsi` arrays

In the same way, `ParticleFixedAttrsi` and `ParticleFixedAttrsj` arrays follow the order of attributes in `ParticleFixedAttrsFile` file. The order of attributes in `IntegFieldAttrsi` and `IntegFieldAttrsj` arrays are arbitrarily defined by the user. An example of the order of elements in these arrays is shown in Figure A.9.

```
IntegFieldAttrsi(1) = x-force of i    IntegFieldAttrsj(1) = x-force of j
IntegFieldAttrsi(2) = y-force of i    IntegFieldAttrsj(2) = y-force of j
IntegFieldAttrsi(3) = z-force of i    IntegFieldAttrsj(3) = z-force of j
```

Figure A.9 – Example of attributes order in `IntegFieldAttrsi` and `IntegFieldAttrsj` arrays

A.6. Running PDQ

To run PDQ, open the PBS (Portable Batch System) script, `PDQ.PD.pbs`, with `vi`, in the run directory and change the `RUNDIR=` and `remotescratch=` to the run directory, which is */username/*`PDQ`*/modelname/*`run/`. Define the number of processors as follows. First, note that `nnodes` multiplied by `ppn` results in the total number of requested processes. On `nano`, the maximum number of processors per node, `ppn`, is four. In the PBS script, note that `ppn` and `cores_per_node` should be the same; thus the number in front of `setenv cores_per_node` should be the same as `ppn`. Figure A.10 represents an example of the first few lines of the PBS script.

```
#!/bin/csh
#PBS -l nodes=8:ppn=4
#PBS -l walltime=48:00:00
#PBS -N Cant

# must set cores_per_node = PBS variable 'ppn'
# variable smp corresponds to 'rack-level' grouping of nodes
#   i.e., number of racks

setenv cores_per_node 4
```

Figure A.10 – First few lines in the PBS script file

From the `/modelname/run` directory, submit the job with `qsub PDQ.PD.pbs`.

The following are some useful Linux/PBS commands to use when submitting jobs to the supercomputer (`nano`, `pequena`). They work regardless of which directory you are currently in:

- `qstat`: outputs the status of submitted jobs on the machine. If a job is running, R is written in front of it. If it is queued, Q is the letter found in

front of it. You can also see more details by additional flags to the command, for example by typing `qstat –an`.

- `qgrok`: shows the number of total, occupied and free nodes.
- `qdel`: with this command you can delete your submitted job by typing `qdel` *`jobID`*, for instance `qdel 12423`. The `jobID` is integer in the first column of the submitted job.

A.7. Post-processing

Each sample model directory has a postprocessor directory containing Matlab files used for graphical post processing of the results.

Copy the `*.dat` files from */modelname/*`run` directory to the */modelname/*`postprocessor` directory and run the file whose name starts with `readfiles_`. Do this by typing the name of that starts with `readfile_` with the time step you want to post process as an input argument. For instance in the Matlab prompt window type `readfiles_ConcBeam(1000)` for the `Cant` model. This will show a deformed shape of the beam after 1000 time steps.

File “timing.o” in the run directory includes timing performance of the run. This is a helpful file for studying the scalability and timing performance of the code. The elapsed time and the percentage time spent on different parts of the code are tabulated in this file.

REFERENCES

Allen M. P. and Tildesley D. J. (1987). *Computer Simulation of Liquids*, Oxford Science Publications, Oxford.

Anderson T. L. (2005). *Fracture Mechanics: Fundamentals and Applications*, 3rd Ed., CRC Press, Boca Raton, FL.

Atlas S. R., Cummings J. C., and Reynders J. V. W. (1996). "Parallel Molecular Dynamics Simulation in the POOMA FrameWork", paper presented at the 1996 Conference on Parallel Object-Oriented Methods and Applications, Santa Fe, NM.

Atlas S. R. (1999). "PDQ, a Portable, Parallel and Extensible Molecular Dynamics Simulation Program", Technical Report, University of New Mexico.

Atlas S. R. and Valone S. M. (2011). "Density Functional Theory of the Embedded-Atom Method: Multiscale Dynamical Potentials with Charge Transfer", preprint, Physical Review B, to be submitted.

Atlas S. R., Wright A. F., Ramprasad R. and Cano L. (1998-2011). "Vernet: A Parallel Planewave Pseudopotential Code for Density Functional Electronic Structure Calculations in Solids", University of New Mexico.

Barney B. (2010). "Introduction to Parallel Computing", Lawrence Livermore National Laboratory, `https://computing.llnl.gov/tutorials/parallel_comp/`.

Bazant Z. P. and Jirasek M. (2002). "Nonlocal Integral Formulations of Plasticity and Damage: Survey of Progress", Journal of Engineering Mechanics, 128(11): 119-149.

Beazley D. M. and Lomdahl P. S. (1994). "Message-Passing Multi-Cell Molecular Dynamics on the Connection Machine 5", Parallel Computing, 20(2): 173-195.

Bowers K. J., Chow E., Xu H., Dror R. O., Eastwood M. P., Gregersen B. A., Klepeis J. L., Kolossvary I., Moraes M. A., Sacerdoti F. D., K. Salmon, Shan Y., Shaw D. E. (2006). "Scalable Algorithms for Molecular Dynamics Simulations on Commodity Clusters", Conference on High Performance Networking and Computing Archive, Proceedings of the 2006 ACM/IEEE Conference on Supercomputing, Tampa, Florida, Article No. 84.

Bowers K., Dror R. and Shaw D. E. (2006). "The Midpoint Method for Parallelization of Particle Simulations", Journal of Chemical Physics, 124: 184109.

Bowers K., Dror R. and Shaw D. E. (2007). "Zonal methods for the parallel execution of range-limited N-body simulations", Journal of Computational Physics, 221 (1): 303-329.

Brown D. and Maigret B. (1999). “Large Scale Molecular Dynamics Simulations using the Domain Decomposition Approach”, Proceedings of the 24th SPEEDUP Workshop, Berne, Sept. 24-25, 12(2): 33-41.

Bruck J., Ho C., Kipnis S. and Weathersby D. (1994). “Efficient Algorithms for All-To-All Communications in Multi-Port Message-Passing Systems”, Proceedings of the 6th Annual ACM Symposium on Parallel Algorithms and Architectures, Cape May, NJ, ACM Press, 6: 298-309.

Cusatis G., Bazant Z. P. and Cedolin L. (2006). “Confinement-Shear Lattice CSL Model for Fracture Propagation in Concrete”, Computer Methods for Applied Mechanics and Engineering, 195: 7154–7171.

Fincham D. and Ralston B. J. (1981). “Molecular Dynamics Simulation Using the Cray-1 Vector Processing Computer”, Computer Physics Communications, 23(2): 127-134.

Fincham D. (1987). “Parallel Computers and Molecular Simulation”, Molecular Simulation, 1: 1-45.

Gerstle W. and Sau N. (2004). “Peridynamic Modeling of Concrete Structures”, Proceedings of the 5th Intl. Conf. on Fracture Mechanics of Concrete Structures, Li, Leung, Willam, and Billington, Eds., Ia-FRAMCOS, Vail, CO, 2: 949-956.

Gerstle W., Sakhavand N. and Chapman S. (2010). “Comparison of Peridynamic and Continuum Mechanics Models for Concrete”, 7th International Conference on Fracture Mechanics of Concrete and Concrete Structures, ACI, Korea.

Gerstle W. H., Sau N. and Sakhavand N. (2009). “On Peridynamic Computational Simulation of Concrete Structures”. Technical Report SP265-11, American Concrete Institute, 265: 245-264.

Gerstle W., Sau N. and Silling S. (2005). “Peridynamic Modeling of Plain and Reinforced Concrete Structures”, Proceedings of the 18th Intl. Conf. on Structural Mechanics in Reactor Technology (SMiRT 18), Atomic Energy Press, Beijing China, Aug. 7-12, 949–956.

Gerstle W. H., Sau N. and Aguilera E. (2007a). “Micropolar Modeling of Concrete Structures”, Proceedings of the 6th Intl. Conf. on Fracture Mechanics of Concrete Structures, Ia-FRAMCOS, Catania, Italy, June 17-22.

Gerstle W., Sau N. and Aguilera E. (2007b). "Micropolar Peridynamic Constitutive Model for Concrete”, 19th Intl. Conf. on Structural Mechanics in Reactor Technology (SMiRT 19), Toronto, Canada, August 12-17, B02/1-2.

Gerstle W., Sau N. and Silling S. (2007). “Peridynamic Modeling of Concrete Structures”, Nuclear Engineering and Design, 237(12-13): 1250-1258.

Gerstle, W., Silling, S., Read, D., Tewary, V. and Lehoucq, R. (2008). “Peridynamic Simulation of Electromigration”, Computers, Materials and Continua, Tech Science Press, 8(2): 75-92.

Heffelfinger G. S. (2000). “Parallel Atomistic Simulations”, Computer Physics Communications, 128(19): 219-237.

Hendrickson B. and Plimpton S. (1992). “Parallel Many-Body Simulations Without All-To-All Communication”, Technical Report SAND92-0792, Sandia National Laboratories, Albuquerque, NM.

Hess B., Kutzner C., van der Spoel D. and Lindahl E. (2008). “GROMACS 4: Algorithms for Highly Efficient, Load-Balanced, and Scalable Molecular Simulation”, Journal of Chemical Theory and Computation, 4: 435–447.

Kadau K., Germann T. C. and Lomdahl P. S. (2006). “Molecular Dynamics Comes of Ages: 320 Bilion Atom Simulation on BlueGene/L”, Modern Physics, 17(12): 1755-1761.

LAMMPS code, (2011). Large-scale Atomic/Molecular Massively Parallel Simulator, available at [`http://lammps.sandia.gov`].

Lindahl E., Hess B. and van der Spoel D. (2001). “GROMACS 3.0: A Package for Molecular Simulation and Trajectory Analysis”. Journal of Molecular Modeling, 7(8): 306-317.

Mase G. T., Smelser R. E. and Mase G. E. (2009). *Continuum Mechanics for Engineers*, 3rd Ed., CRC Press, Boca Raton, FL.

Mel'cuk A. I., Giles R. C. and Gould H. (1991). “Molecular Dynamics on the Connection Machine”. Computers in Physics 5: 311-318.

Metcalf M., Reid J. and Cohen M. (2004). *Fortran 95/2003 Explained (Numerical Mathematics and Scientific Computation)*, 3rd Ed., Oxford University Press, USA.

Newton I. (1999). *The Principia*, 1687. See *A New Translation*, by Cohen I. B. and Whitman A., University of California Press, Berkeley.

Nguyen V. B., Chan A. H. C. and Crouch R. S. (2005). “Comparisons of Smeared Crack Models For RC Bridge Pier Under Cyclic Loading”, 13th ACME conference, University of Sheffield, pp. 111-114.

Pacheco P. S. (1998). “A User’s Guide to MPI”, Department of Mathematics, University of San Francisco, ftp://math.usfca.edu/pub/MPI/mpi.guide.ps.

Parks M. L., Lehoucq R. B., Plimpton S. J. and Silling S. A. (2008). “Implementing Peridynamics within a Molecular Dynamics Code”, Computer Physics Communications, 179: 777-783.

Phillips J. C., Braun R., Wang W., Gumbart J., Tajkhorshid E., Villa E., Chipot C., Skeel R. D., Kalé L. and Schulten K. (2005). “Scalable molecular dynamics with NAMD”, Journal of Computational Chemistry, 26(16): 1781–1802.

Plimpton S. J., (1995). “Fast Parallel Algorithms for Short-Range Molecular Dynamics”, Computational Physics, 117: 1-19.

Rapaport D. C. (2004). *The Art of Molecular Dynamics Simulation*, 2nd Ed., Cambridge University Press, Cambridge, UK.

Reynders J. V. W., Hinker P. J., Cummings J. C., Atlas S. R., Banerjee S., Humphrey W. F., Karmesin S. R., Keahey K., Srikant M., and Tholburn M. (1996). “POOMA: A Framework for Scientific Simulation on Parallel Architectures”, in: G Wilson and P Lu, eds., *Parallel Programming Using C++*, MIT Press, Cambridge.

Runzell B., Shield C. K., French C. W. (2008). “Shear Capacity of Prestressed Concrete Beams”, Technical Report MN/RC 2007-47, Minnesota Department of Transportation, St. Paul.

Sau N. (2008). “Peridynamic Modeling of Quasi-Brittle Structures”, Ph.D. Dissertation, University of New Mexico, unpublished.

Silling S. (1998). “Reformulation of Elasticity Theory for Discontinuities and Long-Range Forces”, Technical Report SAND98-2176, Sandia National Laboratories, Albuquerque, NM.

Silling S. (2002). “Dynamic Fracture Modeling with a Meshfree Peridynamic Code”, Technical Report SAND2002-2959C, Sandia National Laboratories, Albuquerque, NM.

Silling S. A., Epton M., Weckner O., Xu J. and Askari E. (2007). “Peridynamic States and Constitutive Modeling”, Journal of Elasticity, 88: 151-184.

Steinbrugge K. V. (1992). “The Earthquake Engineering Online Archive, Karl V. Steinbrugge Collection”, NISEE, University of California, Berkeley, http://nisee.berkeley.edu/elibrary/Image/S4034.

The Economist (2009). “Cloud computing: Clash of the clouds”, Oct. 15th 2009.

Timoshenko S. P. (1983). *History of Strength of Materials*, Dover Publications, New York.

Valone S. M. and Atlas S. R., (2006). "Electron Correlation, Reference States, and Empirical Potentials", Philosophical Magazine 86: 2683.

Verlet L. (1967). "Computer Experiments on Classical Fluids. I. Thermodynamical Properties of Lennard-Jones Molecules", Yeshiva University, New York, Physical Review, 159: 98–103.

Zienkiewicz O. C., Taylor R. L. (2005). *The Finite Element Method for Solid and Structural Mechanics*, 6th Ed., Elsevier, Oxford.